UNIVERSITAT POLITÈCNICA DE CATALUNYA
BARCELONATECH
Escola d'Enginyeria de Barcelona Est

MASTER THESIS

Màster en Enginyeria Química

VALIDATION OF FLACS CODE FOR RISK ANALYSIS OF HYDROCARBON POOL FIRES

Report and Appendices

Author: Brais Gómez-Reino Martínez

Director: Eulàlia Planas

Co-Director: Borja Rengel

Call: June 2017

UNIVERSITAT POLITÈCNICA DE CATALUNYA
BARCELONATECH
Centre for Technological Risk Studies

1 Abstract

Fires have been object of study over the last decades due to their destructive power. Fire's hazardous nature and its ability to inflict damage to property, the environment and people, has produced a need to understand how it works in every aspect. Currently, the main focus is to estimate the fire characteristics and main effects, in order to accurately design emergency plans and prevention measures.

Due to the needs previously stated, fires have been studied and analyzed mainly from an experimental point of view. However, experimental data is arduous and extremely expensive to obtain due to the amount of resources needed. Additionally, small-scale models, which are generally easier to be undertaken, cannot be extrapolated to full-scale models. Considering this, semi-empirical methods were developed, but can only be applied to simple scenarios and they cannot fully model them. To achieve complete models of fires, CFD (Computational Fluid Dynamics) modeling has been recently used as a way to achieve a cheaper and easier method to study the fire development of full-scale fires in a wide range of conditions. Nevertheless, CFD models require a huge validation effort before they could be widely applied.

The main objective of this thesis is to analyze the performance and if possible validate the CFD code FLACS-Fire v10.5 (Flame Accelerator Simulator) for pool-fires. FLACS is a Computational Fluid Dynamic (CFD) program, which solves the compressible conservation equations for mass, momentum, enthalpy, and mixture fraction using a finite volume method. To model a fire it is necessary to include, among others, processes that involve submodels for: turbulence, combustion, thermal radiation, and soot generation. It is of utmost importance, while developing fire models, to validate them against experimental data in pursuance of being able to conclude whether the simulation is valid or not, and to determine the inherent error in comparison with reality. This process consists in a replication of the experimental setup in the CFD, in this case FLACS, and compare it with experimental data previously available.

In the present work, gasoline and diesel fuel experimental pool fires were modeled with FLACS-Fire v10.5 code. Simulations considered different pool fire experiments with diameters ranging from 1.5 to 4 meters. In addition, simulations were run with the Eddy Dissipation Concept (EDC) as combustion model; with the κ-ε model as turbulence model; and with the Discrete Transfer Model (DTM) as the radiation model. The predicted results of temperature's evolution at different heights, burning rate, and thermal radiation were compared with experimental measurements.

The results for gasoline and diesel pool fires indicate that FLACS-Fire v10.5 is able to model pool fires. Pool model 3 (PM3) was able to run all simulations, and Pool Model 1 (PM1) does not perform well with pool diameters higher than 1.5m. Predicted values of the proposed parameters are in a fair concordance with experimentally obtained values. Temperatures measured at the centerline of the flame are in most cases overestimated.

Burning rates are well approximated with small and large pool fires (0.15 kg/s-0.5kg/s) but largely over predicted in gasoline pool fires of medium size. Thermal radiation is also forecasted with values larger than their experimental counterparts.

Chapter 1, contains a brief introduction to the master thesis. It gives a general understanding of the importance of pool fires in the industry. It also gives a global introduction to Computational Fluid Dynamics (CFD), and its relevancy in the study of accidents, especially in the case of pool fires.

Chapter 2, consists of a theoretical background of fire phenomena and the combustion process, with a special focus on pool fires. First, a brief and simple explanation of the combustion process is given. Then, an introduction to heat transfer is provided, in order to show the essentials of how thermal energy is transferred and how it affects pool fires. Finally, an introduction to pool fires characteristics and their mechanisms is given, with an emphasis on the zones composing the fire as well as its main features.

Chapter 3, mainly covers the existing work concerning the ongoing topic. It covers authors who have worked with pool fires, especially in the validation of FLACS-Fire; as well as others who gather experimental data.

Chapter 4, comprises the crucial elements in fire modeling using FLACS-Fire v10.5. Principally, it contains the submodels FLACS uses for: fluid flow, turbulence, radiation, combustion, soot formation, and pool modeling. This chapter shows a theoretical understanding and the basis from which the simulations are later performed.

Chapter 5, is constituted by a detailed explanation of the experimental data used in the present thesis. Instrumentation used in the experiments is thoroughly analyzed, as well as the fuels used and the experiments performed.

Chapter 6, includes the simulations performed in the present thesis, as well as, a comprehensive analysis of the data obtained. Initial simulations studying various variables such as grid, radiation model and pool model are studied. Final simulations are also evaluated, which especial emphasis on the discrepancies with the experimental data.

2 Resumen

Los incendios han sido objeto de estudio a lo largo de las últimas décadas debido a su gran poder destructivo. La naturaleza peligrosa y la capacidad de infligir daño a las propiedades, medioambiente y a las personas, han generado una necesidad de comprender el funcionamiento de los incendios en todos sus aspectos. Actualmente, los esfuerzos se centran en estimar las características del fuego y sus efectos principales, para así, poder diseñar certeramente planes de emergencia y medidas de prevención adecuadas.

Debido a las necesidades mencionadas anteriormente, los incendios han sido estudiados y analizados principalmente desde un punto de vista experimental. Sin embargo, obtener datos experimentales es arduo y es extremadamente costoso por la cantidad de recursos necesarios. Adicionalmente, los modelos a pequeña escala, que generalmente son más asequibles, no son extrapolables a los modelos completos. Se han generado modelos semi empíricos, pero estos solo se pueden aplicar en casos simplificados y no son capaces de modelar completamente un sistema real. La obtención de modelados completos se ha realizado en los últimos años mediante el uso de códigos CFD (Computational Fluid Dynamics). Los CFD se han utilizado recientemente estudiar el desarrollo de incendios completos en gran variedad de condiciones de una manera más sencilla y menos costosa. No obstante, los modelos CFD requieren grandes esfuerzos en su validación antes de poder ser utilizados en todos los casos deseados.

El objetivo principal del presente Trabajo Final de Máster es el analizar el funcionamiento, y si es posible, validar el código CFD, FLACS-Fire v10.5 (Flame Accelerator Simulator) en el caso de incendios de balsa. FLACS es un programa CFD que resuelve, para fluidos compresibles, las ecuaciones de conservación de masa, momento, entalpía y fracción mezclada utilizando un método de volúmenes finitos. El modelado de un fuego necesita incluir, entre otros, procesos que engloban submodelos de: turbulencia, combustión, radiación térmica y generación de hollín. Tiene gran importancia durante el desarrollo del modelado del fuego, el validar dichos modelos con valores experimentales; para así conseguir discernir si las simulaciones realizadas son válidas o no, y determinar el error inherente de un modelo matemático implementado en relación con la realidad. Este proceso consiste en realizar réplicas de un montaje experimental, pero en el CFD, en este caso FLACS, y comparar los resultados con los datos experimentales previamente obtenidos.

En el presente trabajo se han simulado con FLACS-Fire v10.5 incendios de balsa de gasolina y diésel. Las simulaciones han considerado diferentes experimentos de incendios de balsa con diámetros desde 1.5 hasta 4 metros. Además, cabe resaltar que las simulaciones se han realizado utilizando el Eddy Dissipation Concept (EDC) como modelo de combustión; con un modelo κ-ε para tratar la turbulencia y Discrete Transfer Method (DTM) como modelo para la radiación térmica. Los resultados obtenidos son

de: la evolución de la temperatura a diferentes alturas, la tasa de combustible quemado y la radiación térmica se han comparado con las medidas experimentales en las mismas condiciones.

Los resultados de los incendios en balsa de gasolina y diesel, indican que FLACS-Fire v10.5 es capaz de modelar incendios de balsa. Pool Model 3 (PM3) es capaz de correr todas las simulaciones, en cambio el Pool Model 1 (PM1) no es capaz de desarrollarse con normalidad en balsas con diámetros mayores a 1.5m. Los valores simulados de los parámetros propuestos concuerdan con los valores obtenidos experimentalmente. Las temperaturas medidas en el centro de la llama se sobreestiman en gran parte de los casos. Las tasas de quemado (burning rate) se aproximan a los valores experimentales para incendios de pequeño y gran tamaño (0.15 kg/s-0.5 kg/s) pero se obtienen valores mayores a los experimentales en los casos de incendios de tamaño medio. Las radiaciones térmicas que se han obtenido son sustancialmente superiores a sus homólogos experimentales.

El capítulo 1, contiene una breve introducción al presente trabajo. Se trata de aportar un conocimiento general de la importancia de los incendios de balsa en la industria. También es una introducción global a los Computational Fluid Dynamics (CFD), y su relevancia en el estudio de accidentes, especialmente en el caso de incendios de balsa.

El capítulo 2 consiste en el trasfondo teórico de los fundamentos del proceso de combustión, enfocándolo hacia los incendios de balsa. En primer lugar, es necesario dar una breve explicación sobre el proceso de combustión. Después, se presenta una introducción a los fenómenos de transferencia de calor, mostrándose lo esencial de como se la energía es transferida y su afecto en los incendios de balsa. Por último, se tratarán las características principales de los incendios en balsa, enfatizando principalmente en cómo se componen y distribuyen.

El capítulo 3 analiza el trabajo ya existente a cerca del tema principal de este estudio. Se han tratado trabajos de autores que han trabajado con incendios en balsas, especialmente si estos están enfocados en la validación de FLACS-Fire.

El capítulo 4 trata los elementos cruciales del modelado de fuegos utilizando FLACS-Fire v10.5. Principalmente, este capítulo contiene los submodelos que FLACS utiliza para: el flujo de fluidos, turbulencia, radiación, combustión, formación de hollín y modelado de las balsas.

El capítulo 5 está constituido por una exposición detallada de la obtención de datos experimentales utilizados en el presente trabajo. La instrumentación utilizada en los experimentos se estudia pormenorizadamente, así como, los combustibles y los experimentos realizados.

El capítulo 6 incluye las simulaciones realizadas en este trabajo, además se han analizado exhaustivamente los datos obtenidos. En primer lugar se analizarán unas simulaciones iniciales que estudian variables como la malla, el modelo de radiación y el modelo de balsas o el modelo de formación de hollín. Se han evaluado también las simulaciones finales, con especial énfasis en las discrepancias con los datos experimentales.

3 Resum

Els incendis han sigut objecte d'estudi al llarg de les darreres dècades degut al seu gran poder destructiu. La naturalesa perillosa i la capacitat d'infringir mal a les propietats, mediambient i a les persones, han generat una necessitat de comprendre el funcionament dels incendis en tots els seus aspectes. Actualment, els esforços es centren en estimar les característiques del foc i els seus efectes principals, per així, poder dissenyar encertadament plans d'emergència i mesures de prevenció adequades.

Degut a les necessitats mencionades anteriorment, els incendis han sigut estudiats i analitzats principalment des d'un punt de vista experimental. Malgrat això, obtindre dades experimentals és feixuc i és extremadament costós per a la quantitat de recursos necessaris. Adicionalment, els models a petita escala, que generalment són més assequibles, no són extrapolables als models complets. S'han generat models semi empírics, però aquests només es poden aplicar en casos simplificats i no són capaços de modelar completament un sistema real. L'obtenció de modelats complets s'han realizat en els darrers anys mitjançant l'ús de codis CFD (Computational Fluid Dynamics). Els CFD s'han utilitzat recentment per estudiar el desenvolupament d'incendis complets en gran varietat de condicions d'una manera més senzilla i menys costosa. No obstant, els models CDF requereixen grans esforços en la seva validació abans de poder ser utilitzats en tots els casos desitjats.

L'objectiu principal del present Treball Final de Máster és el d'analitzar el funcionament, i si és posible, el de validar el codi CFD, FLACS-Fire v10.5 (Flame Accelerator Simulator) en el cas d'incendis de bassa. FLACS és un programa CFD que resol, per a fluids compressibles, les equacions de conservació de massa, moment, entalpia i fracció mesclada utilitzant un mètode de volums finits. El modelat d'un foc necessita incloure, entre d'altres, processos que engloben submodels de: turbulència, combustió, radiació tèrmica i generació de sutge. Té una gran importància durant el desenvolupament del modelat del foc, el validar aquests models amb valors experimentals; per així aconseguir discernir si les simulacions realitzades són vàlides o no, i determinar l'error inherent d'un model matemàtic implementat en relació amb la realitat. Aquest procés consisteix en realizar rèpliques d'un muntatge experimental, però en el CFD, en aquest cas FLACS, i comparar els resultats amb les dades experimentals prèviament obtingudes.

En el present treball s'han simulat amb FLACS-Fire v10.5 incendis de bassa de gasolina i dièsel. Les simulacions han considerat diferents experiments d'incendis de bassa amb diàmetres des de 1.5 fins a 4 metres. A més, cal ressaltar que les simulacions s'han realitzat utilitzant el Eddy Dissipation Concept (EDC) com a model de combustió; amb un model κ-ε per a tractar la turbulència i Discrete Transfer Method (DTM) com a model per a la radiació tèrmica. Els resultats són de: l'evolució de la temperatura a

diferents alçades, la taxa de combustible cremat i la radiació tèrmica s'han comparat amb les mesures experimentals a les mateixes condicions.

Els resultats dels incendis en bassa de gasolina i dièsel, indiquen que FLACS-FIRE v1.05 és capaç de modelar incendis de bassa. Pool model 3 (PM3) és capaç de córrer totes les simulacions, en canvi el Pool Model 1 (PM1) no és capaç de desenvolupar-se amb normalitat en basses amb diàmetres majors a 1.5 m. Els valors simulats dels paràmetres proposats concorden amb els valors obtinguts experimentalment. Les temperaturas mesurades en el centre de la flama es sobreestimen en gran part dels casos. Les taxes de cremat (burning rate) s'aproximen als valors experimentals per a incendis de petita i gran mida (0.15 kg/s-0.5 kg/s) però s'obtenen valors majors als experimentals en els casos d'incendis de mida mitjana. Les radiacions tèrmiques que s'han obtingut són substancialment superiors als seus homòlegs experimentals.

El capítol 1, conté una breu introducció al present treball. Es tracta d'aportar un coneixement general de la importància dels incendis de bassa a la indústria. També és una introducció global als Computational Fluid Dynamics (CFD), i la seva rellevància en l'estudi d'accidents, especialment en el cas d'incendis de bassa.

El capítol 2 consisteix en el rerefons teòric dels fonaments del procés de combustió, enfocant-lo cap als incendis de bassa. En primer lloc, és necessari donar una breu explicació sobre el procés de combustió. Després, es presenta una introducció als fenòmens de transferència de calor, monstrant-ne l'essencial de com l'energia és transferida i el seu efecte als incendis de bassa. Per últim, es tractaran les característiques principals dels incendis de bassa, emfatitzant principalment en com es componen i distribueixen.

El capítol 3 analitza el treball ja existent sobre el tema principal d'aquest estudi. S'han tractat treballs d'autors que han treballat amb incendis en basses, especialment si aquests estan enfocats a la validació de FLACS-Fire.

El capítol 4 tracta els elements crucials del modelat de focs utilitzant FLACS-Fire v10.5. Principalment, aquest capítol conté els submodels que FLACS utilitza per: el flux de fluids, turbulència, radiació, combustió, formació de sutge i modelat de les basses.

El capítol 5 està constituït per una exposició detallada de l'obtenció de dades experimentals utilitzades en el present treball. La instrumentació utilitzada en els experiments s'estudia detalladament, així com, els combustibles i els experiments realitzats.

El capítol 6 inclou les simulacions realitzades en aquest treball, a més s'han analitzat exhaustivament les dades obtingudes. En primer lloc s'analitzaran unes simulacions inicials que estudien variables com la malla, el model de radiació i el model de basses o el model de formació de sutge. S'han evaluat també les simulacions finals, amb especial èmfasi a les discrepàncies amb les dades experimentals.

4 Nomenclature

Symbol	Description
Ø	Equivalence ratio
N	Number of moles
Q	Total thermal heat
K	Thermal conductivity
A	Exposed area
ΔT	Temperature increment
L	Thickness
H	Pool height
h	Height of atmospheric mixing layer
h	Convective heat transfer coefficient
E	Emissivity
E	Emitted radiation
Σ	Steffan-Boltzmann constant
U	Velocity
M	Dynamic viscosity
Γ, D	Diffusion coefficient
Φ	Scalar variable
β	Configuration factor
β_v	Volume porosity
k_f	Specific reaction rate constant
X	Fractions of reacting fine structures
T	Turbulent time scale
ε	Dissipation of turbulent kinetic energy
σ_κ, σ_ε	Prandtl number in *k* and ε model
Re	Reynolds number
P	Pressure
T	Time
T	Temperature
X	Distance
H	Specific enthalpy
G	Gravity acceleration
F	Force
F_g	Specific gravity force
F_τ	Specific friction force
$\sigma_{i,j}$	Stress tensor
D, d	Diameter
K	Turbulence kinetic energy
ΔH_c	Heat of combustion
u*	Fine velocity scale
L	Length

c_p	Heat capacity at constant pressure
S	Source term
X	Mol fraction
Y	Mass fraction
Z	Element mass fraction
R	Universal gas constant
L_V	Evaporation heat of fuel
H_F	Flame height
S	Burning velocity
E_a	Activation energy

4.1.1 Subscripts

St	Standard conditions
i, j	Species index, spatial index
T	Turbulence
Rad	Radiation
Conv	Convection
Cond	Conduction
F	Fuel
L	Laminar
L	Losses
Ox	Oxygen
k	Kinetic energy
ε	Dissipation of kinetic energy
w	Wall conditions
v	Volume
f	Flow
D	Drag

4.1.2 Superscripts

”	Fluctuating value
*	Fine structure state
-	Mean value
o	Surrounding fluid state
~	Mass weighted
′	Root mean square
+	Dimentionless

5 Contents

1 Introduction

Over this introductory chapter, it will be explained what the main objective of the thesis is, historical data of pool fires will also be treated, as well as, a brief introduction to CFD simulation.

1.1 Objective

The objective of this work is to perform a validation of FLACS-Fire v10.5 to simulate large pool fires. The validation of a model consists in a comparison process between experimental and simulated data and using the disparities to ameliorate the already existing model.

In the present thesis, the modeling of turbulent diffusion pool fires was used to validate FLACS-Fire code. Simulations of gasoline and diesel pool fires were based on experimental work, and key parameters such as temperature at various heights, thermal radiation, and burning rate were predicted. Forecasted values were compared with their experimental counterparts and evaluated accordingly, to determine the accuracy of the proposed FLACS model.

In order to obtain a suitable model for the pool fires, preliminary simulations were performed. These were intended to find out the influences of the most important simulation tool parameters: the grid size, the radiation model, the emissivity, the soot model, and the pool model.

1.2 Historical data of pool fires

Accidents involving fires are among the most common major accidents in process plants, transportation, and loading/unloading of hazardous materials. It is often difficult to determine the frequency of each type of accident because the information is incomplete and in many cases many events happen simultaneously. Regardless of the source, most concur that fires are one of the most, if not the most, frequent accident in the industry. Casal et al. [19] describes how approximately 47% of all major accidents involved a fire, 40% involved an explosion and in 13 % there was a gas cloud. Regarding the type of fire, these authors found that the most recurrent event was pool, followed by flash fire and, with a much smaller frequency, jet fire; with frequencies of 66%, 29%, and 5% respectively.

The damaged area caused by pool fire accidents is much smaller than those related to other major accidents such as explosions or toxic clouds. The area affected of the fire engulfment or the thermal radiation is rather small. Nevertheless, this area generally contains equipment that is susceptible to thermal change and it can be severely damaged. Nearby equipment affected may increase the accident via the domino effect.

Koteswara et al. [18] collected and analyzed data from accidents occurred in the chemical process industry between 1998 and 2015 and found the following percentages for the cause of accidents:

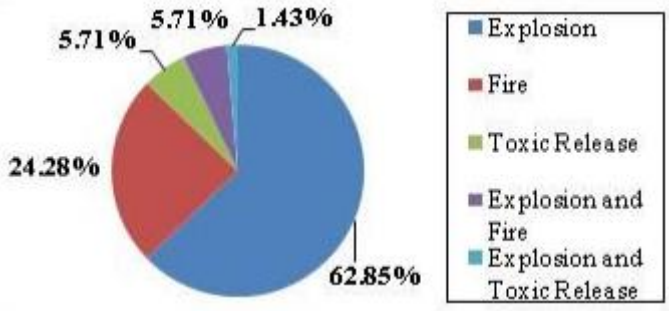

Figure 1: Frequencies of accident occurrence (source: Koteswara et al., 2016 [18])

Regarding the nature of the chemicals involved in the accident, the same authors established the following proportions:

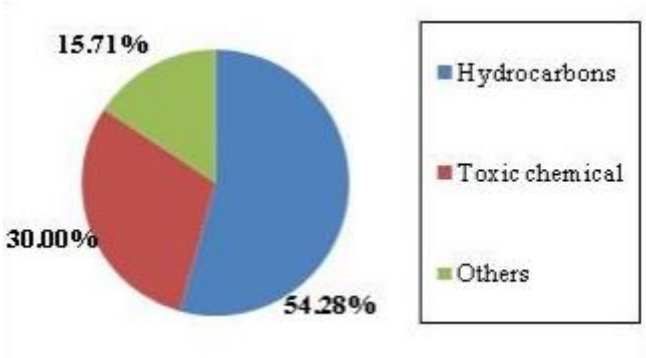

Figure 2: Major chemical causes of process accidents (source: Koteswara et al., 2016 [18])

All in all, it is interesting to study hydrocarbon pool fires since it is one of the most common accident in industrial facilities among with explosions. Both accidents are occurring using hydrocarbons due to their flammability and explosive nature. It is also interesting to note that explosions and fires are intimately related, because an explosion can cause a fire and vice-versa. A fire can increase drastically the temperature of adjacent vessels, this can possibly increase the vaporization of a liquid, and hence the pressure augments too. Pressure increase can end in an explosion, and the other way around, the liberation on energy in an explosion can lead to a fire.

1.3 Introduction to Computer Fluid Dynamics

Almost all CFD simulators are based on the Navier–Stokes (NS) equations, which define any single-phase viscous fluid flow. NS equations describe turbulent flow and since most realistic fire scenarios are turbulent, it is one of the most important models in the whole system. In contrast to laminar flow, turbulent flow with fluctuations of

velocity, leads to fluctuation in density, temperature and mixture composition. For this reason, numerical solution of the NS equations for turbulent flow is extremely difficult. Turbulence flow can be implemented in the NS equations and solved with Direct Numerical Simulations (DNS), but this will require prohibitive amount of computational time. The main reason for this time-consume is that the small scales in turbulent flows require far more grid points than the analogous laminar flow. In practical CFD modeling of turbulent flow time-average equations such as Reynolds average Navier Stokes (RANS) equations or Large Eddy Simulations (LES) method are used. In contrast to RANS equations, which do not solve any scale of the turbulence, the LES method resolves the largest scales (eddies). Both methods require additional turbulence models for the unsolved eddies to close the system of equations. Among different turbulence models the two-equation model called *k-ε* model is one of the most popular and it is the one implemented in FLACS. Two extra transport equations represent the turbulent properties of the flow. κ represents the turbulent kinetic energy and ε represent the dissipation rate of turbulent kinetic energy. [10].

2 Background

This chapter covers the fundamentals of fire dynamics and the combustion process. Generalities about the combustion of a fuel, heat transfer and pool fires; all of them are the foundation of fire behavior as well as show what is happening in a process involving fire.

2.1 Combustion

There are many different definitions of what a fire is, depending on the source that is consulted:

> *NFPA 921: *"A rapid oxidation process, which is a chemical reaction resulting in the evolution of light and heat in varying intensities"*. [15]
>
> *Webster's Dictionary: *"A fire is an exothermic chemical reaction that emits heat and light"*. [15]
>
> *FARLEX: *"Rapid, persistent chemical change that releases heat and light and is accompanied by flame, especially the exothermic oxidation of a combustible substance"*. [15]

A fire can only exist if it can continuously burning, and this happen only under certain conditions. These conditions are usually summarized in a fire square or tetrahedron as it can be seen in Figure 3. A fire can only start if a flammable fuel is mixed with a sufficient quantity of an oxidizer, commonly oxygen, and is exposed to a sufficient source of energy to allow ignition. Energy may come in different ways like a sparking source or even temperature itself can be enough if it reaches a value above the flash point for the fuel-oxygen mixture. This covers three of the four sides of the tetrahedron/square, but it would only ensure the initiation of a fire but not its continuity. In order to achieve continuous burning, a rapid oxidation process must take place that can keep the chain reactions in motion.

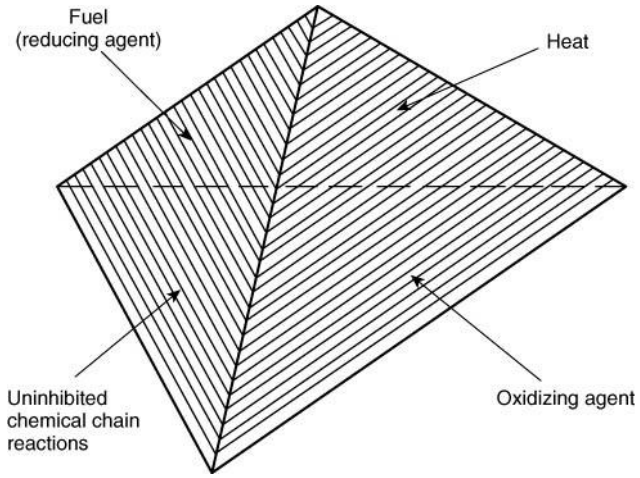

Figure 3: Fire tetrahedron (**Source: the NFPA (National Fire Protection Association) [13]**

The definitions of each of the sides of the tetrahedron according to the NFPA (National Fire Protection Association) [13] are:

> *Fuel*: Any substance that can undergo combustion. It exists in three states of the matter: solids, liquids and gases. Solid and liquids do not burn directly but, instead, combustion occurs in a vaporous area above the surface of the fuel. This region is created by heating the solid or liquid above its ignition temperature in a process known as pyrolysis or evaporation, respectively. Gases do not require pyrolysis to undergo combustion.
>
> *Oxidizing agent*: As it was previously stated, oxygen is the most common oxidizing agent. Air contains approximately 21% oxygen, but the higher the concentration of oxygen the more severely it will burn. There are several other typical oxidizing agents such as nitrates, peroxides, iodine, chlorine, etc.
>
> *Heat*: Initial energy must be provided by an outer source such as a spark or environmental temperature. Heat is produced by an exothermic reaction (a chemical reaction that produces more energy than needed for the reaction to occur, causing the excess energy to be released). Heat transfers from an area of higher temperature to areas of lower energy due to the temperature gradient existent. Energy transfers by three main phenomena: Conduction, convection and radiation. Continuous burning requires rapid oxidation to produce chain reactions.

Combustion takes place when an oxidizing agent reacts with a fuel. The combustion process for hydrocarbons reacting with oxygen will yield CO_2 and H_2O as combustion products. Usually the oxidizer is the oxygen in the air, so it is a mixture of nitrogen and oxygen. Therefore, most real cases ratios of the reactants are seldom stoichiometric. There are two cases that may happen: fuel lean or fuel reach combustion. Fuel lean combustion lacks enough fuel to react with all the oxygen present, this case is usual in open fires where the flow of oxygen is never an issue. On the other hand, fuel rich combustion is the opposite of fuel lean, there is an excess of fuel, thus, not enough

oxygen to combust all the fuel. It is important to point out that in the case that is to be studied, the combustion will always be fuel lean and always with excess of oxygen. Nevertheless, the environmental conditions and magnitude of the experiments makes impossible the perfect and complete combustion in all parts of the flame.

A parameter to describe the proportion of the reactant mixture is the equivalent ratio, this ratio is defined by the following dimensionless parameter:

$$Ø = \frac{n_{fuel}/n_{ox}}{(n_{fuel}/n_{ox})_{st}} \quad [1]$$

Equivalence ratio takes into consideration the actual molar ratio between the fuel and the oxidizer with the stoichiometric ratio. If Ø =1, the equivalence ratio is met and complete combustion occurs; if Ø <1 the mixture is fuel lean and, on the other hand, if Ø >1 the combustion is fuel rich.

The reaction that takes place for complete burning is:

$$C_xH_y + z(O_2 + 3.76N_2) \xrightarrow{yields} aCO_2 + bH_2O + cN_2 + Q$$

This reaction is stoichiometric, there is no fuel nor oxygen left after the reaction is fully developed.

If the case of incomplete burning, the equation would change drastically, especially in the case of incomplete combustion due to lack of oxygen. Combustion with an excess of oxygen will simply have oxygen in the byproducts of the reaction. Combustion lacking oxygen, fuel rich, will yield to products such as CO, H_2, or others depending on the fuel used. [4]

It is especially important to mention that in the case of a real fire, the combustion gases are composed of hundreds of compounds, these compounds affect the overall combustion process. The real reaction process is not implemented in any CFD because of its complexity and unpredictability. Not all species are taken into account, just the major or the more probable ones; this is a limitation that all CFDs share.

2.2 Heat transfer

Fire dynamics require a broad spectrum of physics branches to be applied into the understanding of its particularities. Among these necessary branches of physics, lies heat transfer. Heat transfer is known to happen through conduction, convection and radiation, all these three transfer mechanisms appear during a fire but usually they are relevant in different stages of the fire.

Conduction is the heat transfer through a solid material, going with a gradient from the higher temperature to a lower temperature zone. Fourier's law can calculate provide the energy being transferred:

$$q = \frac{k \cdot A \cdot \Delta T}{L} \quad [2]$$

Where k is the thermal conductivity of the solid material, A is the exposed area through which the thermal conductivity occurs, L is the thickness of the solid, and ΔT is the temperature difference between the hot and the cold side.

This transfer method is most significant in the ignition phase and spread of flame over other combustible solids and it is remarkably important when it comes to fire safety measures such as fire walls, integrity of structures, etc. [16]

Convection is another heat transfer method produced by the movement of a fluid due to being in a higher energy state than its surroundings. Convection happens throughout all stages in a fire, hot air moves spreading the energy produced, but it is most important in the early stages of the fire, when the thermal radiation levels are still too low to be significant. Convection can be free or forced and it changes drastically the fire. A free or natural convection is a self-sustained flow driven by buoyancy forces created due to density differences, and the density differences are caused by temperature gradients in the fluid. Buoyancy forces influences the shape and behavior of the flame. Forced convection occurs when fluid motion is generated by an external source like a pump device and the flow is independent of density differences. Buoyancy forces also exist, but usually they have only a small effect. Convection can be explained with Newton's empirical equation [16]:

$$q = h \cdot A \cdot \Delta T \quad [3]$$

Where h is the convective heat transfer coefficient, A is the exposure area, and ΔT is the temperature difference.

Remarkably, the convective heat transfer coefficient, h, depends on various characteristics of the system, geometry, properties of the fluid, etc. This fact make it arduous to estimate if the system is not controlled because, for example, geometry changes as it burns, properties vary as temperature increases, etc.

Radiation is a heat transfer mechanism involving electromagnetic waves, thus not involving any conducting medium linking the emitter and receiver of energy. Radiation is a type of energy that can be absorbed, transmitted or reflected in a surface in the whole electromagnetic spectrum. Radiation is the most dominant form of heat transfer when the fire is fully developed, especially important in fires with a diameter larger than 0.3 m. Be noted that, radiation does not require a medium and therefore can heat objects

afar from the fire and even produce an auto ignition in other fuels. Radiation can be explained through Stefan Boltzmann's law [16]:

$$E = \varepsilon \cdot \sigma \cdot T^4 \quad [4]$$

Where ε is the emissivity, σ is the Stefan-Boltzmann constant ($5.67 \cdot 10^{-8}$ $W \cdot m^{-2} \cdot K^{-4}$), and E is the emissive power which is the total thermal radiation energy. The black body is a perfect emitter and has an emissivity equal one. In any non-ideal system, there has to be a geometrical relationship between the emitter and the receiver, the so called view factor, then the radiation can be calculated as:

$$E = \varepsilon \cdot \sigma \cdot T^4 \cdot \beta \quad [5]$$

Where β is the view factor, geometrical relationship between emitter and receiver.

There are large differences in the radiative emission characteristics of fires depending on the fuel composition. Large chain hydrocarbons produce high concentrations of soot. In contrast, methanol burns cleanly with no soot. Hydrocarbon pool fires are extremely luminous due to significant concentrations of soot particles, which emit radiation in the whole range of the thermal radiation spectrum. Gas species such as carbon monoxide and hydrocarbon intermediates emit radiation in more discontinuous bands of the spectrum [9].

2.3 Pool fires

Pool fires are the main subject to be discussed in this thesis, therefore this section will cover briefly, what a pool fire is and how it works. A pool fire is defined as a turbulent diffusion flame produced by a horizontal pool of a fuel that is vaporizing at a low rate. In this type of fire, the liquid pool receives heat from the flame via convection and radiation, and exchanges heat with the soil with conduction. Once the fire is in a stationary state, a feedback mechanism is settled which governs the supply of volatile fuel to the flame. Eventually, the fuel vaporization reaches a maximum value limited by the radiative heat transfer from the flame.

Figure 4: Outdoor pool fire, representative of the modeled system (Source: F. Ferrero et al., 2006 [7])

Heat transfer to the substrate might be significant in certain cases, for example in fuel spills over water (the sea, a lake, etc.) or metals. The heat rate that is transferred between the fuel and the soil depends highly on the composition of both. In the case of water at atmospheric temperature, heat loss can be determinant since it can lower the evaporation rate to such small values that the flame can no longer withhold itself. This same scenario can happen with a metallic surface at a lower temperature than the fuel, since the thermal conductivity will have a relatively high value, the temperature drop can make the evaporation rate diminish to critical values.

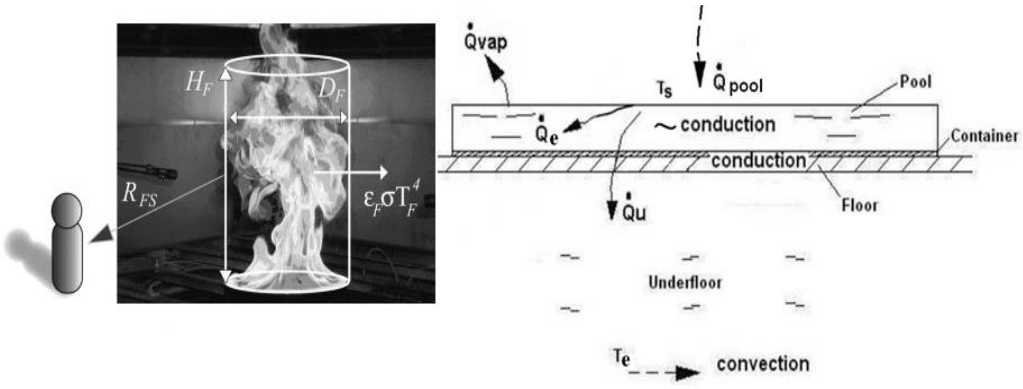

Figure 5: Pool fire heat transfer schematic
(Source:https://www.researchgate.net/figure/273456236_fig3_Figure-3-Pool-fire-heat-transfer-scheme)[24]

Large diameter pool fires, greater than one meter, have a remarkably high soot production.

Hot combustion gases rise, due to density difference, entraining the air around and producing turbulence, which further mixtures the air around the fire, the fuel and the combustion gases. As it has been previously stated, combustion is seldom complete; this incomplete combustion produces, among hundreds of products, soot. Incomplete combustion is what confers its particular orange-yellow color to fires; also soot will act as a gray body absorbing radiation from the fire and afterwards emitting it. Soot forms a black-gray layer of smoke that blocks the radiation from the fire affecting the overall radiation intensity.

Pool fires do not present structured flame geometry, unlike jet fires which do have a structure. Nevertheless, for pool fires with diameters from 0.03 to 0.3 m it can be observed that the flame shows certain flame structuration (usually due to the regime being laminar or in transition from laminar to turbulent) even though it may not be stable in all areas. Therefore, the fact that flames can have a certain geometrical structure depends greatly in the diameter and the flow from the pool. [8]

The structure of a turbulent fire plume in pool fires with diameters greater than 30 cm can be divided into three regions:

- Persistent flame zone: it is the zone immediately above the surface of the fuel; it is a fuel rich region where oxygen has not completely entered. This region represents approximately a 20% of the flame height, it is an area where temperature is relatively low, and it is also rich in intermediate components of the pyrolysis.
- Intermittent flame zone: air entrained by the turbulence penetrates radially to the flame and it is where the pyrolysis products react with the oxygen producing the combustion products and the pertinent intermediates depending on the conditions and the fuel. This zone is where most part of the reaction takes place; therefore it is also where most of the energy is produced. Turbulence in this system creates swirls, which entrain the air generating great vortices that grow larger and ascend until the fuel within extinguishes or the temperature is low enough to keep the oxidation from occurring. The moment a vortex can no longer withhold the reaction, the edge of the visible flame falls to the original height and a new swirl starts to grow a new vortex.
- Smoke plume: This zone has little to no chemical reactions and the temperature drops exponentially as air is entrained to the interior of the smoke.

3 Literature Review

The main objective of this literature search was to find other validations or accurate simulations of FLACS' code to retrieve information about the modeling.

Table 1: Literature review overview

Reference	Main measurements	Simulators FLACS/CFD		Pool fire simulation	Fuel	Pool diameter (m)	Publication date
C. Gutiérre-Montes et al. [12]	Temperature Burning rate Velocity	×	✓	✓	Heptane	0.92, 1.17	2009
N. Pedersen [9]	Temperature Soot fraction Flame height	✓	×	✓	Heptane	0.3, 0.5	2012
L. Skarsbo [10]	Temperature Flame height HRR	✓	✓	✓	Heptane	0.1, 0.15, 0.2, 0.3, 0.6	2006
T. Magnusson et al. [21]	Mass flow Pressure Temperature	×	✓	✓	Tetrapropylene	0.5, 0.71	2012
S. Biao et al [20]	Mass flow HRR Viscosity	×	✓	✓	Liquefied natural gas	3.8, 4.5	2010
P. Middha [22]	Pressure Burning velocity	✓	×	×	Hydrogen	×	2010

After going through the different publications about pool fires, a main conclusion is drawn from the research, FLACS has not been thoroughly validated yet. Only two master thesis were found that validated the software, both with heptane pools. N. Pedersen (2012) [9] performed simulations of heptane pool fires of 0.3 and 0.5m. Conditions for this experiments were of 293K temperature, atmospheric pressure of 1 atm, turbulence intensity of 0.01 for the 0.3 m pool, and 0.1 for the 0.5 m pool; and turbulent length scale of 0.015 and 0.02 m respectively for each pool fire.

L. Skarsbø (2006) [10] simulated the experiments presented by Gutiérrez et al (2009) using two CFDs: FDS and FLACS. Conditions for these experiments were the same as Pedersen (2012) [9], since they are extracted from the same set.

Middha (2010) [22] also validated FLACS but in this case, the validation went towards the dispersion and explosion areas using jets of hydrogen. Even though the simulations are rather useful and test many of the features in the software, they do not validate the Fire module.

On the other hand, there are more than enough simulations and validations of other CFDs, among the most common appears Fire Dynamics Simulator (FDS). Gutiérrez-Montes et al. (2009) [12] performed experiments for heptane pool fires of 0.92 and 1.17

m approximately at various ambient conditions, 13-18ºC and 0-1 m/s wind speed. Magnusson et al (2012) [21] tested tetrapropylene pool fires of 0.5 and 0.71 m using FDS. Simulations were performed using varying parameters such as: air supply position, air flow, and burning rates. Biao et al (2010) performed simulations using LNG (liquefied natural gas) pool fires with the commercial code FLUENT v13.0. Initial conditions of these experiments were very broad with varying compositions of the LNG, pool diameter, and also with wind velocities from 2.7 to 10.1 m/s depending on the experiment.

Regarding results, Pedersen (2012) [9] stated that temperatures are over predicted compared to the experimental values. Temperatures simulated are strongly influenced by the radiation model used. L. Skarsbø (2006) [10] on the other hand, found out that both temperature and smoke velocity are well predicted using the 6-Flux radiation model above the fire, but show deviation around the fire.

4 FLACS-Fire

This section covers the models that are implemented in FLACS-Fire, making an overview of the theoretical foundation for physical and chemical models. Among all the models that are needed to obtain a valid simulation of a fire, the most important are: turbulence model, radiation model, combustion model, soot formation models, and pool models.

4.1 Fluid flow and Turbulence

Accidental fires are practically all inherently dependent on fluid flow, therefore it is necessary to implement in the system a model for the fluid flow that can describe it perfectly. Governing equations for fluid flow include equations for: momentum, enthalpy transport, mass fraction transport, mixture fraction, turbulent kinetic energy, dissipation rate of turbulent kinetic energy, effective viscosity, and stress tensor.

A general equation for the momentum:

$$\frac{\partial}{\partial t}(\beta_v \rho u_i) + \frac{\partial}{\partial x_j}(\beta_j \rho u_i u_j) = -\beta_v \frac{\partial p}{\partial x_i} + \frac{\partial}{\partial x_j}(\beta_j \sigma_{ij}) + F_{o,i} + \beta_v F_{w,i} + \beta_v(\rho - \rho_o) g_i \quad [6]$$

The transport equation for turbulent kinetic energy is described:

$$\frac{\partial}{\partial t}(\beta_v \rho k) + \frac{\partial}{\partial x_j}(\beta_j \rho u_j k) = \frac{\partial}{\partial x_j}\left(\beta_j \frac{\mu_{eff}}{\sigma_k}\frac{\partial k}{\partial x_j}\right) + \beta_v P_k - \beta_v \rho \varepsilon \quad [7]$$

The transport equation for the dissipation rate of turbulent kinetic energy:

$$\frac{\partial}{\partial t}(\beta_v \rho \varepsilon) + \frac{\partial}{\partial x_j}(\beta_j \rho u_j \varepsilon) = \frac{\partial}{\partial x_j}\left(\beta_j \frac{\mu_{eff}}{\sigma_\varepsilon}\frac{\partial \varepsilon}{\partial x_j}\right) + \beta_v P_\varepsilon - C_{2\varepsilon}\beta_v \rho \frac{\varepsilon^2}{k} \quad [8]$$

The stress tensor in the above equation is given by:

$$\sigma_{ij} = \mu_{eff}\left(\frac{\partial u_i}{\partial x_j} + \frac{\partial u_j}{\partial x_i}\right) - \frac{2}{3}\delta_{ij}\left(\rho k + \mu_{eff}\frac{\partial u_k}{\partial x_k}\right) \quad [9]$$

Remarkably, realistic pool fires are usually turbulent, therefore turbulence is a crucial parameter to be taken into account.

4.2 Turbulence

FLACS has implemented a two-equation model named κ-ε model. This model is an eddy viscosity model that proposes to solve one equation for the turbulent kinetic energy and another for the dissipation of turbulent kinetic energy; all this, following Boussinesq eddy viscosity assumption, which leads to a Reynolds stress tensor:

$$-\rho\widetilde{u_i'' u_j''} = \mu_{eff}\left(\frac{\delta u_i}{\delta x_j} + \frac{\delta u_j}{\delta x_i}\right) - \rho\frac{2}{3}k\delta_{ij} \quad [10]$$

Additionally, FLACS provides a set of turbulent Prandtl-Schmidt numbers, which compare the diffusion of a desired variable to the dynamic viscosity.

$$\sigma_h = 0.7 \quad \sigma_{fuel} = 0.7 \quad \sigma_\xi = 0.7 \quad \sigma_\kappa = 1.0 \quad \sigma_\varepsilon = 1.3 \quad \sigma_b = 0.9$$

4.3 Radiation

Thermal radiation is one of the most important factors and a key component in the overall heat transfer in burning systems. Thus, to perform a CFD simulation, an accurate modeling of the radiation generated is required.

During a fire, energy is transferred from the high temperature areas to the lower temperature ones, via radiation and convection, this heat transfer is essentially energy loss that has to be represented in the general energy conservation equation. A fire is very well modeled using the equation for energy conservation for compressible fluids:

$$\rho C_v \frac{DT}{D_t} = \rho C_v \left(\frac{\partial T}{\partial t} + v \cdot \nabla T\right) = \nabla \cdot (k \nabla T) - \nabla \cdot q_R - p \nabla \cdot v + \mu\varphi + Q''' \qquad [11]$$

Radiation intensity depends vastly on the gas temperature as well as on the composition of the fuel. Radiation can be a very complex phenomena depending on the system, which for the purpose of this thesis is an absorbing, emitting and scattering medium; for which the governing equation is the Radiative Transfer Equation (RTE):

$$\mu \frac{dI(\tau, \mu, \varphi)}{d_\tau} = -I(\tau, \mu, \varphi) + (1 - \omega) I_B[T] + \frac{\omega}{4\pi} \int_{\mu'=-1}^{1} \int_{\varphi'=0}^{2\pi} I(\tau, \mu, \varphi) \varphi(\mu', \varphi'; \mu, \varphi) d\mu' d\varphi' \qquad [12]$$

This transfer equation is of integro-differential nature, this mathematical complexity increases the computational needs; also there are several different methods to solve said equation, each of this methods uses a specific model to obtain a solution. Several of these models have been compared:

No	Requirements	MCM	DTM	DOM, FVM, DDOM	6-Flux
1	**Accuracy**	Very Good	Very Good	Very Good	Not accurate
2	**Speed of Computation**	Very Slow	Fast	Fast	Very Fast
3	**Treating Complex Geometries**	Very Good	Very Good	Poor	Good
4	**Treating Entire Range of Optical Thickness**	Very Good	Very Good	Very Good	Poor
5	**Parallelization**	Easy	Easy	Difficult	Difficult
6	**Treating Spectral dependence**	Very Good	Very Good	Very Good	Very Good
7	**Treating Non uniform Radiative properties**	Very Good	Very Good	Very Good	Very Good
8	**Treating Anisotropic Scattering**	Very Good	No	Very Good	No
9	**Ability to handle conjugate problems**	Poor	Very Good	Very Good	Poor

Figure 6: Comparison of the degree of detail among radiation models (Source: GexCon. FLACS v10.4 User's Manual, 2015 [1])

FLACS incorporates two radiation models, DTM and 6-Flux, both have been tested and used for various simulations. However, the lack of accuracy in the 6-Flux model makes it a very poor choice for a system that requires a high degree of accuracy or if it is composed of transparent gases since this model does not contemplate the absorbed radiant energy [1].

4.3.1 Discrete transfer radiation model

The discrete transfer method (DTM) is one of the commonly used problems where the medium is a participating agent of the system. DTM successfully combines advantages from other methods such as the Monte Carlo, flux and zonal methods.

DTM solves the RTE for imaginary rays that connect boundaries or solid surfaces in the computational domain. Rays are fired from solid surface elements into a finite amount of solid angles covering the domain; the main simplification assumed by DTM is that the intensity through a solid angle is approximated by a single ray. Therefore, DTM solves the RTE for each ray from one solid boundary to another solid in the geometry and it can calculate the radiation intensity distribution in an arbitrary shaped, three dimensional complex geometry.

The input parameters that characterize the medium (gas temperature and absorption coefficient of the medium, temperature and emissivity of walls, number of rays and directions) are needed for the radiative transfer calculations.

The primary advantages of the DTM are:

- Numerically exact and geometrically flexible.

- It is used to solve conjugate heat transfer problems.
- Ideal for implementing on parallel computer architectures.
- Accurate for a wide range of optical thicknesses.

The main limitation of the DTM is the fact that it depends largely on the number of rays used to simulate. Large number of rays are very CPU-intensive requiring either high performance computers or extensive amounts of time. [1]

4.3.2 Six Flux model

The Six-flux model solves the RTE by approximation of the equation to the six first order differential equations, which are obtained by discretization of the angle so that the effect of the radiation is accounted for by the positive and negative radiation fluxes in each of the coordinates. Afterwards, these six differential equations can be transformed into three second order ordinary differential equations by using the composite-flux definitions.

Although the Six-flux model has the attractive appeal of being simple and computationally fast; it has severe limitations that affect the results of the simulation, including:

- In case of transparent gases, radiation passes from one surface to another without affecting the gas. The Six-flux model will not yield very accurate results, since its transmission occurs in coordinate directions only, neglecting the oblique effects.
- Only scattering arises between the radiation fluxes in the different coordinate directions.
- The model is not readily extended to coordinate systems which are neither Cartesian nor cylindrical-polar. [1]

4.4 Combustion

One of the crucial phenomenon of this thesis is combustion, therefore it is of upmost importance to fully understand how FLACS-Fire approaches this issue. FLACS has implemented the Eddy Dissipation Concept (EDC). This model stablishes the interactions between chemistry and turbulence. This section will also thoroughly treat how FLACS-Fire models flames and the burning velocity. Flame model used is a diffusion flame model since the case studied is in a non-premixed state and it is regulated by the diffusion rate.

4.4.1 Flame model

This case scenario treats diffusion flames. Diffusion coefficient is calculated from the transport equation:

$$D = \frac{\mu_{eff}}{\sigma_{fuel}} \qquad [13]$$

In industrial applications, the reaction zone in a premixed flame is thin compared to practical grid resolutions. It is therefore necessary to model the flame. In FLACs, the flame zone is thickened by increasing the diffusion with a factor β and reducing the reaction rate with a factor $1/\beta$. Hence, the flame model in FLACS-Fire is called the β-model

It is possible to define a dimensionless reaction rate, named W. In the β-model, the diffusion coefficient D, and the dimensionless reaction rate W are readjusted:

$$W^* = \frac{W}{\beta} = W\frac{l_{LT}}{\Delta_g} \quad [15]$$

$$D^* = D\beta = D\frac{\Delta_g}{l_{LT}} \quad [16]$$

If an eigenvalue analysis of the burning velocity is applied, the following relationship between D and W is obtained for a quenching limit of the progress variable χ_q=0.05:

$$WD = 1.37S_u^2 = W^*D^* \quad [17]$$

The progress variable is an indicator of how much of the potential fuel has burnt already:

$$\chi = \frac{Y_{fuel}}{Y_{fuel}^0 + \zeta\left(Y_{fuel}^1 - Y_{fuel}^0\right)} \quad [18]$$

D^* and W^* depend on the grid size and the burning velocity, hence:

$$W^* = c_{1\beta}\frac{S_u}{\Delta \mathrm{g}} \quad [19]$$

$$D^* = c_{2\beta}S_u\Delta_{\mathrm{g}} \quad [20]$$

Finally, the reaction rate of the fuel is modeled by the expression ahead:

$$R_{fuel} = -W^*\rho\left[\min\left(\delta_H(\chi - \chi_q), \chi, 9 - 9\chi\right)\right] \quad [21]$$

having to take into account that δ_H is the Heaviside step function. [1]

4.4.2 Burning velocity model

Burning velocity is highly dependent on the conditions in which the reaction is happening. There are two burning velocity states: laminar and turbulent.

The full burning process and how it evolves and develops starts as laminar when a fuel cloud is ignited with a weak ignition source and it has to be under quiescent conditions. In this case, the flame front is smooth, and the propagation is only ruled by thermal and/or molecular diffusion. After the initial stable moments, instabilities may appear coming from different possible sources such as ignition, flow dynamics, Rayleigh-

Taylor instabilities, etc. These instabilities will develop wrinkling of the flame surface and the speed increases to a quasi-laminar state. Developing the flame fully, always depending on the flow conditions, will eventually reach a turbulent burning regime.

Laminar burning velocities depend on the type of fuel, the fuel-air mixture and the pressure under which the system is held. Burning velocities at different equivalence ratios for different fuels are tabulated. The laminar burning velocity of a mixture of fuels has to be estimated by a volume-weighted average. Finally, the pressure dependency on the velocity can be adjusted as follows:

$$S_L = S_L^0 \left(\frac{P}{P_0}\right)^{\gamma P} \quad [22]$$

γ is a parameter dependent on the nature of the fuel. The intermediate state of a quasi-laminar regime can be parametrized by the equation:

$$S_{QL} = S_L(1 + \chi \left[\min((\frac{R^{0.5}}{3}),1)\right] \quad [23]$$

The correlation for the turbulent burning velocity is a simplification of a general expression presented as:

$$\frac{S_T}{S_L} = 0.875K^{-0.392}\frac{u'}{S_L'} \quad [24]$$

In which the K stands for the Karlovitz stretch factor which can be calculated as:

$$K = 0.157\left(\frac{u'}{S_L}\right)^2 Re_T^{-0.5} \quad [25]$$

Merging all equations into one and rearranging:

$$S_T = 1.81{u'}^{0.412}\tilde{l}_I^{0.196}S_L^{0.784}\mu^{-0.196} \quad [26]$$

[1]

4.4.3 Eddy Dissipation Concept model

Most events involving a fire are in non-premixed conditions, which leads to diffusion flames, a combustion process where fuel and oxidant are combined via diffusion. Combustion rates are controlled by the mixing of fuel and air, this situation makes optimal the use of a Mixed Is Burnt (MIB) combustion model. Currently, FLACS-Fire utilizes an Eddy Dissipation Concept (EDC) for the turbulence-chemistry interaction. Advantages of this model are that it can be either fast or heavily detailed chemistry-wise, and extinction can be modeled. The transport equation for the fuel mass fraction is:

$$\frac{\delta\bar{\rho}\widetilde{Y}_{fuel}}{\delta t}+\frac{\delta\bar{\rho}\widetilde{Y}_{fuel}\tilde{u}_j}{\delta x_j}=\frac{\delta}{\delta x_j}\left(\bar{\rho}D\frac{\widetilde{Y}_{fuel}}{\delta x_j}\right)-\frac{\delta}{\delta x_j}\left(\bar{\rho}\widetilde{Y''_{fuel}u''_j}\right)+\bar{\rho}\tilde{\omega}_{fuel} \qquad [27]$$

From this general model, the EDC connects the turbulent flow and the chemical reactions. The main equations of this model are presented:

$$\tilde{\omega}_{fuel}=-\frac{\dot{m}\chi}{1-\Upsilon^*\chi}\tilde{Y}_{min} \qquad [28]$$

$$\tilde{Y}_{min}=\min\left(\tilde{Y}_{fuel},\frac{1}{r}\tilde{Y}_{ox}\right) \qquad [29]$$

EDC model works under the premise that the chemical reaction can only occur in the fine structures. Dissipation of turbulent energy is largest in fine structures. Fine structures are then assumed as a homogeneous reactor at constant pressure. Following this assumption, the reaction rate of species per time and volume can be calculated from a mass balance of this supposedly homogeneous reactor. The expression for the mass balance within the reacting system is:

$$-\bar{R}_i=\bar{\rho}\dot{m}\chi(Y_i^0-Y_i^*) \qquad [30]$$

It is often also assumed that the reaction occurs infinitely fast, and then the mean chemical reaction rate can be written as:

$$-\bar{R}_f=\frac{\bar{\rho}\dot{m}\chi}{1-\Upsilon^*\chi}\tilde{Y}_{min} \qquad [31]$$

EDC can be assimilated to a homogeneous fine structures reactor, which is depicted in the following figure:

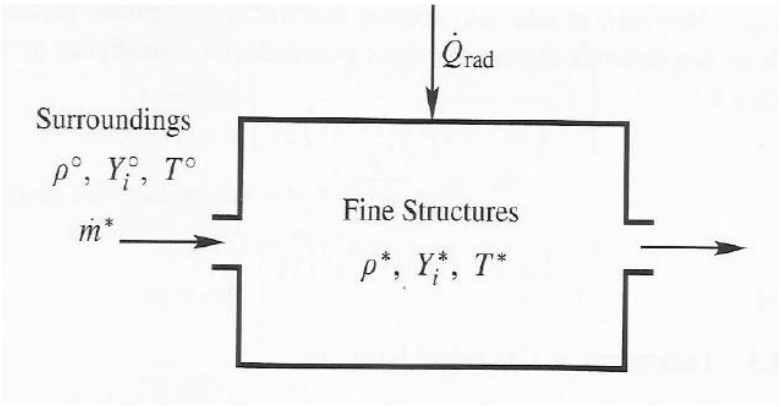

Figure 7: Diagram of the homogeneous reactor of fine structures
(Source: Natalja Pedersen (2012). "Modeling of jet and pool fires and validation of the fire model in the CFD code FLACS."

4.5 Soot

Appropriate prediction of soot formation is an important parameter well-known for its implications in heat transfer especially in the radiation area. Soot is an arduous phenomenon to parametrize; this is because of the lack of knowledge about its formation and growth within the control volume. Heat transfer is affected by soot since it will absorb and emit part of the energy from the flame, this will affect the temperature of the flame (as well as the temperature received by the thermocouples).

There are several models to calculate soot formation, from complex to very simplified models. Regardless of their complexity, none of these can perfectly predict the formation of soot without further adjustments.

FLACS' approach in this matter is by using two different models, the Conversion Factor Model (CFM) and the Formation-Oxidation model (FOX). [1]

4.5.1 Conversion Factor Model (FCM)

The CFM has a fixed amount of the fuel carbon converted directly into soot regardless of equivalence ratio, temperature, time, or any other given variables other than the fuel composition. Common soot yields for the fuels available in FLACS:

Table 2: Typical soot yields for different fuels

Fuel	Soot yield
Methane	0,70%
Ethane	2,0%
Propane	9,0%
Butane	10,0%
Pentane	10,0%
Hexane	10,0%
Heptane	12,0%
Octane	12,0%
Nonane	12,0%
Decane	12,0%
Hendecane	12,0%
Dodecane	12,0%
Ethylene	12,0%
Propylene	16,0%
Acetylene	23,0%

4.5.2 Formation-oxidation model (FOX).

FOX depends on two terms in the transport equation, being one of them the modelization of the soot formation and the other one models the oxidation/combustion

of soot. Soot formation is a rather complex process; specifically nuclei formation needs a certain mixture, temperature, and time. Soot formation can be divided in 5 differentiated steps: soot inception, soot surface growth, oxidation, coagulation, and agglomeration. For modelling of nuclei formation and oxidation, one more transport equation has to be added to the system, that at this moment FLACS has not yet implemented [1].

The transport equation for the soot mass fraction is very similar to the one used in the overall combustion process but, in this case the parameters are for the soot formation:

$$\frac{\delta \bar{\rho} \widetilde{Y}_{soot}}{\delta t} + \frac{\delta \bar{\rho} \widetilde{Y}_{soot} \tilde{u}_j}{\delta x_j} = \frac{\delta}{\delta x_j}\left(\bar{\rho} D \frac{\widetilde{Y}_{soot}}{\delta x_j}\right) - \frac{\delta}{\delta x_j}\left(\bar{\rho} \widetilde{Y''_{soot} u''_j}\right) + \bar{\rho} \widetilde{\omega}_{soot} \qquad [32]$$

Currently, even in the use of this FOX model, the upper limit for the mass fraction of soot is limited by the soot yield value previously shown in Table 2. [1]

4.6 Pool model

FLACS v10.6 presents two main options for pool modeling. Pool model 1 (PM1) is a static pool and the evaporation is ruled by Antoine vapor pressure equation. Pool model 3 (PM3) is a dynamic pool and allows the spill to move in the XY-plane, therefore, for our purpose, requires an obstruction. Pool model 1 and 3 may be used for the same study given that the pool is restricted from moving by including extra obstructions in the geometry. The models have been validated for pool spread with and without obstacles at adiabatic conditions, for evaporation of a liquid methane pool at rest on soil and for spreading of LNG on water. [1]

4.6.1 Pool modeling

PM1 does not present any kind of movement; therefore, this section does only apply to PM3. FLACS calculates the spreading of a pool by the shallow-water equations in two dimensions (XY). The shallow- water equations are solved on a Cartesian grid, identical to the XY-grid provided in FLACS. The equation for the spill height is:

$$\frac{\delta h}{\delta t} + \frac{\delta h u_i}{\delta x_i} = \frac{\dot{m}_L - \dot{m}_V}{\rho_L} \qquad [33]$$

and the momentum equation is written as:

$$u_j \cdot \frac{\delta h u_i}{\delta x_j} + \frac{\delta h_i}{\delta t} = F_{g,i} + F_{\tau,i} \qquad [34]$$

where the gravity term is modeled with the following equation:

$$F_{g,i} = hg\Delta \frac{\delta(h+z)}{\delta x_i} \qquad [35]$$

The elevation of the ground, z, has been included such that spills on sloping terrains and the effects of obstacles and embankments can be introduced in the model. The

parameter DELTA is equal to 1on solid surfaces and delta varies depending on the density if the surface is water. The shear stress between the pool and the substrate is given by:

$$F_{\tau,i} = \frac{1}{8} f_f u_i |u_i| \quad [36]$$

The friction factor must be included in the model and it depends on the regime of the flow, for a laminar regime:

$$f_{f,lam} = \frac{64}{4Re_h} \quad [37]$$

Friction factor in turbulent regimes is estimated by Haaland's approximation to the classical method of the Moody chart. The equation varies depending on the relative roughness of the system:

$$f_{f,turb} = \begin{cases} \left\{-1.8\log\left(\frac{1.72}{Re_h} + \left(\frac{\epsilon_g}{12h}\right)^{1.11}\right)\right\}^{-2} & if\ \frac{\epsilon_g}{h} < 0.2 \\ 0.125\left(\frac{\epsilon_g}{h}\right)^{1/3} & if\ \frac{\epsilon_g}{h} \geq 0.2 \end{cases} \quad [38]$$

The friction factor chosen is the largest among the values obtained. The friction factor between a pool and water is less than between a pool and solid soil. Water reduces the ground roughness to zero and the laminar friction factor to a fourth of its original value. [1]

4.6.2 Pool heat and mass transfer

The transport equation for specific enthalpy reads:

$$\frac{\delta h\theta}{\delta t} + u_i \frac{\delta \theta}{\delta x_i} = \frac{\dot{m}_L}{\rho_L}(\theta_L - \theta) + \frac{1}{\rho_L}\left(\dot{q_c} + \dot{q_{rad}} + \dot{q_g} + \dot{q_{evap}}\right) \quad [39]$$

further explaining this equation:

- The first term is the enthalpy due to the leak.
- q_c is convective heat transfer between the pool and air.
- q_{rad} is the radiative heat transfer received from the surroundings and the sun.
- q_g is heat transfer with the substrate in which the pool lies.
- q_{evap} is heat loss due to evaporation of the fuel.

For cryogenic liquids like liquid H_2, liquid N_2 and LNG, the heat transfer is dominated by the heat from the substrate. Heat transfer from solid and rough grounds and for all grounds at non-boiling conditions is approximated by:

$$\dot{q}_{g,cond} = \begin{cases} \dfrac{\lambda_g (T_g^{\infty} - T_p)(1.5 - 0.25(t - t_{gw})}{\sqrt{\pi \alpha g}} & if\ t < 4s \\ \dfrac{\lambda_g (T_g^{\infty} - T_p)}{\sqrt{\pi \alpha g}(t - t_{gw})} & if\ t \geq 4s \end{cases} \quad [40]$$

where λ_g is the thermal conductivity of the ground, αg is the thermal diffusivity of the ground, and t_{gw} is the point in time the ground was wetted. Infinite ground is assumed in the derivation of the expressions above and T_g^{∞} is the ground temperature at an infinite position that equals the ground temperature before the ground was wetted. Furthermore, the equation above is only valid for conductive heat transfer. Spreading pools will also have a convective contribution to the heat transfer between the pool and the substrate. The convective heat transfer can be expressed as follows:

$$\dot{q}_{g,conv} = 0.0133 Re_h^{0.69} Pr_l^{0.4} \frac{\lambda_g}{h} \left(T_g^s - T_p\right) \quad [41]$$

where λ_l and Pr_l are conductivity and Prandtl number of the pool liquid and T_g^s is the ground temperature at the surface. The total heat transfer for pools on solid and rough grounds and for non-boiling conditions is found by using a cubic blending function:

$$\dot{q}_{s,nb} = \left(\dot{q}_{g,cond} + \dot{q}_{g,conv}\right)^{\frac{1}{3}} \quad [42]$$

In the expression for the convective heat transfer, the surface temperature of the substrate is used, which is calculated as follows:

$$T_g^s = T_g^{\infty} + 2\frac{\bar{\dot{q}}_s}{\lambda_g}\sqrt{\frac{\alpha_g (t - t_{gw})}{\pi}} \quad [43]$$

On smooth surfaces such as water and metal, the expressions for boiling heat transfer are used. Nucleate boiling is assumed for slight superheats. Slight superheat is defined as the conditions when the surface temperature of the substrate is at least 4 K higher than the boiling point temperature of the pool liquid and the heat transfer is below the critical heat flux. Cooper's correlation is used to calculate the nucleate boiling heat transfer:

$$\dot{q}_{s,nb} = 0.55 p_r^{0.12} (-\log p_r)^{-0.55} M^{-0.5} \left(T_g^s - T_p\right) \quad [44]$$

where the reduced pressure, $p_r = p_{sat}/p_c$ where p_{sat}, is the saturation pressure and p_c is the critical pressure. The nucleate boiling heat transfer replaces the conductive heat transfer in the cubing blending function for the effective heat transfer from the ground. The expressions for transition boiling and film boiling heat transfer and for selection of boiling regime:

$$\dot{q}_g = \begin{cases} \dot{q}_{g,film} & if\ Re_h \le 15 \\ \dot{q}_{g,film} + \frac{1}{2}(\dot{q}_{g,film}\left(\frac{1500 - Re_h}{1485}\right) + \dot{q}_{g,conv}\left(\frac{Re_h - 15}{1485}\right) & if\ 15 \le Re_h \le 1500 \\ \frac{1}{2}\dot{q}_{g,film} + \frac{1}{2}\dot{q}_{g,conv} & if\ Re_h \ge 1500 \end{cases} \quad [45]$$

where $\dot{q}_{g,film}$ refers to the film boiling heat transfer for a fluid in rest. Convective heat and mass transfers are based on boundary layer theory and wall functions similar to those for the momentum equation are used. The convective heat transfer reads:

$$\dot{q}_c = \frac{\rho_c C_\mu^{\frac{1}{4}} k^{\frac{1}{2}} c_{p,g}(T_g - T_p)}{T^+} \quad [46]$$

where T^+ is given by a two-layer model:

$$T^+ = \begin{cases} Pr y^+ & if\ y^+ < E^+ \\ E^+ Pr + \frac{Pr_T}{\kappa}\ln\frac{y^+}{E^+} & if\ y^+ \ge E^+ \end{cases} \quad [47]$$

The expression for the convective mass transfer is similar to that for heat transfer:

$$\dot{m}_c = \frac{\rho_g C_\mu^{\frac{1}{4}} k^{\frac{1}{2}} \frac{P_0}{RT_p}(x - x_{sat})}{x^+} \quad [48]$$

where $x=P_g/P_0$ and x^+ is given by:

$$x^+ = \begin{cases} Sc\ y^+ & if\ y^+ < E^+ \\ E^+ Sc + \frac{Sc}{\kappa}\ln\frac{y^+}{E^+} & if\ y^+ \ge E^+ \end{cases} \quad [49]$$

Both the sun and the surroundings contribute to the radiative heat transfer:

$$\dot{q}_{rad} = (1 - \omega)\dot{q}_{sun} + \epsilon_g \sigma T_g^4 - \epsilon_p \sigma T_p^4 \quad [50]$$

Two mechanisms contribute to the evaporation rate, the convective mass transfer and boiling:

$$\dot{m_V} = \dot{m}_c + \dot{m}_{boil} \quad [51]$$

Evaporation due to boiling hinders the pool temperature to rise above the boiling point temperature and is calculated as follows:

$$\dot{m}_{boil} = max\left\{\frac{\dot{q}_g + \dot{q}_c + \dot{q}_{rad}}{\Delta h_{fg}} - \dot{m}_c\ , 0\right\} \quad [52]$$

Finally, the heat transfer due to evaporation can be determined by:

$$\dot{q}_{evap} = -(\dot{m}_c + \dot{m}_{boil})\Delta h_{fg} \quad [53]$$

[1]

4.6.3 Coupled pool fire physics

When modelling pool fires with FLACS-Fire there are two options: Either one models the evaporation from the pool with an area leak, or by modeling evaporation from the pool by Pool model 1 or 3. In the present thesis, the latter option has been used because an area leak requires a certain burning rate to be set, and it is an important parameter to be estimated via simulation.

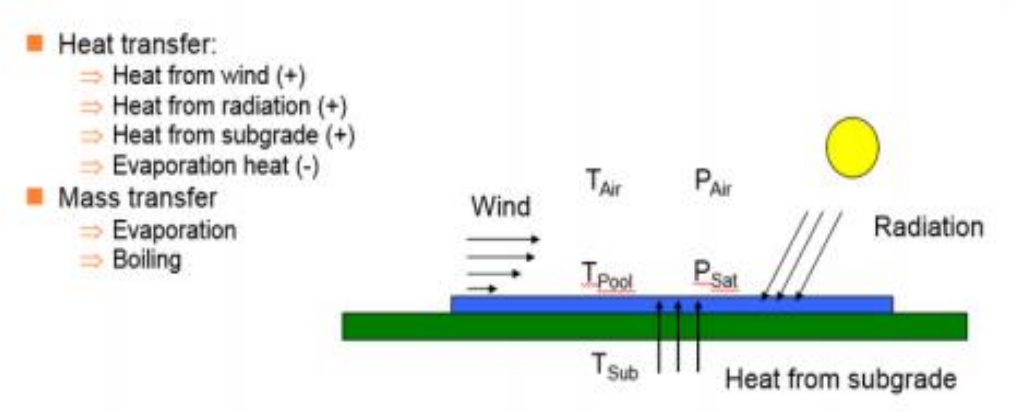

Figure 8: Coupled pool fire heat transfer
(Source: GexCon. FLACS v10.4 User's Manual 2015 [1].)

In the coupled pool fire model radiation from the flame is fed back to the pool model through the heat transfer balance for the pool, illustrated in the previous figure. In addition to the heat from the combustion, the heat balance also includes heat from the wind, the subgrade and the heat of evaporation. The radiative heat can be calculated with either the Discrete Transfer Model (DTM) or the Six-flux model. A minimum radiative heat on the pool surface may be set to enforce higher evaporation rates prior to the ignition of the combustible cloud forming over the pool. Combustion modelling currently applies the Eddy Dissipation Concept (EDC). [1]

5 CERTEC Experiments

This chapter of the thesis is going to review thoroughly the pool fires experiments performed by the CERTEC group over the past years. The experiments are directly related to the PhD theses developed by M Muñoz et al. (2005) [8] and F. Ferrero et al. (2006) [7].

CERTEC experiments were conducted in a training center called "Centro de Formación de Seguridad Can Padró" located in the town of Sant Vincenç de Castellet in the Barcelona province. This training center hold facilities to perform different firefighting drills ranging from small controlled fires to fires in tanks, buildings, etc. Can Padró also withholds incorporates an experimental area with enough space to carry out the pool fire experiments with the safety measures required.

The experimental facility can be seen in Figure 9 and is composed by the following parts:

- Storage and control room.
- 5 reinforced concrete concentric pools (1.5, 3, 4, 5, and 6 meters of diameter).
- Support structure for the thermocouples
- Training center's facilities: liquid residue disposal, weather station, water pumping station, hydrants, etc.
- Auxiliary equipment: fire extinguishers, wiring, insulation, instrumentation, fuel tanks, etc.

Figure 9: Overview of the experimental facility. (Source: M. Muñoz, E. Planas, J. Casal (2005). "Estudio de los parámetros que intervienen en la modelización de los efectos de grandes incendios

de hidrocarburo: geometría y radiación térmica de la llama." [8].)

5.1 Pools for hydrocarbon fires

The pools available in the experimental area are concentric circles made of reinforced concrete with diameters of 1.5, 3, 4, 5, and 6m in diameter. Pools were designed with approximately 10 cm of thickness and they are gradually increasing their height from the inner pool to the outer ones. The walls are high enough not to interfere with the experimental procedures, but also, they do not interfere among themselves; meaning the 3 m wall does not interfere in a 4 m pool fire experiment due to the fact that they are stepped.

Each pool has a galvanized steel pipe that enables the possibility of draining the remaining water and combustion residue. These draining pipes lead to a tank where all the liquid is stored until it can be treated in subsequent waste plant. Both pipes and intermediate storage of waste are inclined with a 2% slope to be able to drain everything by gravitational flow.

Latest improvements to the pools set-up was the incorporation of a 2.5'' steel pipe under the pools bottom. This pipe contains a set the wiring to introduce in the pools thermocouples and radiometers. Instrumentation inside the pools enable the acquaintance of information regarding the fuel layer as well as the heat being transferred from the flame to the surface of the fuel. Moreover, the pools have been waterproof as well as coated with thixotropic cement and with elastic mortar.

Furthermore, it was necessary to be able to determine the combustion rate. Combustion rate is estimated using two communicating vessels. Each pools has a 3/8'' pipe that is connected to a container through a flexible tube. This container is inside of the scale room, which protects from the fire the scale, container, valves, and other utensils. This scale room is located just 1 meter away from the outer ring of the pools set-up, and it is insulated with rock wool.

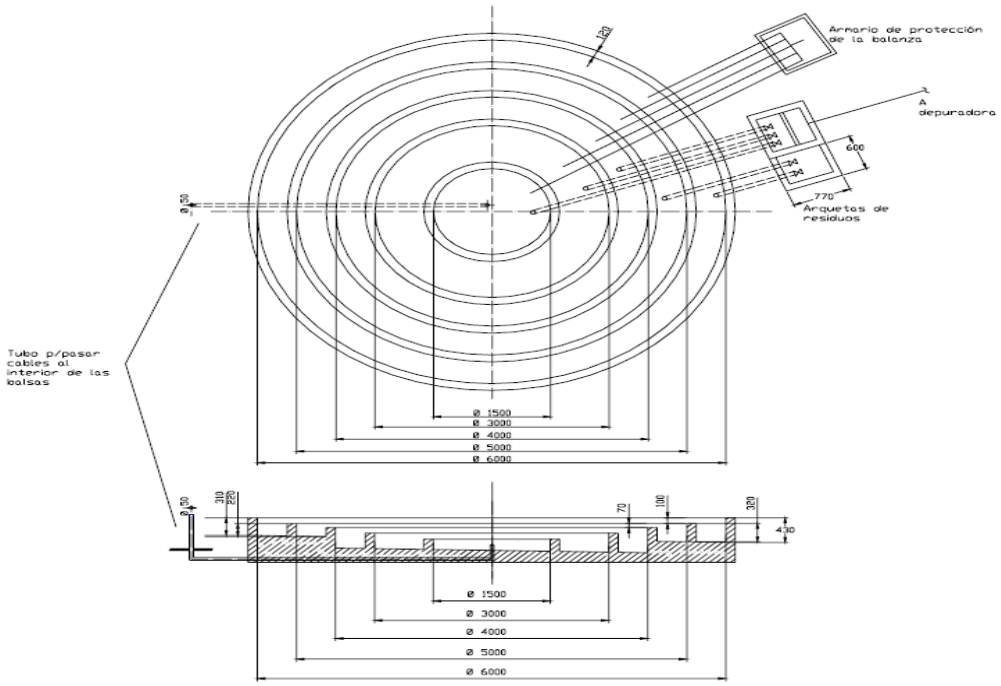

Figure 10: Schematics of the pool set-up (Source: F. Ferrero, J. Arnaldos (2006). "Incendios de hidrocarburos: Estudio de la formación y evolución de boilover de capa fina."[7])

5.2 Instrumentation

This section will cover the instrumentation used in the experiments, but rather than going over everything, it will detail the three main aspects that are essential for this master thesis:

- Temperature measure devices (thermocouples).
- Radiation measure devices (radiometers).
- Mass loss rate measurement system (Communicating vessels and scale).

5.2.1 Thermocouples

CERTEC experiments used two different kind of thermocouples depending on the area that was desired to measure the temperature. There are a total of 32 thermocouples, and they are distributed over three different sections. The first and most important is the metallic tower directly above the pools, the second setup is composed of cables displaced horizontally from the pools, and the third section is inside the fuel.

All the thermocouples used are type K. Type K thermocouples are made of chromel and alumel; chromel is an alloy approximately 90% nickel and 10% chromium, on the other hand, alumel consists of 95% nickel, 2% manganese, 2% aluminum, and 1% silicon. Specifically, the thermocouples used are coated with Inconel600 and have working temperatures between 500-1200ºC and they are apt for oxidizing atmospheres.

- Metallic tower: These thermocouples measure the temperature of hot gas plume above the fire. Six 1mm thermocouples were placed in the metallic tower, and they were protected by an Inconel pod of 3mm and 4.5mm long.

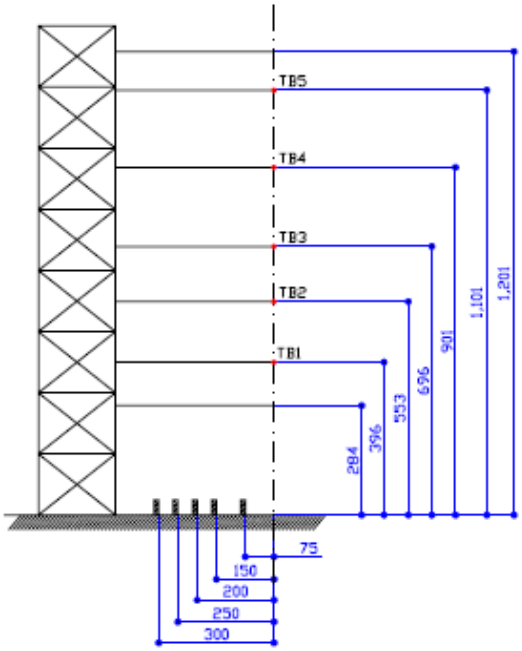

Figure 11: Thermocouple design for the metallic tower
(Source: M. Muñoz, E. Planas, J. Casal (2005). "Estudio de los parámetros que intervienen en la modelización de los efectos de grandes incendios de hidrocarburo: geometría y radiación térmica de la llama."[8]

- Cable setup: There are two kinds of thermocouples depending if they are directly above the flame center or if they are displaced from the center. Thermocouples placed in the center of the flame have a 1.5 mm diameter; external thermocouples have only 1mm. All thermocouples have a 4.5mm pod of Inconel 600.

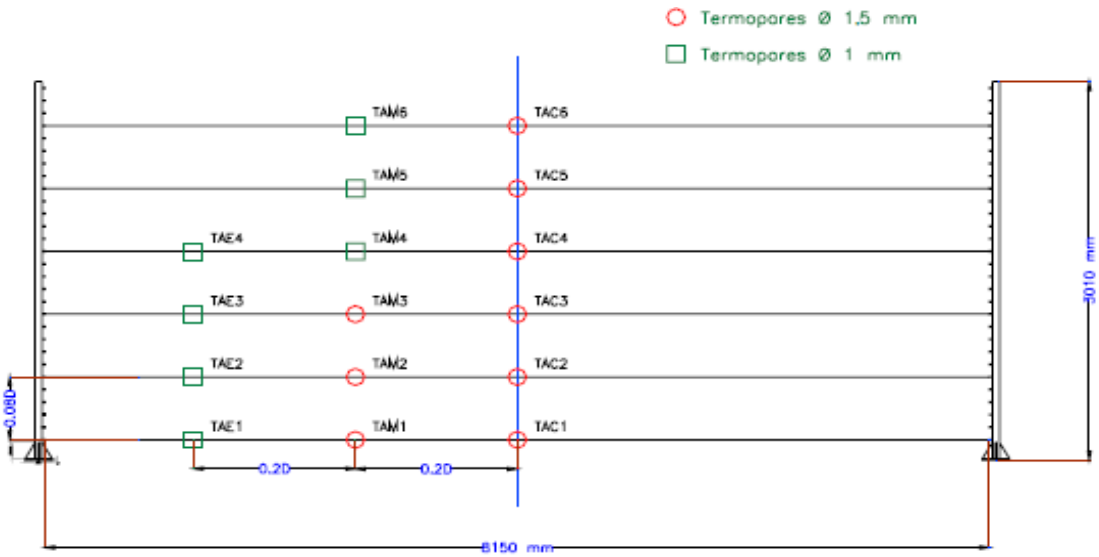

Figure 12: Cable setup for the thermocouples (Source: F. Ferrero, J. Arnaldos (2006). "Incendios de hidrocarburos: Estudio de la formación y evolución de boilover de capa fina."[7])

Thermocouples inside the fuel: This scenario requires 0.3mm thermocouples with an Inconel 600 pod of 1mm diameter and 30cm long.

5.2.2 Radiometers

It is crucial for a proper understanding of a pool fire to measure the heat flux of the fire. CERTEC experiments used Schmidt-Boelter thermopile to gather information about the irradiated heat flux, the emissive power of the flames, and the heat transferred from the flames to the fuel.

Three sensors were used, two heat flux transductors 64-2-16, and a dual sensor, 64-20T-20R(s), that can measure the total heat flux and the radiative one; both manufactured by Medtherm. Specifications for both radiometers can be seen over the next table:

Table 3: Technical specifications of CERTEC radiometers

	64-2-16	**24-20T-20R(S)**
Range	0-23 kW/m^2	0-277 kW/m^2
Output signal	Lineal 0-12 mV	Lineal 0-15 mV
Repetitiveness	±0.5%	±0.5%
Working temperature	200ºC	200ºC
Calibration uncertainty	±3% of the responsiveness to the incident heat flux	±3% of the responsiveness to the incident heat flux
Absorbance of the sensor cover	0.94 nominal, de 0.3 a 15.0μm	0.94 nominal, de 0.3 a 15.0μm
Sensor type	Medtherm Schmidt-Boelter thermopile	Medtherm Schmidt-Boelter thermopile
Impedance	Lower than 1000Ω (250Ω nominal)	Lower than 1000Ω (250Ω nominal)
Critical operating pressure	Not affected by over pressure or vacuum	Not affected by over pressure or vacuum
Refrigeration	Not refrigerated	Water

It is crucial to note that radiometer 24-20T-20R(S) (which later will be coded as Rad91) has incorporated a view restrictor. The view restrictor consists of a sapphire window with a vision angle of 180º. This view restrictor transforms the radiometer into an emissive power measurer; this means that the total emissive power from the flame will be measured and not just the incident radiation.

5.2.3 Mass loss rate

Mass loss rate was determined through the measure of the level in the pool or the equivalent loss of fuel mass. Burning rate is usually determined by a method that can stablish the level difference throughout the experiment, this can be done via differential pressure sensors.

CERTEC experiments measured the burning rate through mass loss, using communicating vessels. This system is constituted by the two vessels, one of them is inside the pool and the other end is connected to a weighting scale, which can register

the weight loss. All the pools are connected to the vessel through steel pipes that are placed in the bottom of the pools. These steel pipes are connected to the measuring vessel with a flexible silicone tube. The whole set up schematics can be seen in the following picture:

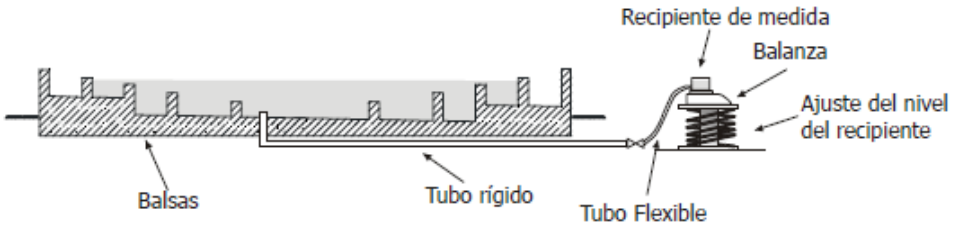

Figure 13: Schematics for the pool and communicating vessels

Source: F. Ferrero, J. Arnaldos (2006). "Incendios de hidrocarburos: Estudio de la formación y evolución de boilover de capa fina." [7]

Pool height diminishes proportionally with the weight loss in the scale, accordingly to:

$$\Delta W = \frac{\rho_f \Delta y}{(\frac{1}{A_p} + \frac{1}{A_R})} \quad [54]$$

A simplification can be made because of the large area difference between the communicating vessel and the pool. If the area of the vessel is disregarded the equation is treated as follows:

$$\Delta W = \Delta y A_R \rho_f \quad [55]$$

The equipment used to measure the weight loss is an electronic balance manufactured by METTLER TOLEDO, model PL-1501-S. Specifications of scale PL-1501-S can be seen in the next table:

Table 4: Specifications of the scale

METTLER TOLEDO: PL-1501-s

Capacity	1510 g
Precision	0.1 g
Repetitiveness	±0.08 g
Linearity	±0.2 g
Plate diameter	160 mm
Interface	RS3222

Weight loss was registered in a computer through data acquisition software, and it was calculated online as the data was recorded. Combustion rate was calculated as:

$$y = \frac{\Delta y}{\Delta t} = \frac{1}{\rho_f A_R} \frac{\Delta W}{\Delta t} \quad [56]$$

5.3 Fuels

Experiments were performed using two kinds of fuel: gasoline and diesel oil. The main reason behind the election of the fuel was their advantages comparing them to other hydrocarbons. Mainly, their advantages are that there are widely used both industrially and domestically; and they are rather easy to obtain. Diesel oil is composed of a wide variety of hydrocarbons, mostly long chain ones; and on the other hand gasoline is a lighter split and it is almost fully made of hexane. Properties of both fuels are detailed in the following table:

Table 5: Properties of the fuels provided

Property	Gasoline	Diesel gasoil
Commercial name	REPSOL 98	REPSOL Tipo C
Maximum water (mg/kg)	200	200
Density at 15ºC (kg/m^3)	725-780	820-860
Boiling temperature (ºC)	40-180	250-370
Autoignition temperature (ºC)	338	280-456
Kinematic viscosity (mm^2/s)	2.7-3.2	2-4.5

5.4 Experiments

The following table shows the set of experiments carried out, as well as some of the conditions in which they were done; overall it is important to point out that the thermocouples are separated as indicated in Figure 11 and Figure 12. Radiometer positioning is detailed in the table below:

Table 6: Information of the experiments performed

Nº Experiment	Name	Diameter (m)	Fuel			Rad 91*		Rad 92*	
			Type	Height (m)	Liters	X (m)	Y (m)	X (m)	Y (m)
1	Foc3_01_D3	3	Diesel	1.27	90.0	12.3	0.9	9	0
2	Foc3_02_D3	3	Diesel	1.5	106.0	15	0	15	0
3	Foc3_03_G3	3	Gasoline	2	141.4	12.3	0.8	15	0
4	Foc3_04_D3	3	Diesel	2	141.4	12.3	0.8	15	0
5	Foc3_05_D3	3	Diesel	2.5	176.7	21	1.5	15	1.5
6	Foc3_06_G6	6	Gasoline	1.5	424.1	14.7	0.9	18	0
7	Foc3_07_D6	6	Diesel	1.5	424.1	14.7	0.9	18	0
8	Foc3_08_G5	5	Gasoline	1.5	294.5	12.3	0.8	15	0
9	Foc3_09_D5	5	Diesel	1.5	294.5	12.3	0.8	15	0
10	Foc3_10_D5	5	Diesel	2	392.7	25	0	15	1
11	Foc3_11_D5	5	Diesel	2	400.0	25	1.5	15	1.5
12	Foc3_12_D6	6	Diesel	2	565.5	30	0	18	1.6
13	Foc3_13_G4	4	Gasoline	1.5	188.5	9.8	0.6	12	0
14	Foc3_14_D4	4	Diesel	1.5	188.5	9.8	0.6	12	0

15	Foc3_15_D4	4	Diesel	2	251.3	20	0	12	1
16	Foc3_16_D4	4	Diesel	2.5	314.2	20	1.6	12	1.6
17	Foc3_17_G3	3	Gasoline	1.5	106.0	15	1.5	9	1.5
18	Foc3_18_D3	3	Diesel	1.2	84.8	15	1.5	9	1.5
19	Foc3_19_M3	3	Mixture	2	141.4	8.5	0.8	9	0
20	Foc3_20_D3	3	Diesel	1.2	84.8	9	1.4	9	0
21	Foc3_21_G1.5	1.5	Gasoline	2	35.3	3.7	0.2	7.5	1.5
22	Foc3_22_D1.5	1.5	Diesel	2	35.3	3.7	0.2	7.5	1.5

*Measured from the center of the pools.

This is the whole collection of experiments that were done; out of this collection in the present thesis there were only simulated: Foc3_22_D1.5, Foc3_21_G1.5, Foc3_01_D3, Foc3_04_D3, Foc3_03_G3, Foc3_17_G3, Foc3_14_D4, and Foc3_13_G4. Not all the experiments were simulated due to time restrictions, the larger the pool fire, higher the simulation time.

6 Results

This section is divided into two different subsections. The first one covers the results of the preliminary simulations performed to correctly set-up some of the simulation parameters, and the second subsection describes the final results obtained in the simulations of the experimental tests. FLACS-Fire requires a set of parameter as inputs to achieve a correct simulation of the case, the most significant are:

- Geometry of the case.
- Monitor points, as well as variables that they measure.
- Grid dimensions.
- Boundary conditions.
- Initial conditions (wind speed, temperature, pressure, ground roughness, etc.).
- Leak data (composition, size, temperature, position, etc.).
- Simulation and output control (simulation time, plotting interval, etc.).
- Ignition region and time.
- Radiation model as well as its parameters (emissivity, absorption coefficient, etc.).
- Combustion model.
- Smoke/Soot model (FOX or CFM fixed value).
- Conduction model.

6.1 Preliminary simulations

This first simulations have a clear purpose of setting the appropriate values to some of the simulation parameters in order to perform adequately the simulations. Preliminary tests have been performed varying the following parameters: grid, radiation model, and soot model. It should be noted that every parameter changed was also tested in both pool models (PM1 and PM3); also, the composition of the fuel is pure hexane as a substitute of gasoline. The simulation used for this initial approach is experiment 21, a gasoline pool fire with a 1.5m diameter. Water has not been placed under the fuel, unlike in CERTEC experiments, due to the fact that FLACS-Fire showed no difference in the results.

Simulations ran on FLACS all have a similar geometry. This geometry consists in a containment with varying dimensions depending on the diameter of the pool fire to simulate. In the following Figure 14, an example of the geometry defined is given:

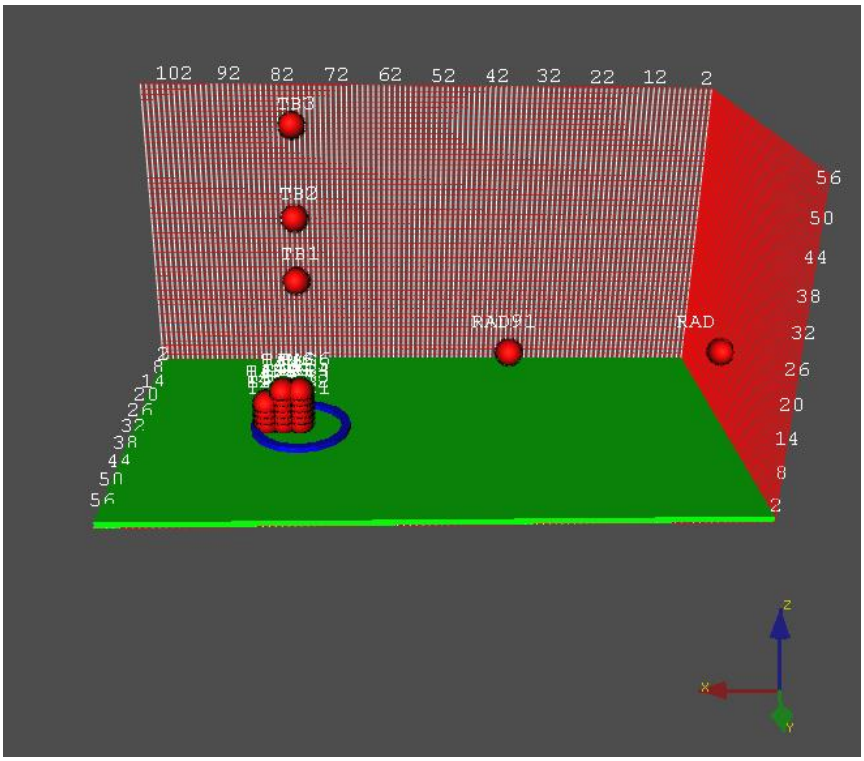

Figure 14: Example of a geometry of a pool in FLACS, with monitor points and grid displaying

The results from the simulations performed are displayed in a simplified way in order to avoid excessive amounts of data. To attain this simplification some key indicators such as thermocouples only at 2.55 meters (TB1), 5.53 meters (TB3) above the pool center, the burning rate, and the radiation are measured. Additionally, the simulations are ran for a short time, around 20 seconds, instead of the full duration of the fire; this decision was made to lower simulation times, and it was acceptable due to how fast the steady state is reached. Simulations performed are recorded in the following table:

Table 7: Initial simulations and their simulation conditions

Simulations	Grid size (m^3)	Radiation model	Soot model
G15_g0.05	0.05x0.05x0.05	DTM	FOX
G15_g0.1	0.1x0.1x0.1	DTM	FOX
G15_g0.2	0.2x0.2x0.2	DTM	FOX
G15_g0.4	0.4x0.4x0.4	DTM	FOX
G15_s0.1	0.1x0.1x0.1	DTM	CFM 0.10
G15_s0.13	0.1x0.1x0.1	DTM	CFM 0.13
G15_SixFlux	0.05x0.05x0.05	Six Flux	FOX

Results will be further discussed in each individual section, but a general result of the data obtained is listed in the next table; it contains the average values for the two thermocouples analyzed and the burning rate:

Table 8: Results for the initial simulations

Simulations	Pool model	TB1 (K)	TB3 (K)	Burning rate (kg/s)
G15_g0.05	PM3	1108.3	553.6	0.06
G15_g0.05	PM1	1082.7	564.1	0.06
G15_g0.1	PM3	1076.4	763.9	0.08
G15_g0.1	PM1	1361.2	662.5	0.10
G15_g0.2	PM3	1186.0	375.7	0.39
G15_g0.4	PM3	898.5	745.5	1.46
G15_s0.1	PM3	1110.4	678.1	0.08
G15_s0.1	PM1	1359.4	726.9	0.08
G15_s0.13	PM3	1017.2	573.8	0.08
G15_s0.13	PM1	1310.2	709.5	0.08
G15_SixFlux	PM3	1283.4	484.6	0.05
G15_SixFlux	PM1	533.0	484.7	0.05

Comparison graphs were constructed and they consist in a representation of the average predicted values versus the measured ones with a diagonal parting the graph. Graphical representations of the data are plotted with a diagonal and two limitation lines defined by a FAC2 factor. FAC2 is recommended for validation by Hanna et al. (2004) [25], and it gives a rapid and unequivocal glance of how valid the data obtained is. FAC2 is calculated as:

$$0.5 \leq \frac{y_P}{y_E} \leq 2 \qquad [57]$$

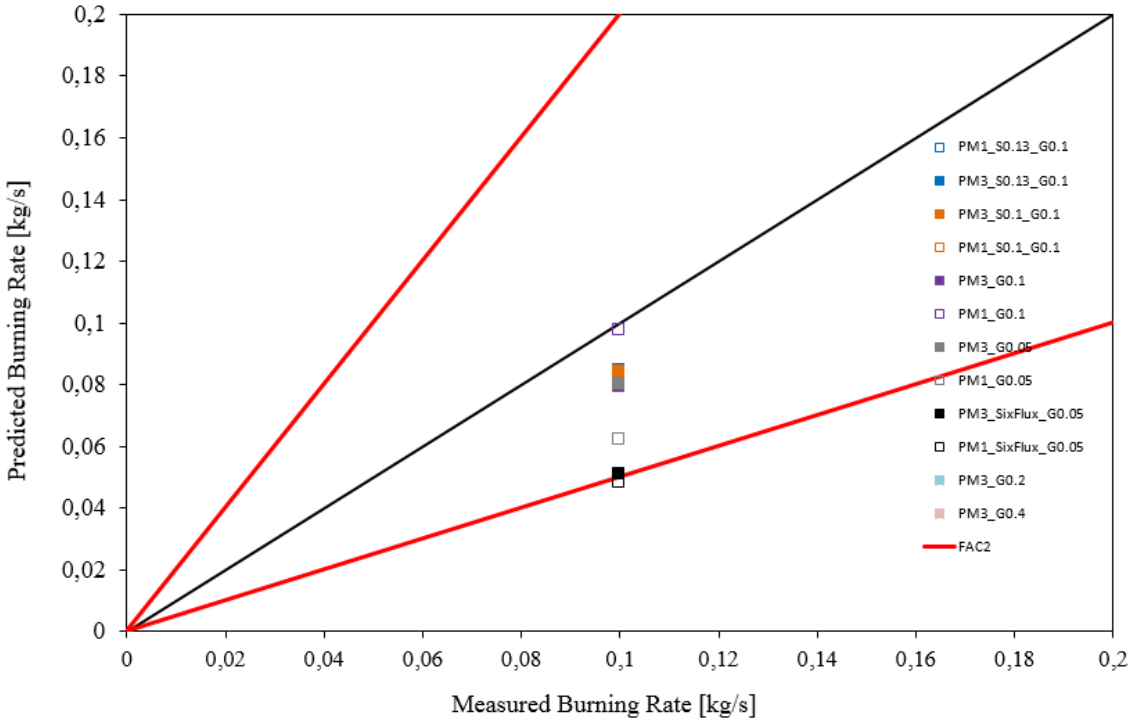

Figure 15: Burning rate results for all initial simulations

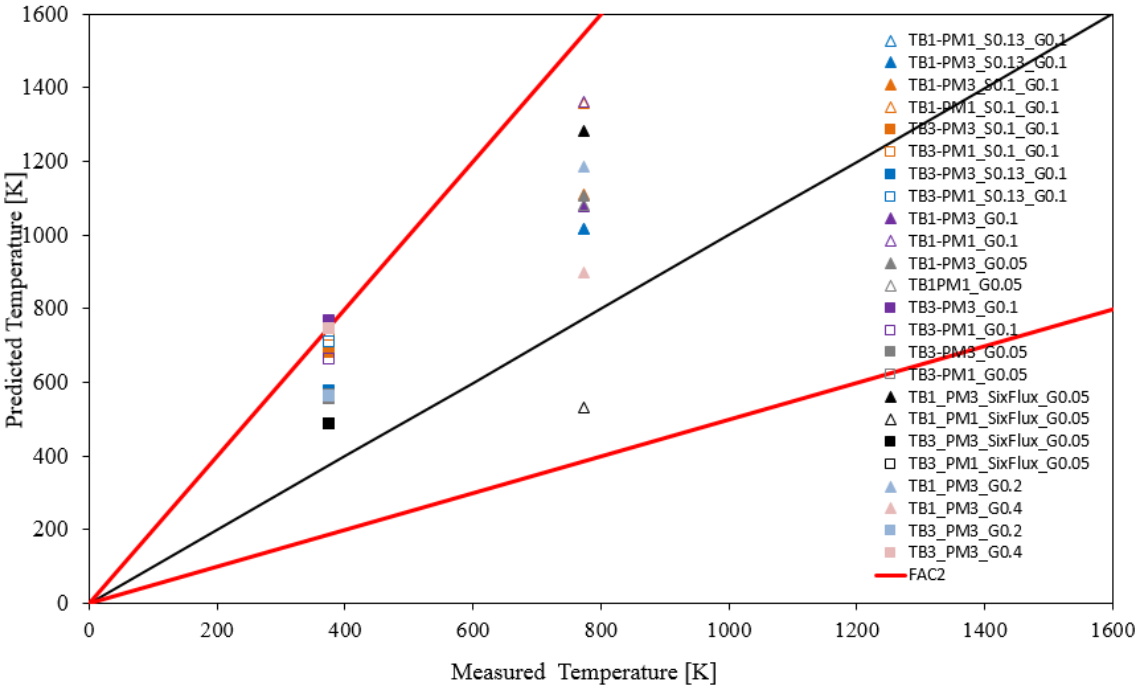

Figure 16: Temperature results for the initial simulations

Now, every set of simulations will be analyzed independently, and conclusions will be drawn to achieve an optimal set of parameters for the final simulations.

6.1.1 Grid

The grid, or mesh, used in a CFD is one of the most significant variables since it is directly related to the amount of operations being carried in the simulation. Tests were performed in order to obtain an acceptable grid that can simulate correctly the system desired, but also does not take excessive computational time.

FLACS uses a grid system consisting in two differentiated grid sections. The main grid is called "core domain" and it represents the refined side of the grid. FLACS also has a "stretch domain" which consists in an enlargement of the core domain, it consists mainly in maximum factor which sets the maximum enlargement of the initial cell size. In the present thesis, all the grids only use a smooth core domain with a defined cell size. Results only for the grid sensitivity analysis are provided in the figure below:

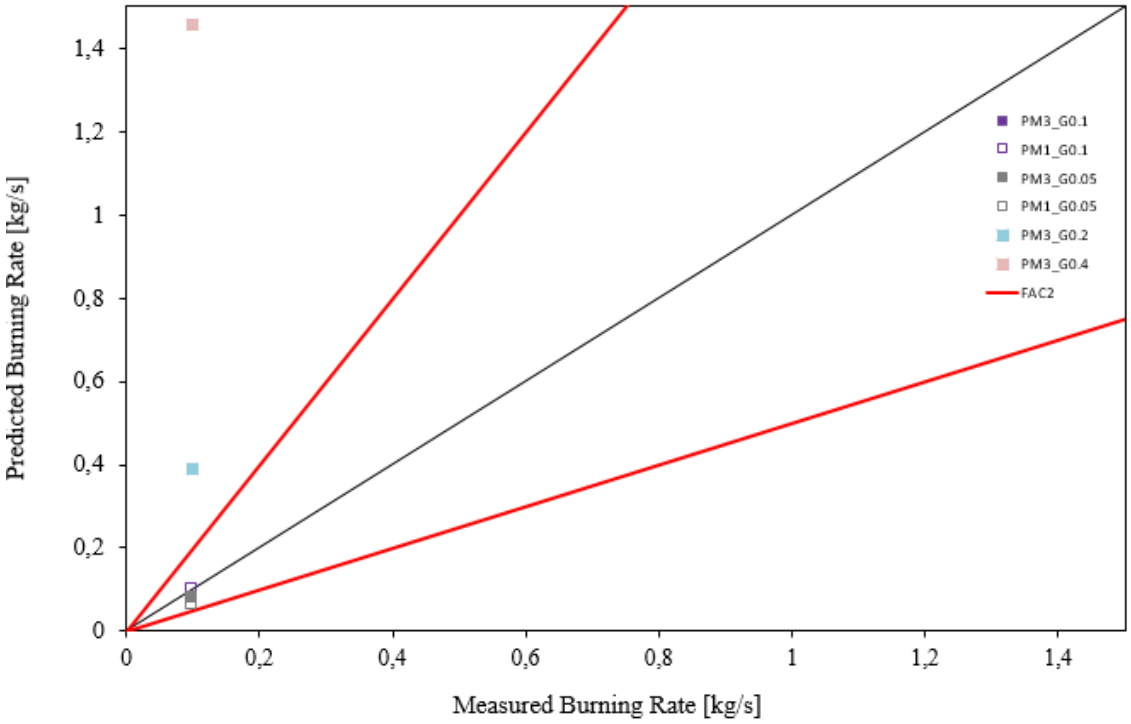

Figure 17: Predicted burning rate for grid sensitivity

Preliminarily, it can be observed that both grids above 0.1x0.1x0.1 have results that are not acceptable. Burning rates as high as the ones obtained in simulations with a grid of 0.2 and 0.4 are so high that the fuel is consumed in only a fraction of the time shortening the simulation drastically. On the other hand, focusing on the 0.05 and 0.1 grids:

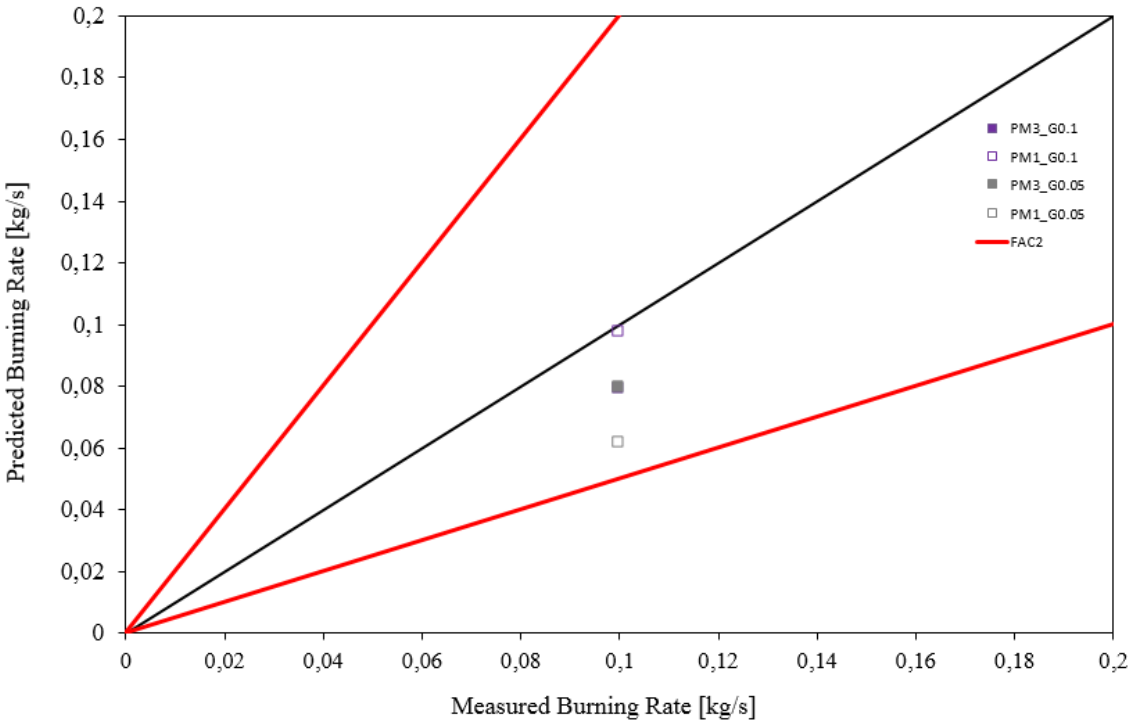

Figure 18: Burning rates for 0.1x0.1x0.1 and 0.05x0.05x0.05 grids

It is observed that the grid definitely has an effect on the burning rate. The results for PM3 on both simulations are practically identical. PM1 with a 0.1 grid shows the best approach to the experimental value; even when the computational time necessary to run a simulation with that gird is smaller than with 0.05; therefore, reducing the grid size it is not always as effective as it might seem. Temperatures are also evaluated in the next figure:

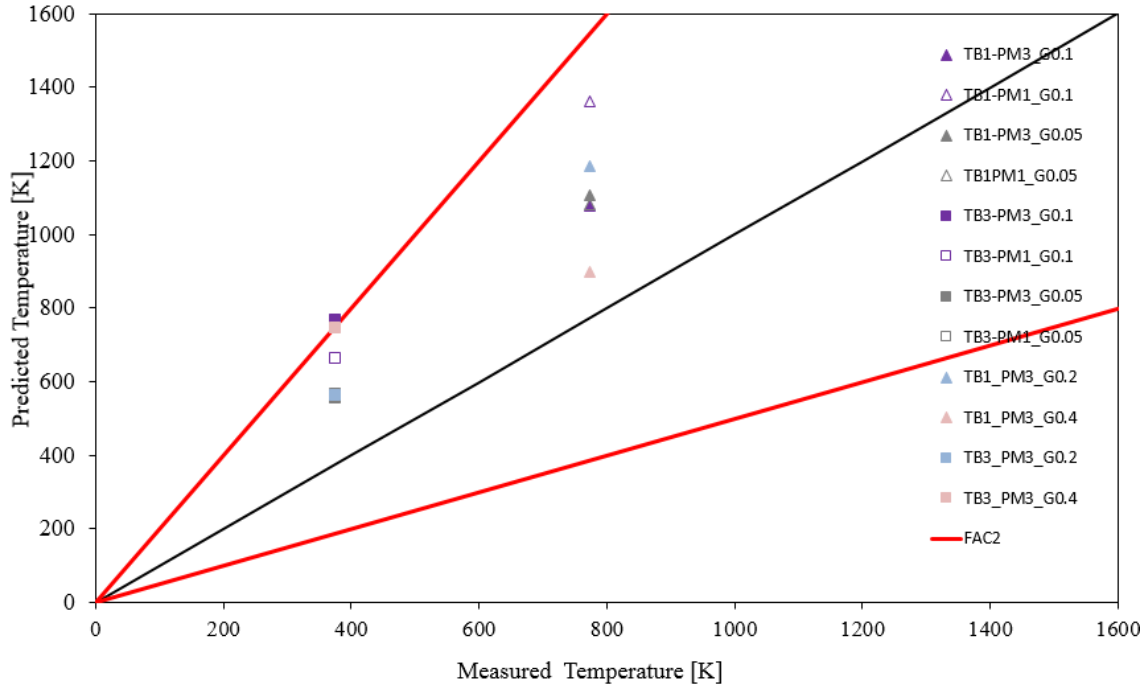

Figure 19: Temperature prediction for grid sensitivity

Grids of 0.4 and 0.2, although they have decent values, they are to be excluded because of their inconsistencies in the burning rate simulation. TB3 is better simulated by the fine grid, but results of PM3 in 0.1 are not far from this value, the difference is not significant enough to justify the computational time. In addition, TB1 has essentially the same values for both grids without any remarkable disparity.

Using the FAC2 criteria, TB1 has all its points remain within the area, only PM1-0.1 shows the biggest discrepancies. For TB3, most of the points fall inside the de FAC2 limits, except for PM3-G0.1 and G0.4. The latter does not hold any importance since this grid is to be excluded directly. In conclusion, a finer grid leads to slightly better results, but the computational time escalates exponentially, which in any practical case is a very precious resource; therefore, with everything taken into account, a grid of 0.1x0.1x0.1 has been selected to run the definite simulations.

6.1.2 Radiation model

It has been stated in previous sections that FLACS has two radiation models that can be used as well as its characteristics, for pool fires the recommendation is to use DTM (discrete transfer method) but the Six-Flux model was also tested to see and prove the differences. Simulations of radiation models were performed in a grid with a cell size of 0.05 how much this radiation would affect the overall result. A finer grid was used due to the fact that SixFlux is a quicker model than DTM, hence the computational time is reduced. The results obtained were plotted and the following graph displays them:

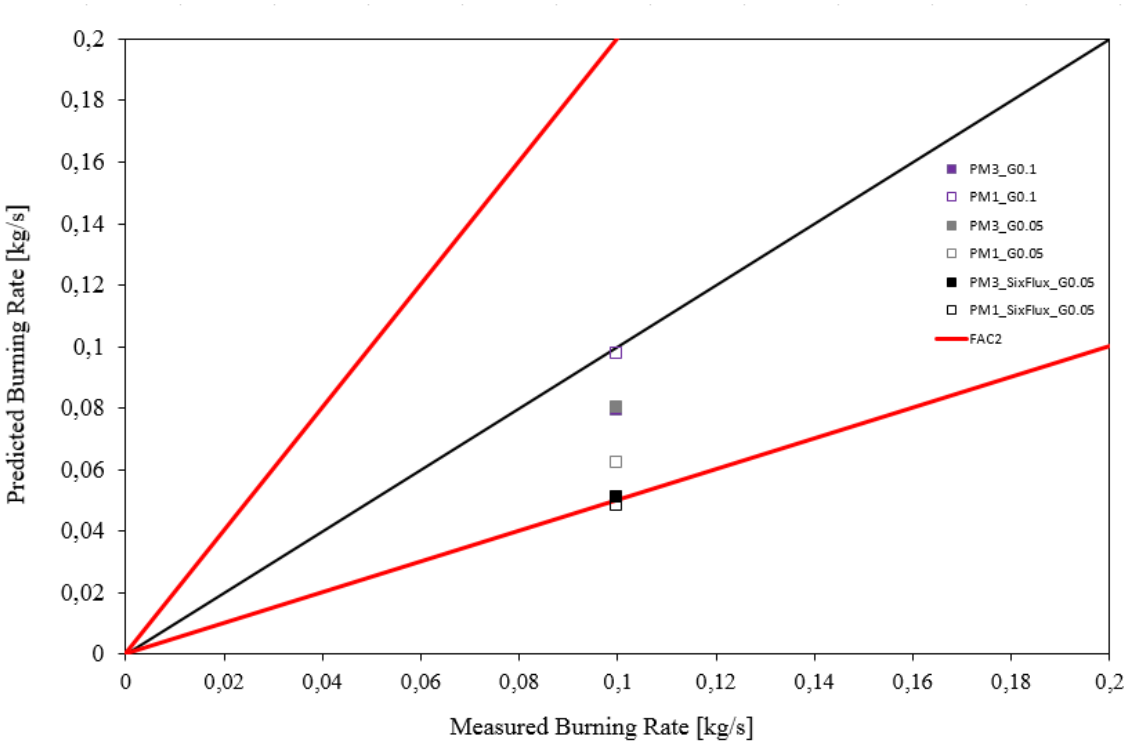

Figure 20: Burning rate prediction for SixFlux model

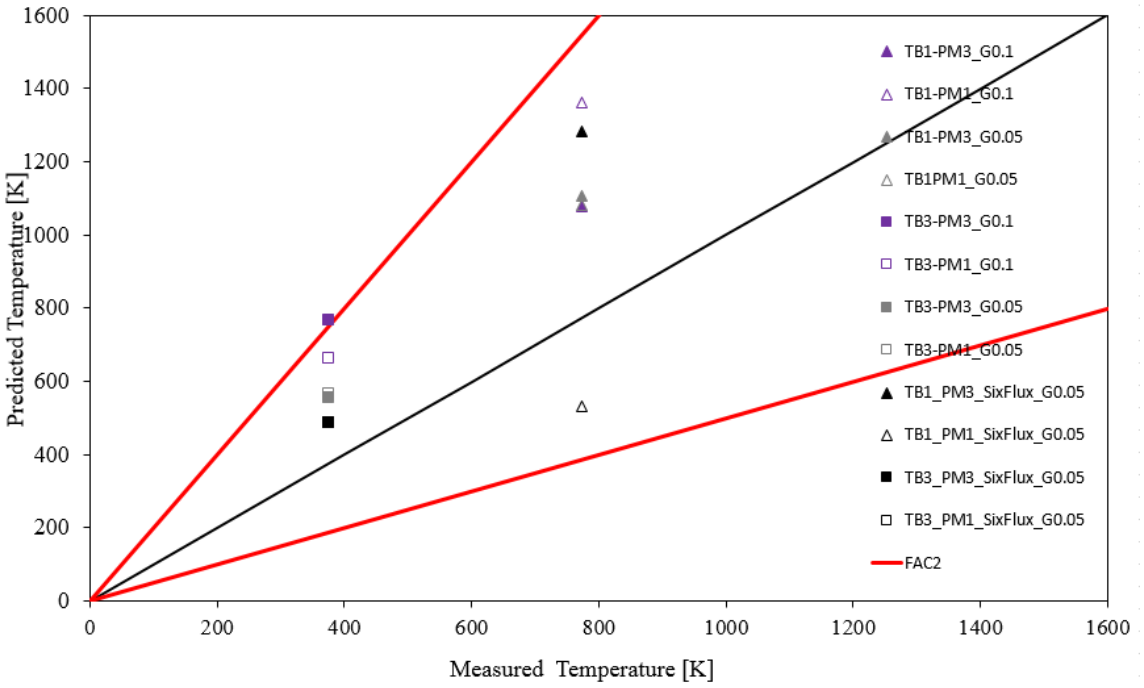

Figure 21: Temperature prediction for SixFlux model

It is observed in the data, that SixFlux does not grant good results in comparison with DTM, regardless of the finer grid. Results for burning rate do not reach acceptable values, they are around 0.5kg/s which is half of the desired value; temperatures are more or less in concordance with the worst values obtained with DTM, which does not grant anything positive towards future simulations. In conclusion, DTM radiation model is a more precise model, which grants better results than SixFlux in approximately the same computational time; consequently, DTM will be used for next simulations.

6.1.3 Soot model

FLACS offers to the user two models for the soot formation, either the Formation-Oxidation model or a fixed conversion factor, which is just an input of a fix value for the soot formation. This master thesis covers the use of Formation-Oxidation since it is the model recommended by the developer but also it has been tested the use of different soot yields that are common among gasoline pool fires. Tests were simulated with soot yield values of 0.1 and 0.13, which are a compromise among the recommended values given in Table 2. Results obtained for the preliminary simulations involving different soot formation approaches are the following figures:

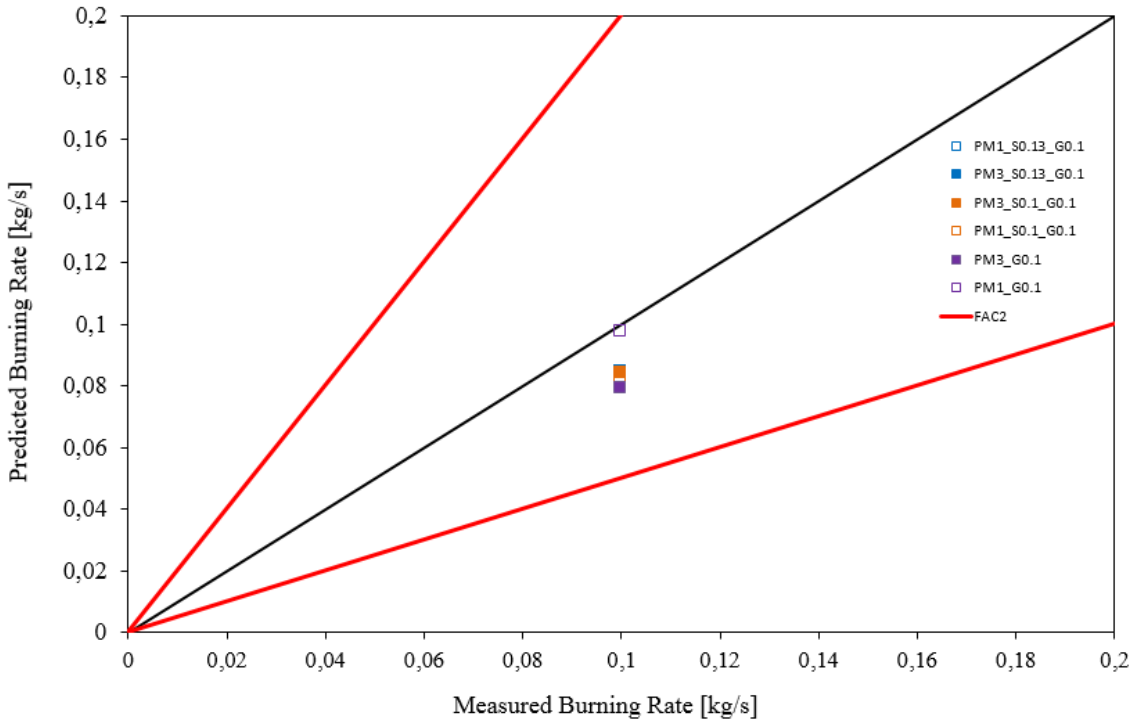

Figure 22: Predicted burning rate with different soot models

Burning rates are approximately the same in all three cases, around 0.08 kg/s which is an acceptable value as it falls inside the area limited by FAC2, and it is indeed close to the diagonal. Temperatures are not very affected by the soot formation either, all the data obtained is inside the desired area. In conclusion, both soot models respond well and it might depend greatly on the type of simulation, therefore for the sake of discerning which soot model is better capable of simulating, both will be implemented in the final simulations.

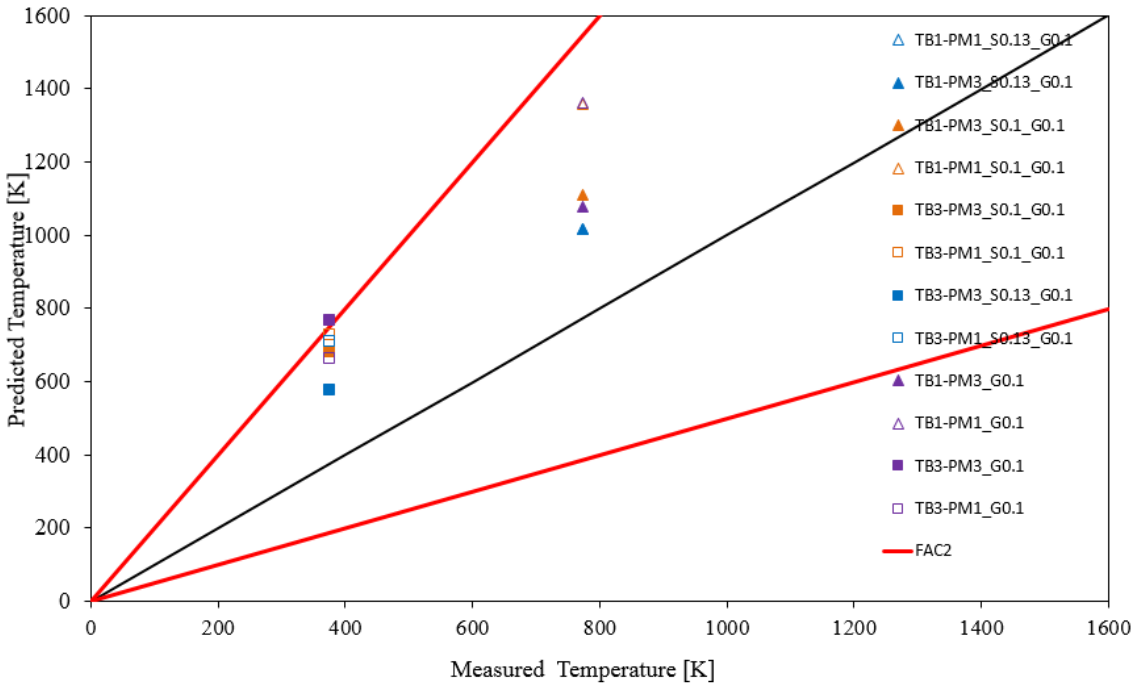

Figure 23: Temperature predictions for different soot models.

Finally, it should be discerned which pool model is a better proposition. Both PM3 and PM1 show great consistency, and results depend highly on which simulation is analyzed. Therefore PM1 is what should be implemented in the simulation, since in reality pools were not dynamic, but it will be further analyzed in PM1 simulations, due to some of inconsistencies that were later found in the final simulations.

6.2 Simulations of the experimental pool fires

The main goal of the present thesis is to validate the capabilities of FLACS to forecast correctly a variety of parameters. This validation is performed throughout a set of simulations based on the previously presented CERTEC experiments and the preliminary simulations performed. Table 9 summarizes the pools simulated:

Table 9: Pool fire experiments simulated in FLACS-Fire.

Simulation	Fuel	Diameter (m)	Solar Radiation (kW/m^2)	Wind speed (m/s)	Emissivity	CFM soot value
FOC_22_D15	Diesel	1.5	465	0.72	0.90	0.10
FOC_21_G15	Gasoline	1.5	400	0.40	0.90	0.10
FOC_01_D3	Diesel	3.0	651	2.10	0.95	0.10
FOC_04_D3	Diesel	3.0	246	0.00	0.95	0.10
FOC_03_G3	Gasoline	3.0	121	0.00	0.95	0.10
FOC_17_G3	Gasoline	3.0	121	1.70	0.95	0.10
FOC_14_D4	Diesel	4.0	434	0.85	0.98	0.13
FOC_13_G4	Gasoline	4.0	290	0.40	0.98	0.13

As it was previously mentioned, steady state is achieved rapidly and thence simulations were only ran for 30 seconds, saving extensive amounts of simulation time. Likewise in the initial simulations, gasoline and diesel could not be introduced as fuels, therefore the same assumption was stablished using dodecane and hexane instead. Ground temperature of the fuel was set to a temperature which grants vaporization of the pool; 490K and 341K for dodecane and hexane respectively.

In chapter 4 it was explained the wide array of possibilities while modeling with FLACS. Table 10 summarizes the four configurations that were taken into account while simulating. Remarkably, CFM soot model enables to use a fixed soot conversion, soot yields from 0.1 kg/kg to 0.13kg/kg were applied.

Table 10: Simulation configurations performed

Configurations	Pool Model	Mesh Size (m)	Soot Model
1st	PM1	0.1 x 0.1 x 0.1	FOX
2nd	PM1	0.1 x 0.1 x 0.1	CFM
3rd	PM3	0.1 x 0.1 x 0.1	FOX
4th	PM3	0.1 x 0.1 x 0.1	CFM

Identically as it was implemented in the initial simulations, the parameters measured are the burning rate, various temperatures and the radiative heat flux. Five thermocouples were taken into account, from the whole set specified in section Thermocouples, these are located in the pool centerline axis at different heights: 2.84 m, 3.96 m, 5.53 m, 6.96 m, and 11.01 m (these heights correspond to thermocouples TB1 to TB5 respectively). For the radiative heat flux, only one radiometer was simulated (Rad92), since as it was explained in section Radiometers, Rad91 measured the total emissive power rather than only the radiant energy. Radiometer distance is shown in the following table:

Table 11: Radiometer location in the different fire scenarios.

Simulation	RAD92 (m)
FOC_22_D15	7.5* – 1.5**
FOC_21_G15	7.5 – 1.5
FOC_01_D3	9 – 0
FOC_04_D3	15 – 0
FOC_03_G3	15 – 0
FOC_17_G3	9 – 1.5
FOC_14_D4	12 – 0
FOC_13_G4	12 – 0

** Represent the radial distance from the pool centre to the radiometer*
*** Represent the axial distance from the pool ground to the radiometer height*

Next section provide the results of the simulations, but for the sake of not over enlarging the size of the thesis it will not be done with all the experiments . Instead of showing

everysingle output of every experiment, validation graphs will be shown appropiately.

6.2.1 PM1 simulations

Prior to the final results analysis via comparison, it is important to note that not all simulations will be displayed, only the ones addressing PM3, the dynamic pool model. This decision was made based on information acquired from all the simulations. PM1 cannot completely simulate most of the fire scenarios as it burns more fuel than it is being evaporated, hence the evaporation rate is lower than the burning rate and the fire stops and might reignite if enough fuel mass is vaporized and accumulated. This affectation occurs in simulations with a pool diameter of 3m and higher.

In the following figure, it can be seen how the burning rate of simulation FOC_04_D3 behaves:

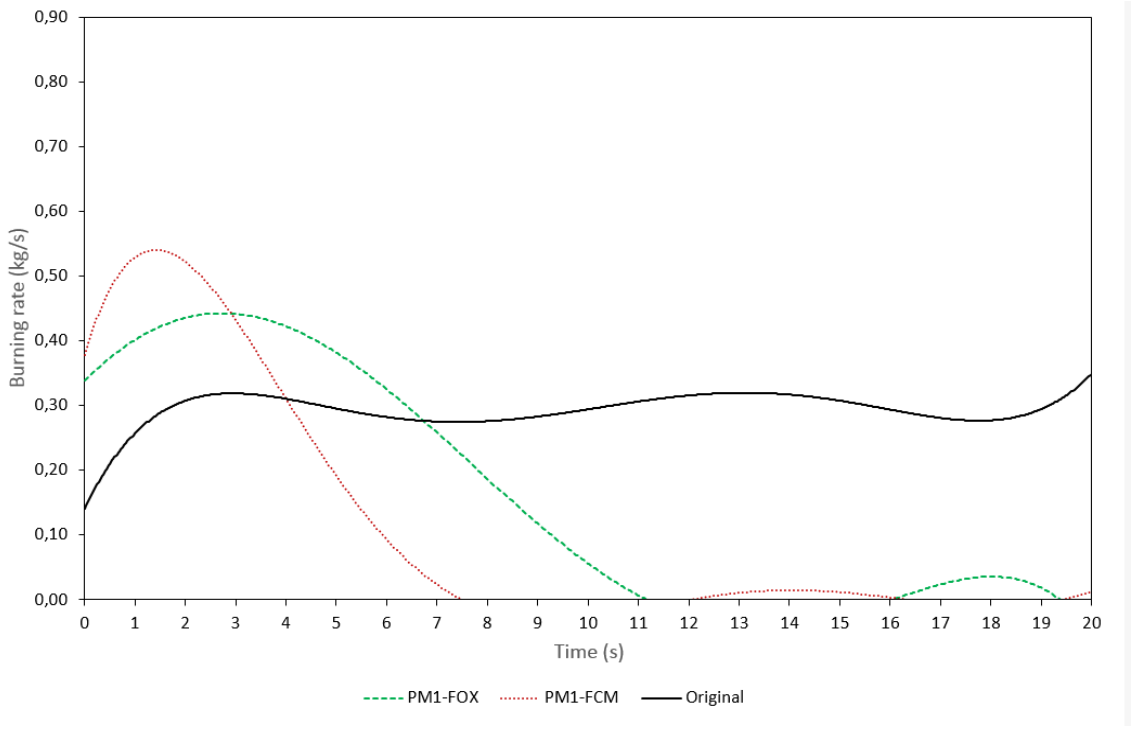

Figure 24: Burning rate of FOC_04_D3

As it is displayed, the burning rate tends to fade away around second 7.5 for the FCM model and around 11 seconds for the FOX model. Afterwards, when enough fuel is vaporized again, it is able to reignite for a few more seconds, but unmistakably, not fully.

6.2.2 Final results and comparison

It can be thoroughly examined all the plots of FLACS' results in

Appendix A- Simulation results, it does not hold much importance to show absolutely every graph, since this will definitely not clearly display if FLACS-Fire is a reliable simulator or not. Alternatively, like it was performed in the initial simulations, a plot with a diagonal and a FAC2 system will be shown with the average values for every parameter studied in every simulation.

The first parameter to be wholly compared is the burning rate. The burning rate from all simulations and experiments are shown in the following graph.

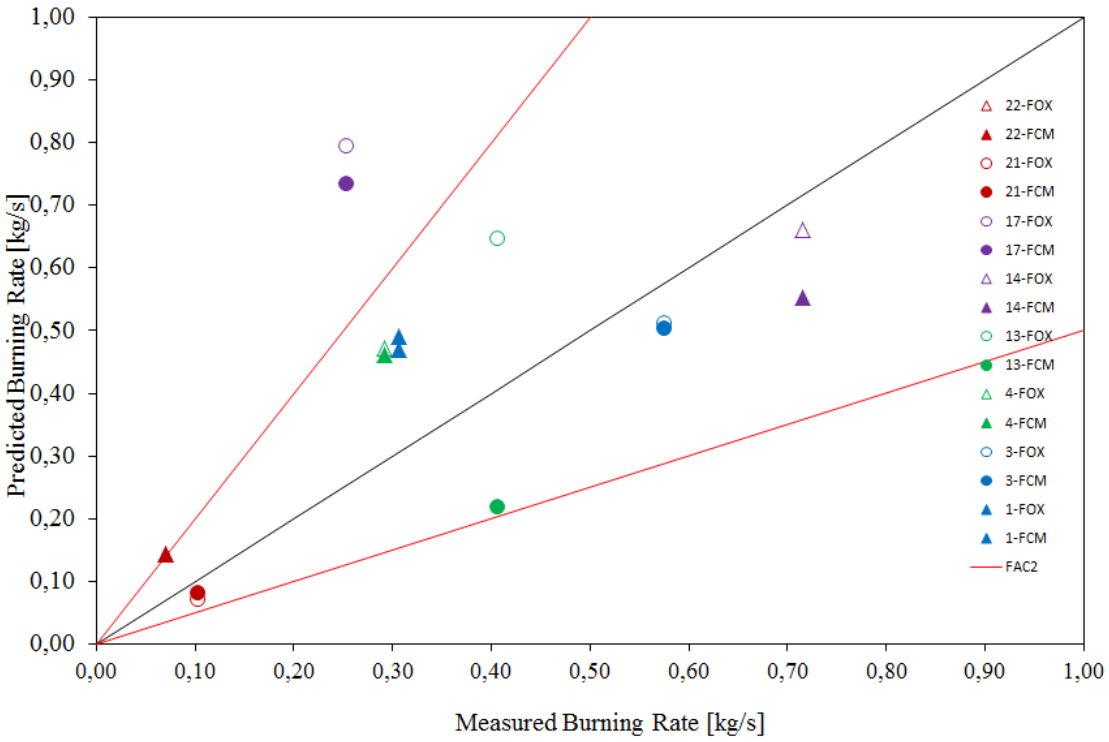

Figure 25: Average burning rates predicted as a function of the experimental measurements.

Generally, the burning rate is well predicted by FLACS-Fire if average values are calculated, as it has been reviewed already, variations and oscillations exist but the average values are indeed similar. This is especially true for simulations of 1.5 m pool diameter where the conditions are very well met. 3m and 4m pool fires match their experimental counterparts adequately on fires 14 and 3, here the fuel does not make a difference (14 is diesel and 3 is gasoline), and even though wind is weak 0.85 m/s in simulation 14 it does not affect the simulation. Simulations 1 and 4 are both diesel pool fires of 3m diameter; their results are in between, values diverge more but still enough to be a fairly acceptable simulation. Remarkably, simulation 1 has the fastest wind speed of 2.1m/s, therefore it is safe to establish that diesel pool fires up to 4 meters are not affected by mild wind conditions.

On the other hand, simulations 13 and 17 disagree strongly with their experimental counterparts. 13 is a 4m gasoline pool fire that has very mild wind conditions (0.4m/s).

13 is 3m gasoline pool fire with 1.7 m/s wind. A rather primitive conclusion for this discrepancies is based on the incapacity of FLACS-Fire to simulate correctly high wind speeds on gasoline, since it has been identified that it is capable to do so with diesel. Simulation 13 has another interesting feature in its results, the FOX model over predicts and the FCM model (using a constant value of 0.13) under predicts it.

To conclude, using the FAC2 system, only simulation 17 falls out of the limits of FAC2, which would mean this simulation's results would not be accepted by the criteria. It is also important to note that, simulation 22 and 13 are very close to the limits of the FAC2, which means they are on the verge of being directly discarded due to over and under prediction respectively.

Temperature is the next parameter to be evaluated. Globally speaking, temperatures are well predicted by FLACS-Fire, being the poorest simulations the ones of 1.5m diameter. Graphical representations analogous to the formerly seen for the burning rate were created:

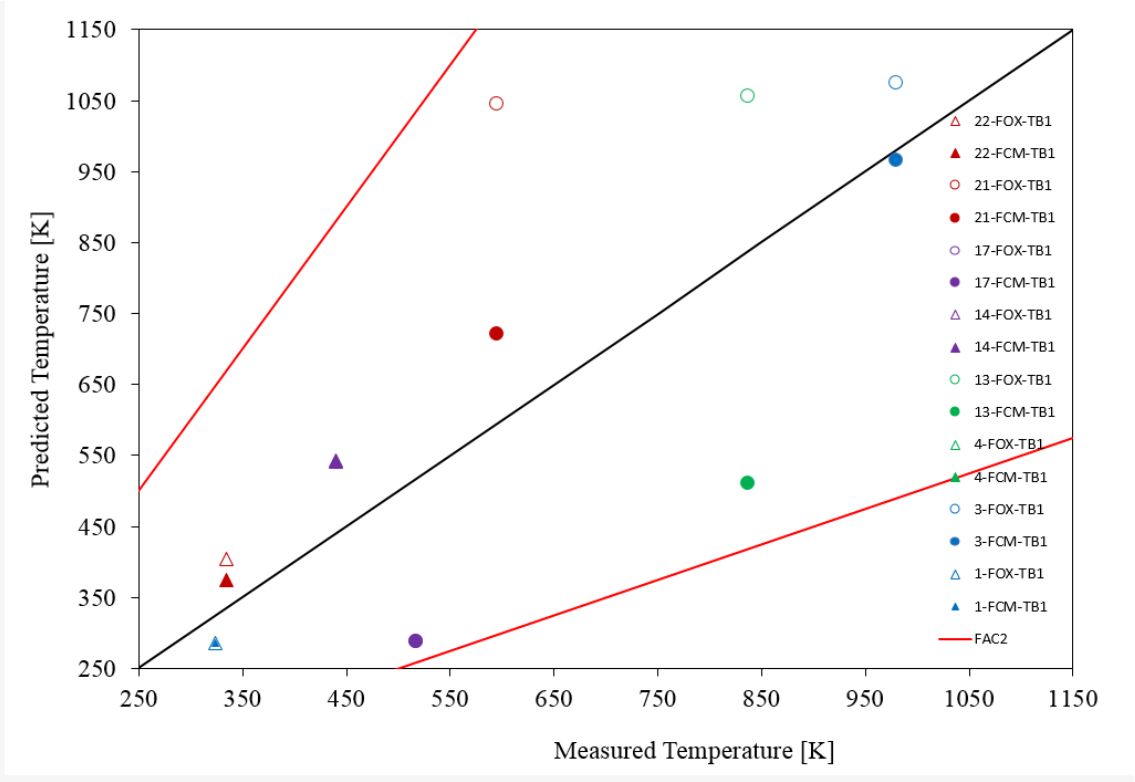

Figure 26: Average TB1 predicted as a function of the experimental measurements.

Specifically TB1 results are in fair concordance with experimental results. It is important to note that soot models concur in the same average values, except in the case of simulation 13, which as it happened in the burning rate discussion, FCM under predicts and FOX over predicts the desired temperature. Experiment 21 is also affected by the soot model, being the FCM tremendously more accurate than the FOX model. Experiment 17 is the only discrepancy that lacks any difference between soot models, again, this is caused by the wind speed moving the flames away from the thermocouples. All values are within the desired limits marked by FAC2.

TB2's results are akin to TB1's, the main difference is the higher accuracy that appears in this results, being the only remarkable discrepancies experiments 13, 17 and 21, which remain imprecise but all still remain inside the FAC2.
Next, TB3's results follow the same pathway as previous thermocouples, this time once again 13-FOX strays away, this divergence appeared in TB1 but not in TB2. Experiments 14 and 21 remain with the poorest validation data.

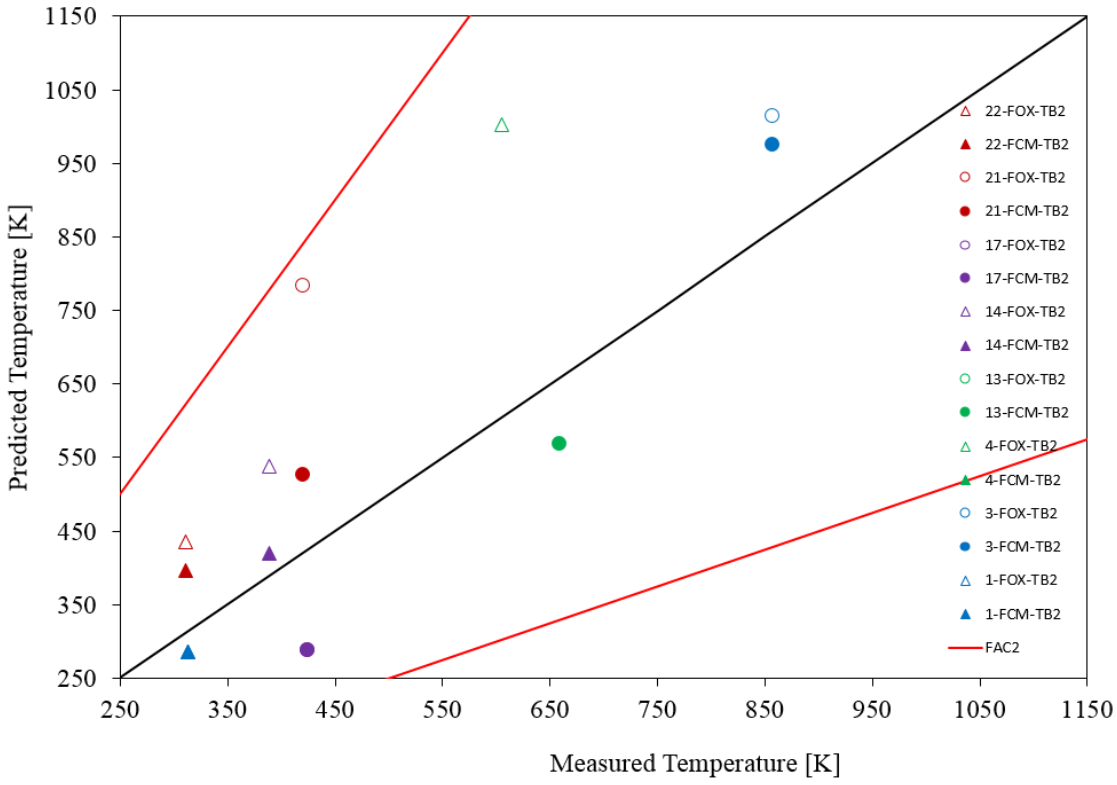

Figure 27: Average TB2 predicted as a function of the experimental measurements.

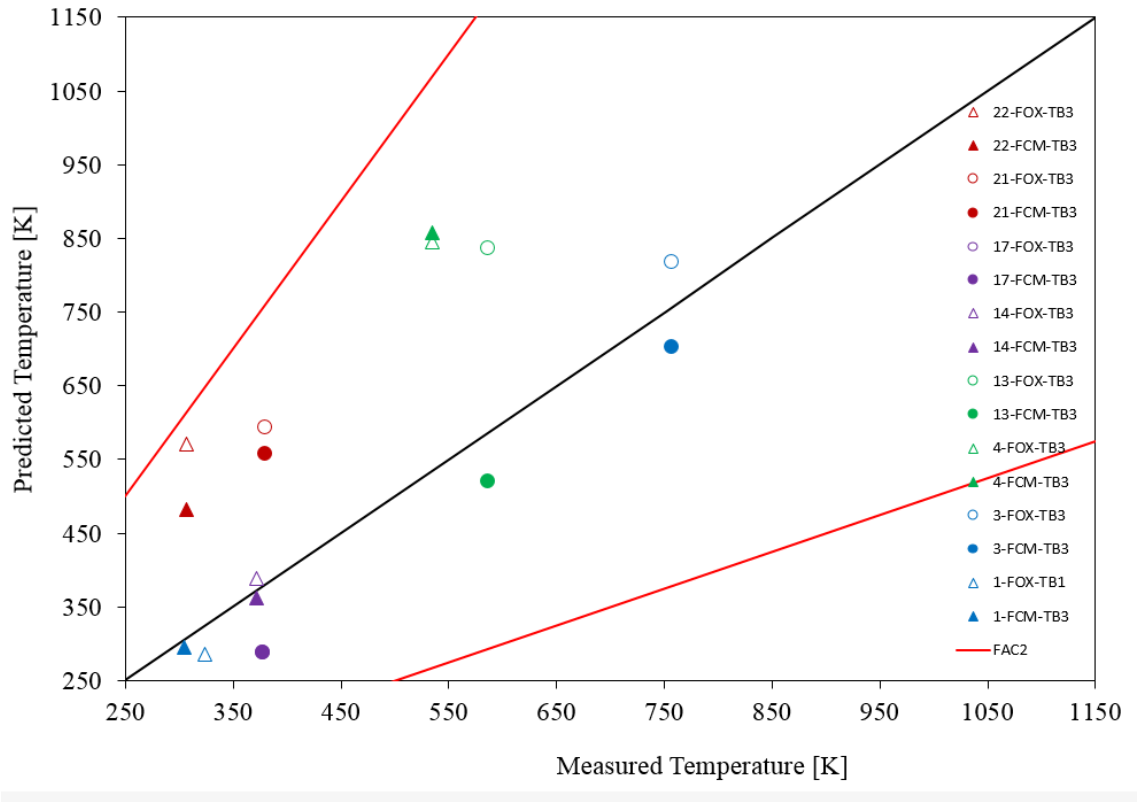

Figure 28: Average TB3 predicted as a function of the experimental measurements.

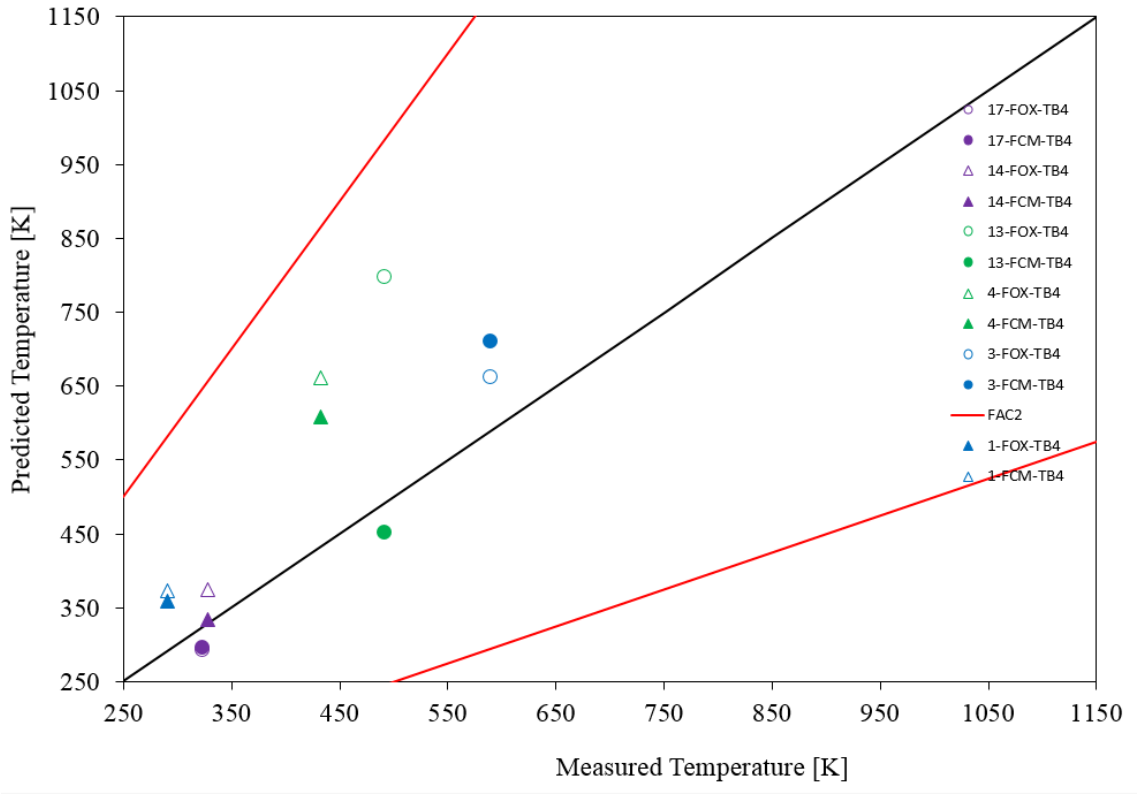

Figure 29: Average TB4 predicted as a function of the experimental measurements.

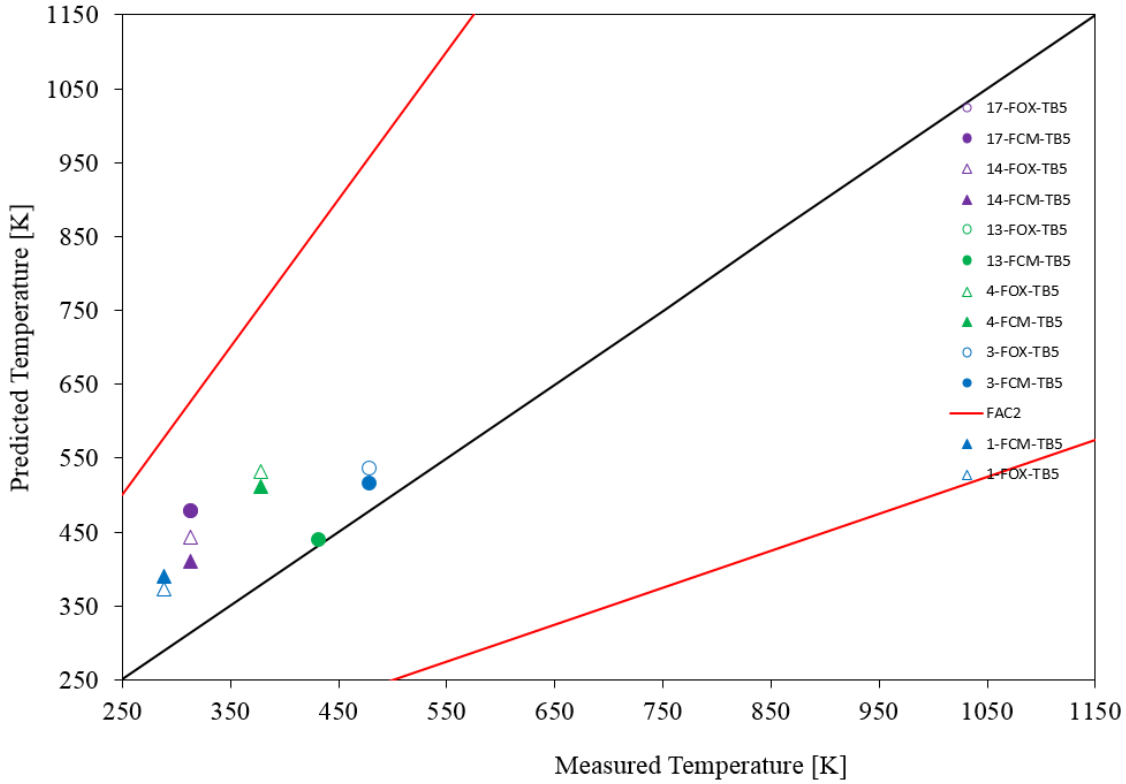

Figure 30: Average TB5 predicted as a function of the experimental measurements.

TB4 is reasonably well predicted in almost any case, the biggest discrepancies occur on simulation 4, both in FOX and FCM, with an average difference of almost 200K. It is interesting to remark that all experiments have a similar behavior for both soot models, except experiment 13 which, again, shows big discrepancies between values. Again all values match the criteria that has been selected (FAC2).

TB5 follows the same pathway as the rest of thermocouples, with minor disparities. It is noteworthy to remark that TB5's temperature for experiment 14 is much higher than TB4, which under normal conditions is not correct, especially with no severe wind. Next figure shows the effect of wind in experiment 1, in contrast with what actually happened during the experiment:

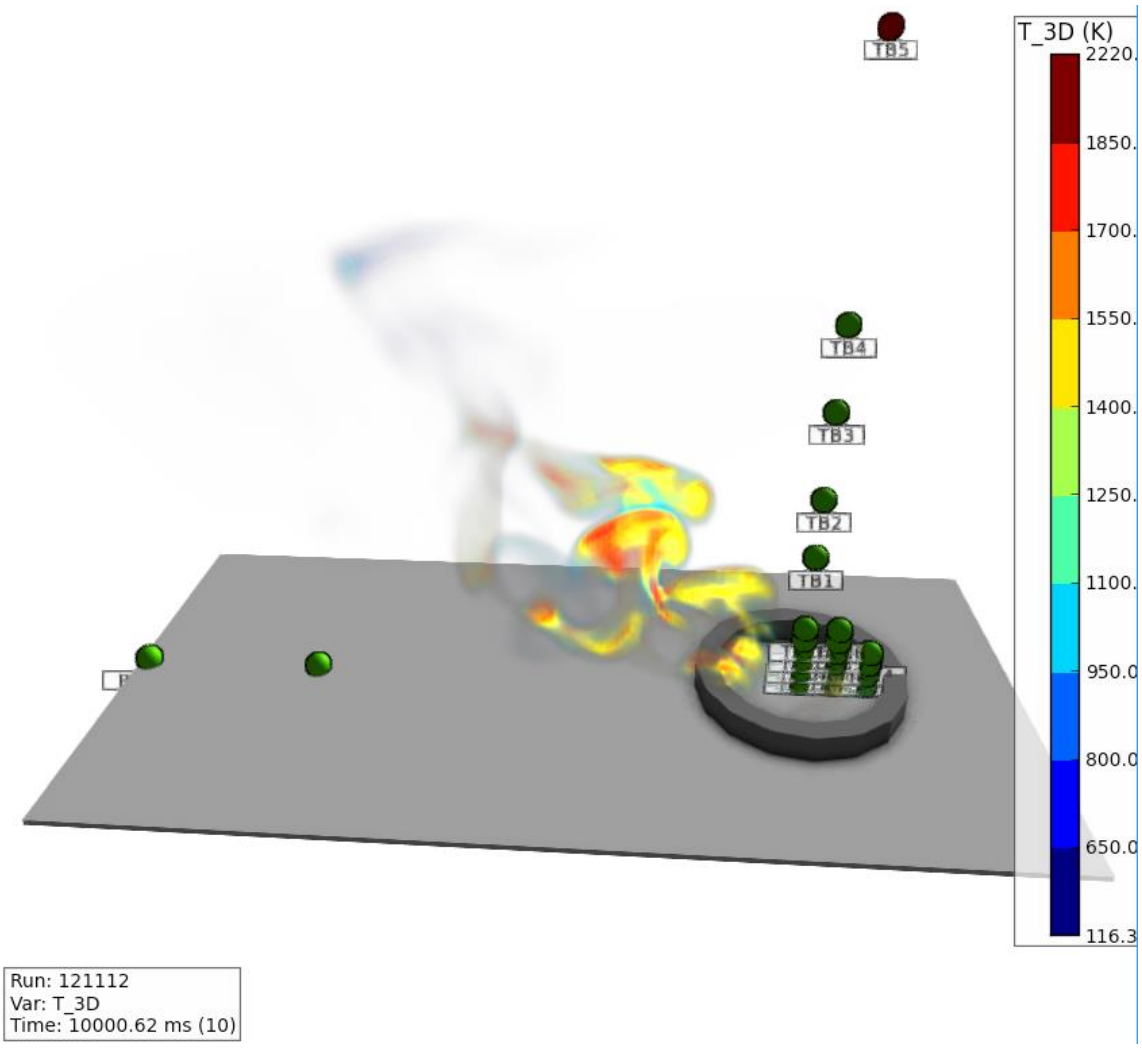

Figure 31: Wind effect in FLACS simulation

As it can be seen in the picture, wind effect is overly exaggerated in the simulations; this may lead to discrepancies in the results if wind is applied. Wind speed for experiment 1 is 2.10 m/s which is a fairly low value compared to average values, this means that for higher values, the effect will be even greater which could lead to errors in the simulation output.

Radiation is the final parameter simulated with FLACS-Fire; the results are displayed in the same graphical representation format. Results are reported in the following figure:

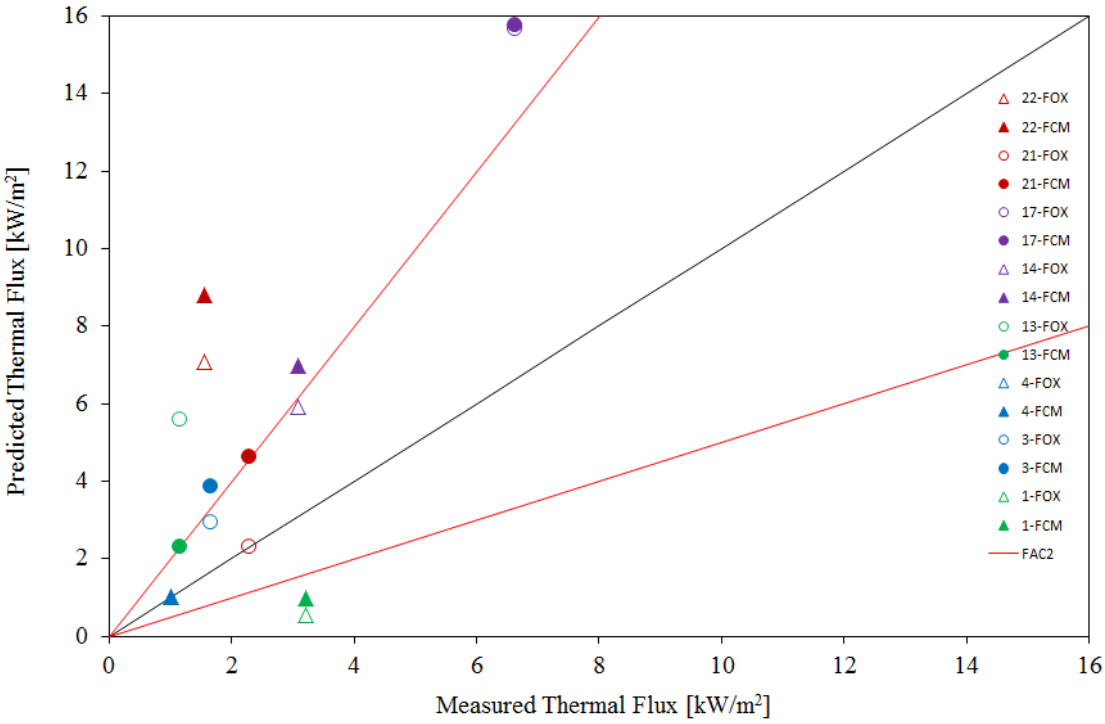

Figure 32: Average radiant heat flux predicted as a function of the experimental measurements.

Radiation is perhaps the most complicated parameter to model, and it affects directly the rest of the variables involved in the burning process, it controls the burning rate through the incident radiation that is absorbed by the fuel pool, which also affects the flame temperature. Results wise, radiation is, generally, the poorest modeled variable.

Experiment 17 is overestimated, being the average simulated value three times higher than the experimental data. This discrepancy is consistent with the fact that burning rate was highly overestimated too in this case, and temperatures were under predicted. Experiment 22 has forecasted values considerably higher than their experimental counterparts.

Soot models do not affect results excessively, except in the case of experiment 13 as it has been previously assessed. Generally, FOX predicts a lower radiation than FCM, which radiation wise, where over prediction occurs in most cases, it is a more precise approach.

To conclude, simulations 17, 22, 13, and 1 are completely out of the range limited by FAC2. Simulation 13 FCM is on the limit on being acceptable but FOX is absolutely out of range. Both simulations 14 are around the limit marked by FAC2, but on the over prediction side. 21 FOX agrees perfectly with the experimental data and FCM is on the border. Simulation 3 like 21, has its FOX trial agree well with the experimental data and FCM is out of range. Simulation 4 is agree perfectly with the experimental data, both FCM and FOX.

6.2.3 Final results, statistical comparison methods

Using as a reference F. Rigas (2005) [26], both the Fractional Bias (FB) and the Normalized mean square error (NMSE) are good approaches to determine the error within a set of data. FB indicates only systematic errors, which lead always to overestimate or underestimate values the measured values, the perfect value for FB would be zero, as it would bean there is no over or under estimation. NMSE measures both systematic and unsystematic (random) errors. The perfect value for the NMSE would be zero as well.

$$FB = \frac{1}{n}\sum_{i=1}^{n} 2\,\frac{y_m - y_e}{y_m + y_e} \qquad [57]$$

$$NMSE = \frac{1}{n}\sum_{i=1}^{n} 2\,\frac{\left(y_m^i - y_e^i\right)^2}{\overline{y_m}\;\overline{y_e}} \qquad [58]$$

y_m denotes the simulated values, and y_e the experimental ones. $\overline{y_m}$ and $\overline{y_e}$ are the averaged values for the simulated and experimental respectively.

Calculations were made with the data obtained with FLACS-Fire, and the results are shown in the next table:

Table 12: Statistical comparison methods

Simulation	Measurement	FB	NMSE	Simulation	Measurement	FB	NMSE
1-PM3-FOX	TB1	-0,10	0,013	**14-PM3-FOX**	TB1	-0,11	0,26
	TB2	-0,07	0,007		TB2	-0,01	0,27
	TB3	-0,05	0,003		TB3	-0,06	0,10
	TB4	0,14	0,037		TB4	0,03	0,04
	TB5	0,17	0,055		TB5	0,21	0,09
	RAD92	-1,27	6,313		RAD92	0,18	0,58
	BR	-0,17	0,200		BR	-0,07	11,73
1-PM3-FCM	TB1	-0,10	0,01	**14-PM3-FCM**	TB1	-0,12	0,27
	TB2	-0,07	0,01		TB2	-0,12	0,12
	TB3	-0,04	0,00		TB3	0,16	0,42
	TB4	0,15	0,05		TB4	-0,01	0,02
	TB5	0,19	0,07		TB5	0,13	0,05
	RAD92	-1,09	4,95		RAD92	0,14	0,71
	BR	-0,13	0,20		BR	-0,19	10,90
3-PM3-FOX	TB1	-0,09	0,49	**17-PM3-FOX**	TB1	-0,50	0,32
	TB2	-0,06	0,51		TB2	-0,34	0,14
	TB3	-0,09	0,46		TB3	-0,24	0,07
	TB4	-0,04	0,33		TB4	-0,09	0,01
	TB5	0,00	0,16		TB5	0,27	0,15

	RAD92	0,28	0,52		RAD92	0,57	0,77
	BR	-0,18	0,17		BR	0,98	34,71
3-PM3-FCM	TB1	-0,19	0,47	**17-PM3-FCM**	TB1	-0,50	0,32
	TB2	-0,14	0,47		TB2	-0,34	0,14
	TB3	-0,25	0,46		TB3	-0,24	0,07
	TB4	-0,04	0,33		TB4	-0,08	0,01
	TB5	-0,06	0,10		TB5	0,30	0,17
	RAD92	0,49	0,76		RAD92	0,62	0,99
	BR	-0,17	0,21		BR	1,00	36,49
4-PM3-FOX	TB1	0,14	0,42	**21-PM3-FOX**	TB1	0,20	0,50
	TB2	0,17	0,44		TB2	0,32	0,42
	TB3	0,10	0,47		TB3	0,32	0,21
	TB4	0,13	0,31		TB4		
	TB5	0,14	0,19		TB5		
	RAD92	0,40	0,69		RAD92	0,02	0,68
	BR	-0,25	0,76		BR	-0,23	0,26
4-PM3-FCM	TB1	0,15	0,39	**21-PM3-FCM**	TB1	-0,08	0,32
	TB2	0,11	0,44		TB2	0,04	0,11
	TB3	0,16	0,42		TB3	0,21	0,10
	TB4	0,17	0,26		TB4		
	TB5	0,16	0,13		TB5		
	RAD92	0,48	0,91		RAD92	0,51	0,87
	BR	-0,31	0,68		BR	-0,14	0,19
13-PM3-FOX	TB1	0,05	0,39	**22-PM3-FOX**	TB1	0,12	0,05
	TB2	0,25	0,45		TB2	0,26	0,10
	TB3	0,12	0,31		TB3	0,51	0,39
	TB4	0,22	0,38		TB4		
	TB5	0,20	0,21		TB5		
	RAD92	1,01	2,45		RAD92	-1,29	6,10
	BR	0,53	12,79		BR	0,71	5,19
13-PM3-FCM	TB1	-0,39	0,50	**22-PM3-FCM**	TB1	0,08	0,06
	TB2	-0,16	0,22		TB2	0,20	0,08
	TB3	-0,09	0,12		TB3	0,38	0,20
	TB4	-0,10	0,11		TB4		
	TB5	-0,03	0,04		TB5		
	RAD92	0,55	0,78		RAD92	1,11	9,12
	BR	0,52	12,48		BR	0,71	5,39

The results obtained are in concordance with the comments previously stated, and the discrepancies show on the calculated data. Radiation has unacceptable values, except for a few simulations. FAC2 was a very useful and fast approach to discriminate, which values were accepted or not. FAC2, on the other hand is a broad spectrum of data, which depending on the application might not be a good approach, therefore a statistical maximum could be fixed and the data filtered with that criteria.

As it can be seen simulations 1, 3, 14, and 17 have most values underestimated, and the rest of the simulations (22, 21, and 4) are all overestimated. In the case of 13, as it has been already commented before FOX model shows values well above the experimental data, and on the other hand FCM is the contrary which is rather contradictory with the rest of the set of simulations.

7 7. Conclusions

The objective of the present work has been validation of the FLACS-Fire v10.5 code by modeling gasoline and diesel pool fires of 1.5, 3, and 4 meters. The combustion model used was the Magnussens´s Eddy Dissipation Concept (EDC). The predicted results were compared to experimental values provided by the CERTEC. The EDC combustion model was used in combination with the Discrete Transfer Radiation model alongside with both soot formation models available; Formation Oxidation (FOX) and Conversion Factor model (FCM). Turbulence was modeled using the κ-ε turbulence model:

- Burning rate predictions agrees with measurements when values are lower than 0.15 kg/s (small pool diameters) or greater than 0.5 kg/s (larger diameters), but overestimates largely the gasoline pool fires with values in between.

- The PM1 fire model cannot completely simulate most of the fire scenarios as it burns more fuel than these being evaporated.

- Predicted temperatures reasonably agree with those measured. Particularly, forecasted values are closed to values measured when simulating pool fires bigger than 1.5 m diameter.

- Radiation values are not estimated as correctly as the other two parameters, most of the experiments comply reasonably, but experiments 14, 17, 22, and 1 show the largest discrepancies.

- Soot model does not affect significantly the results obtained and discrepancies were found to be almost nonexistent. Experiment 13 shows large inconsistencies between both models, depending on the conditions of the measurement. Comparing both FOX and FCM, FCM shows overall better performance, except in the case of radiation, which FOX shows generally better results.

- Grid analysis determined that cell values above 0.1x0.1x0.1 lead to imprecise results. A finer grid of 0.05x0.05x0.05 resulted in a slightly better outcome but with higher computational requirements. Computational time in a simulator that can only perform using one core is a very valuable asset.

- Radiation models differ on the results. DTM shows results with a better concordance to the experimental data than SixFlux. SixFlux on the other hand requires less computational time, given the same mesh.

- Wind affects the simulations greatly, proposed experiments have little to none wind speed. Cases where wind is a key parameter could suffer from discrepancies in various parameters.

- Fuels used in the simulations approximate the real ones. It was assumed that gasoline could be replaced with hexane, and diesel with dodecane. FLACS does not grant any accessible possibility to introduce new fuels.

- FLACS-Fire is presented as a simulator that can only use one core per simulator. This enormous limitation for any simulation that is wished to be made with a fine grid; or one involving a large space. This limitation hindered the progress of the present thesis because of the increase in the simulation time.

- FLACS-Fire reaches stationary state almost automatically which hinders the study of a non-stationary phase. Initial moments of the fire and the decaying phase cannot be studied correctly using FLACS-Fire.

- Results are in concordance with authors such as N. Perdersen (2012) and L. Skarsbø (2011). In most cases, the parameters studied are overestimated to some degree.

8 Recommendations for future work

FLACS is still developing its Fire module so future improvements are to be expected. Validations of future tools as well as many other that are already implemented should be done. Suggestions for further work include:

- Run simulations under the uncoupled approach that FLACS already offers.
- Modeling of confined fires, and the effects of confinement on the flame simulation.
- Thorough investigation of the wind influence in the simulations performed, as well as, other possible simulated cases.
- Analysis of the flame geometry through temperature slices of the fire.
- Simulations with larger pool fires (5 and 6 meters) could be done with the experimental data provided by the CERTEC.
- DTM model should be further analyzed varying the available parameters to obtain better radiation results.
- A grid sensitivity analysis involving finer grids could be performed to determine whether results could be improved.
- Run simulations for the whole duration of the experiment in order to see any possible fluctuation in the values.
- Check differences among combustion models Mixed Is Burned (MIB) and the already used EDC.

9 References

1. GexCon. FLACS v10.4 User's Manual 2015.
2. M. Muñoz, J. Arnaldos, J. Casal, E. Planas (2004). "Analysis of the geometric and radiative characteristics of hydrocarbon pool fires." Combustion and Flame 139: 263-277.
3. E. Planas, J.M. Chatris, C. López, J. Arnaldos (2003). "Determination of flame emissivity in hydrocarbon pool fires using infrared thermography." Fire Technology 39: 261-273.
4. F. Ferrero, M. Muñoz, J. Arnaldos (2007). "Effect of thin-layer boilover on flame geometry and dynamics in large hydrocarbon pool fires." Fuel Processing Technology 88: 227-235.
5. J.M Chandris, J. Quintela, J. Folch, E. Planas, J. Arnaldos, J. Casal (2001). "Experimental study of burning rate in hydrocarbon pool fires." Combustion and Flame 126: 1373-1383.
6. M. Muñoz, E. Planas, F. Ferrero, J. Casal (2007). "Predicting the emissive power of hydrocarbon pool fires." Journal of Hazardous Materials 144: 725-729.
7. F. Ferrero, J. Arnaldos (2006). "Incendios de hidrocarburos: Estudio de la formación y evolución de boilover de capa fina."
8. M. Muñoz, E. Planas, J. Casal (2005). "Estudio de los parámetros que intervienen en la modelización de los efectos de grandes incendios de hidrocarburo: geometría y radiación térmica de la llama."
9. Natalja Pedersen (2012). "Modeling of jet and pool fires and validation of the fire model in the CFD code FLACS."
10. Lars Roar Skarsbø (2011). "An experimental study of pool fires and validation of different CFD fire models."
11. S. Malkeson, T. Jones, R. English (2015). "Jet fire computational fluid dynamics simulations: Validation from an industrial and consultancy perspective."
12. C. Gutiérrez, E. Sanmiguel, A. Viedma, G. Rein (2009). "Experimental data and numerical modelling of 1.3 and 2.3 MW fires in a 20m cubic atrium." Building and Environment 44: 1827-1839.
13. http://www.nfpa.org/news-and-research/news-and-media/press-room/reporters-guide-to-fire-and-nfpa/all-about-fire
14. http://www.firesure.ie/fire_safety_guidance/theory_of_fire.html
15. https://www.nist.gov/%3Cfront%3E/fire-dynamics
16. Hurley, Morgan J., SFPE: "SFPE Handbook of fire protection Engineering". New York, Springer, 2016, 5th edition
17. Kuzmin, D. (2006). "Introduction to Computational Fluid Dynamics". AIAA Journal Vol. 44: 193–193.

18. Koteswara Reddy G, Kiran Yarrakula (2016). "Analysis of Accidents in Chemical Process Industries in the period 1998-2015". International Journal of ChemTech Research vol.9: 177-191
19. J. Casal, M. Gómez-Mares, M. Muñoz, A. Palacios (2012). "Jet Fires: a "Minor" Fire Hazard?". Chemical Engineering Transactions Vol. 26: 13-20.
20. S. Biao, G. Kaihua (2010). "LNG Accident dynamic simulation: Application for hazardous consequence reduction".
21. P. Van Hees, J. Wahlqvist, S. Hostikka, T. Sikanen, T. Magnusson, F. Jörud (2012). "Prediction and validation of pool fire development in enclosures by means of CFD models for risk assessment of nuclear power plants". Nordic Nuclear Safety Research.
22. P. Middha (2010). "Development, use, and validation of the CFD tool for hydrogen safety studies".
23. K. McGrattan, S. Hostikka, R. McDermott, J. Floyd, C. Weinschenk, K. Overholt (2010) "Fire Dynamics Simulator technical reference guide volume 3: Validation".
24. https://www.researchgate.net/figure/273456236_fig3_Figure-3-Pool-fire-heat-transfer-scheme.
25. J. C Chang, S. R. Hanna (2004). "Air quality performance evaluation", Meteorol. Atmos. Phys. vol. 38: 167-196.
26. F. Rigas, S. Sklavounos (2005). "Simulation of Coyote series trials - Part II: A computational approach to ignition and combustion of flammable vapor clouds", Chem. Eng. Sci. 61:1444–1452.

Appendix A- Simulation results

This appendix contains the full graphical representation of the data obtained through the simulations cited in this thesis.

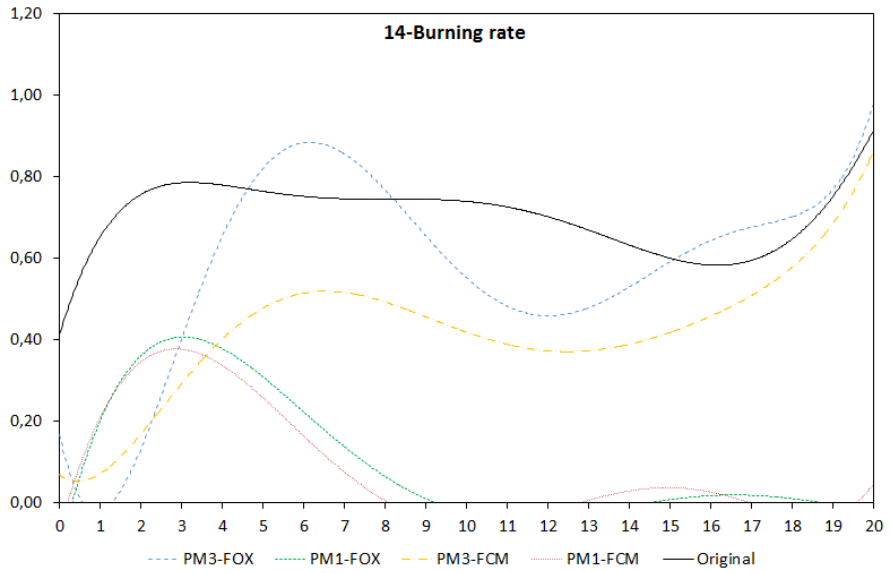

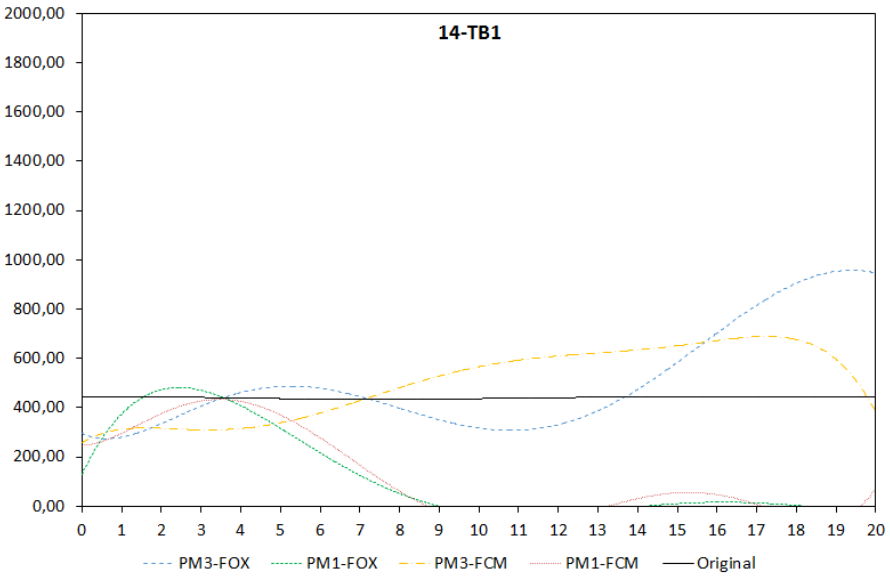

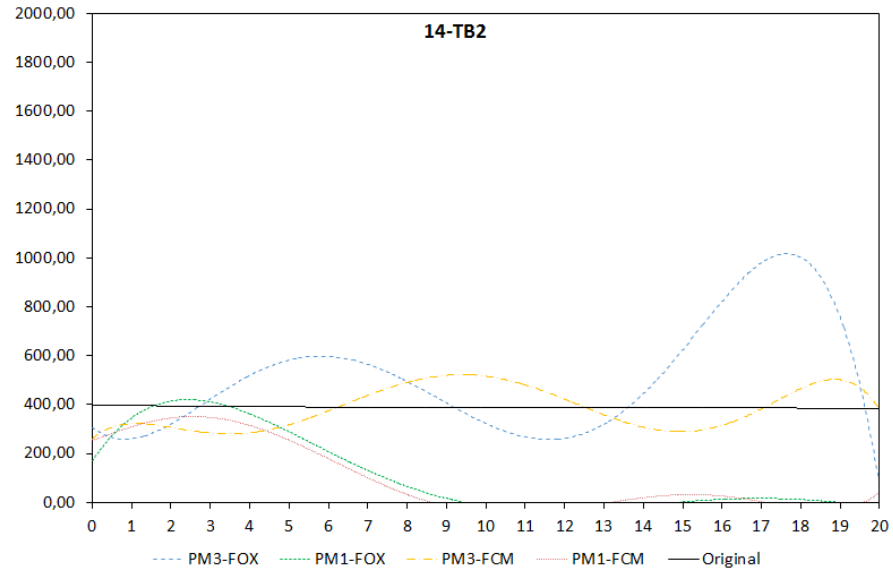
14-TB2
2000,00
1800,00
1600,00
1400,00
1200,00
1000,00
800,00
600,00
400,00
200,00
0,00
0 1 2 3 4 5 6 7 8 9 10 11 12 13 14 15 16 17 18 19 20
PM3-FOX
PM1-FOX
PM3-FCM
PM1-FCM
Original

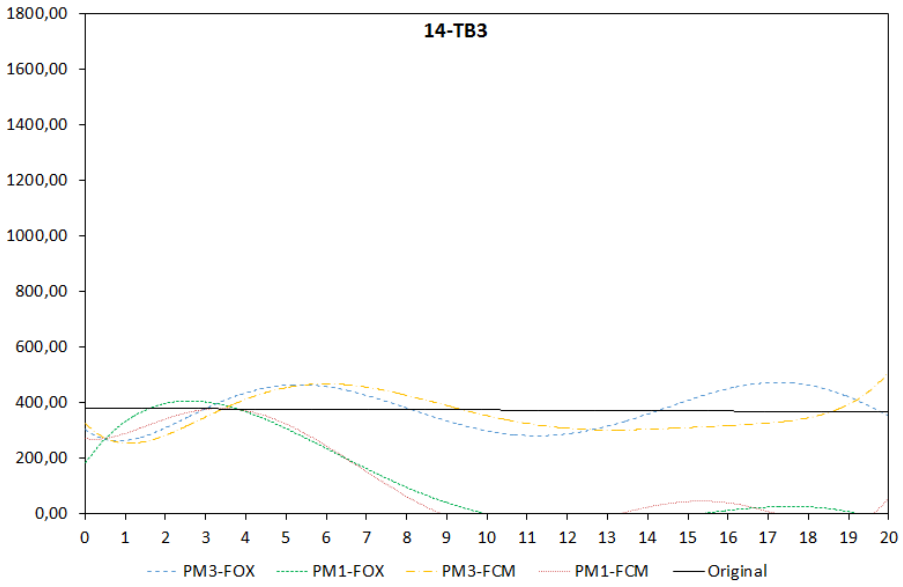
14-TB3
1800,00
1600,00
1400,00
1200,00
1000,00
800,00
600,00
400,00
200,00
0,00
0 1 2 3 4 5 6 7 8 9 10 11 12 13 14 15 16 17 18 19 20
PM3-FOX
PM1-FOX
PM3-FCM
PM1-FCM
Original

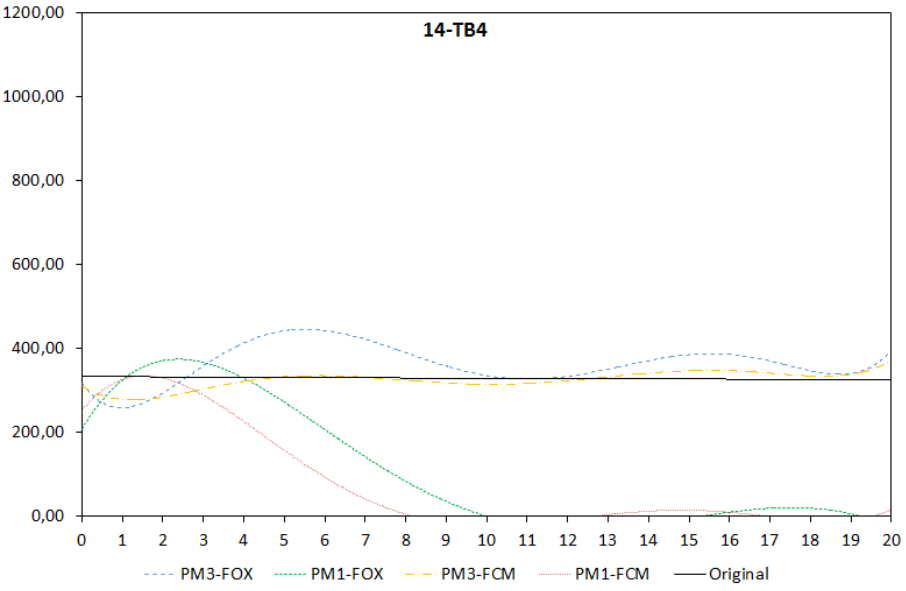
14-TB4
1200,00
1000,00
800,00
600,00
400,00
200,00
0,00
0 1 2 3 4 5 6 7 8 9 10 11 12 13 14 15 16 17 18 19 20
PM3-FOX
PM1-FOX
PM3-FCM
PM1-FCM
Original

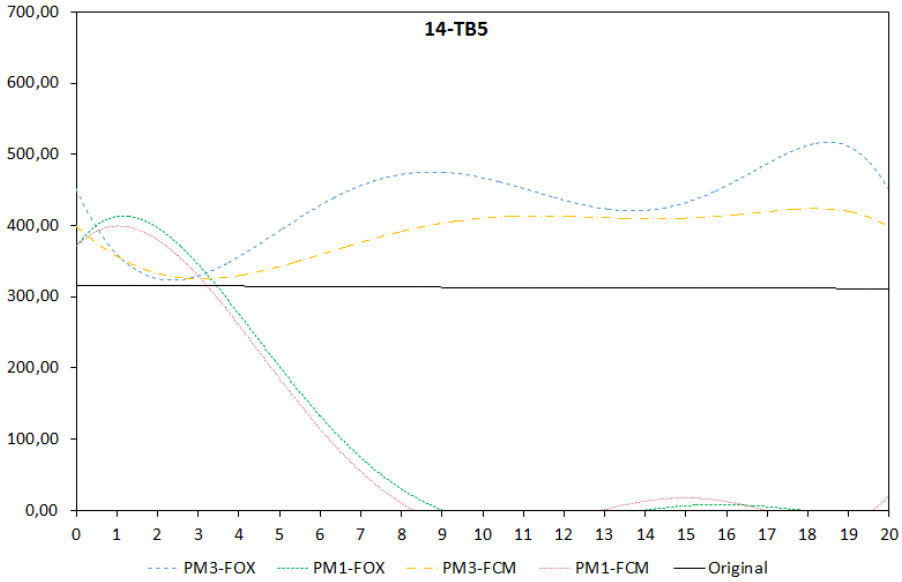
14-TB5
700,00
600,00
500,00
400,00
300,00
200,00
100,00
0,00
0 1 2 3 4 5 6 7 8 9 10 11 12 13 14 15 16 17 18 19 20
PM3-FOX
PM1-FOX
PM3-FCM
PM1-FCM
Original

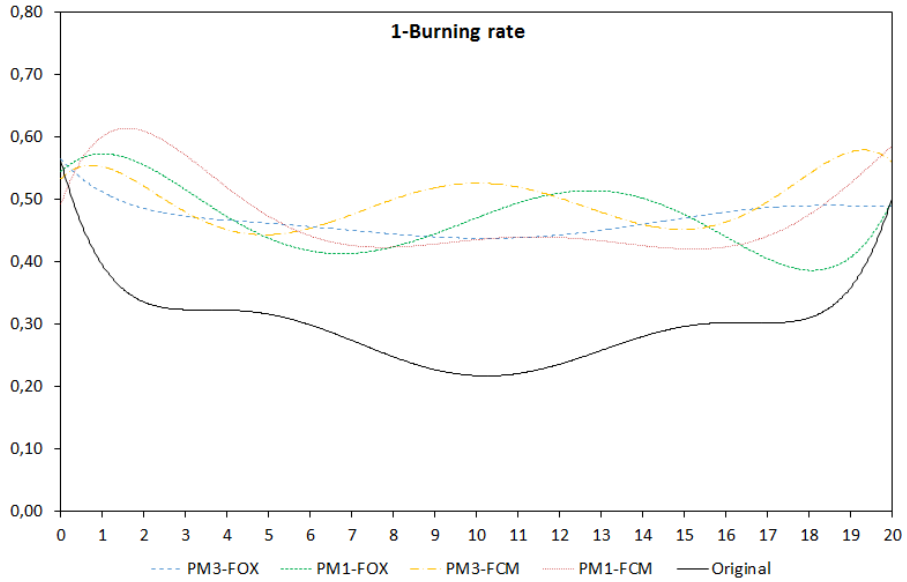
1-Burning rate
0,80
0,70
0,60
0,50
0,40
0,30
0,20
0,10
0,00
0 1 2 3 4 5 6 7 8 9 10 11 12 13 14 15 16 17 18 19 20
PM3-FOX
PM1-FOX
PM3-FCM
PM1-FCM
Original

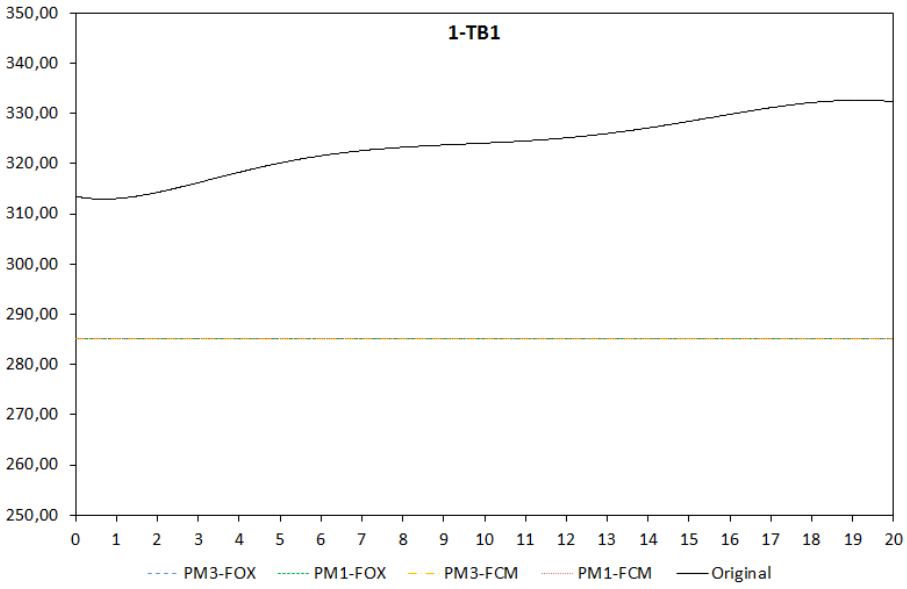
1-TB1
350,00
340,00
330,00
320,00
310,00
300,00
290,00
280,00
270,00
260,00
250,00
0 1 2 3 4 5 6 7 8 9 10 11 12 13 14 15 16 17 18 19 20
PM3-FOX
PM1-FOX
PM3-FCM
PM1-FCM
Original

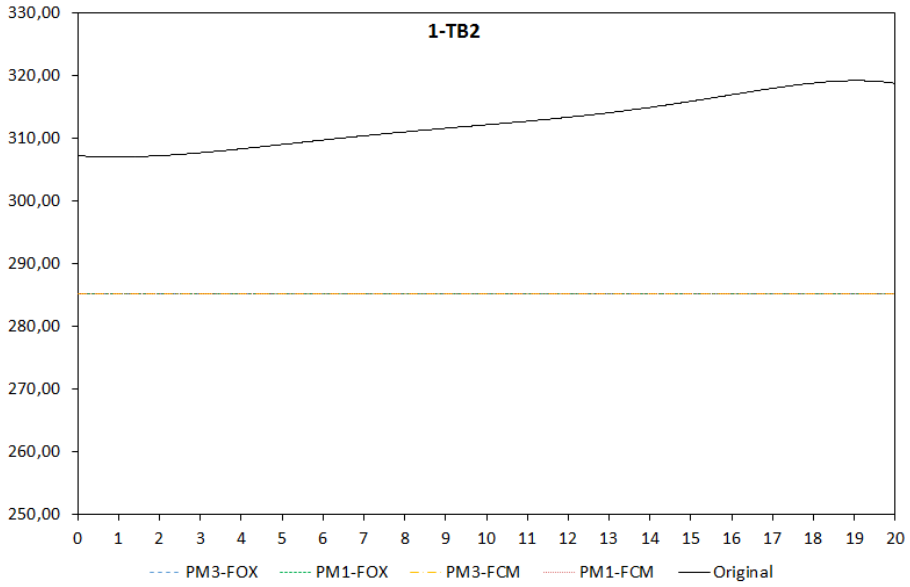
1-TB2
330,00
320,00
310,00
300,00
290,00
280,00
270,00
260,00
250,00
0 1 2 3 4 5 6 7 8 9 10 11 12 13 14 15 16 17 18 19 20
PM3-FOX
PM1-FOX
PM3-FCM
PM1-FCM
Original

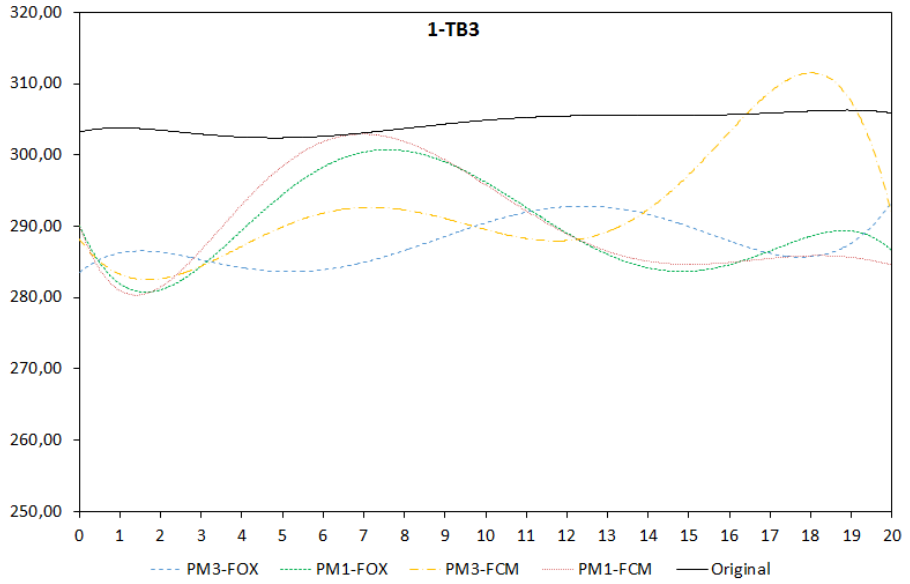
1-TB3
320,00
310,00
300,00
290,00
280,00
270,00
260,00
250,00
0 1 2 3 4 5 6 7 8 9 10 11 12 13 14 15 16 17 18 19 20
PM3-FOX
PM1-FOX
PM3-FCM
PM1-FCM
Original

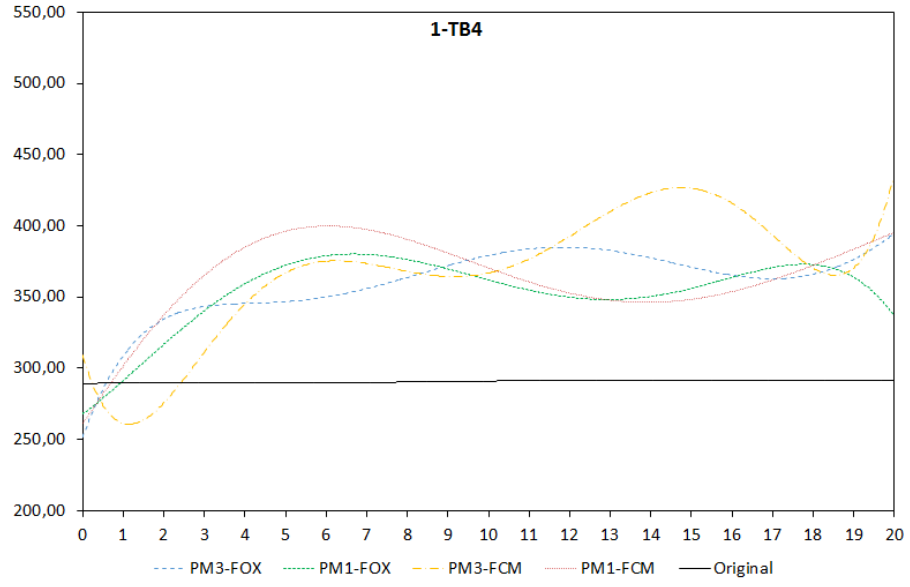
1-TB4
550,00
500,00
450,00
400,00
350,00
300,00
250,00
200,00
0 1 2 3 4 5 6 7 8 9 10 11 12 13 14 15 16 17 18 19 20
PM3-FOX
PM1-FOX
PM3-FCM
PM1-FCM
Original

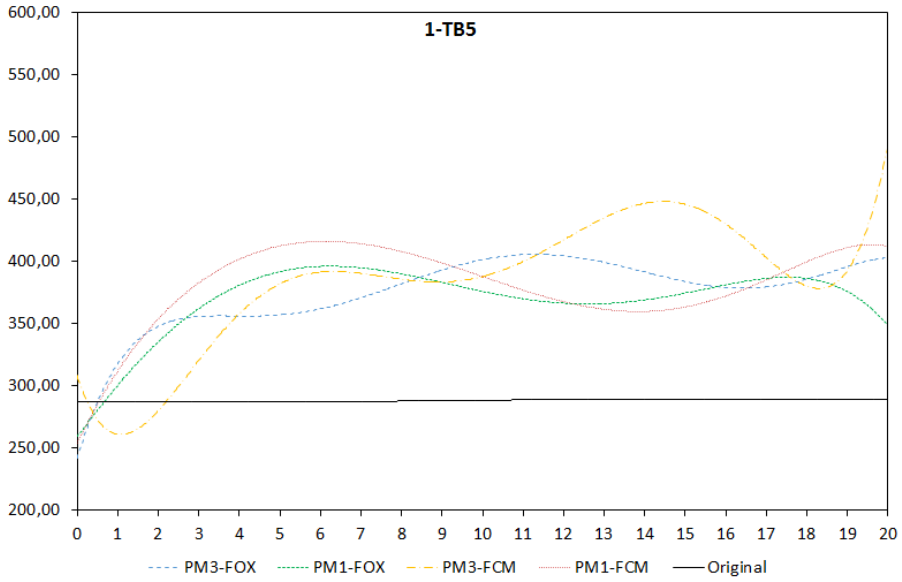
1-TB5
600,00
550,00
500,00
450,00
400,00
350,00
300,00
250,00
200,00
0 1 2 3 4 5 6 7 8 9 10 11 12 13 14 15 16 17 18 19 20
PM3-FOX
PM1-FOX
PM3-FCM
PM1-FCM
Original

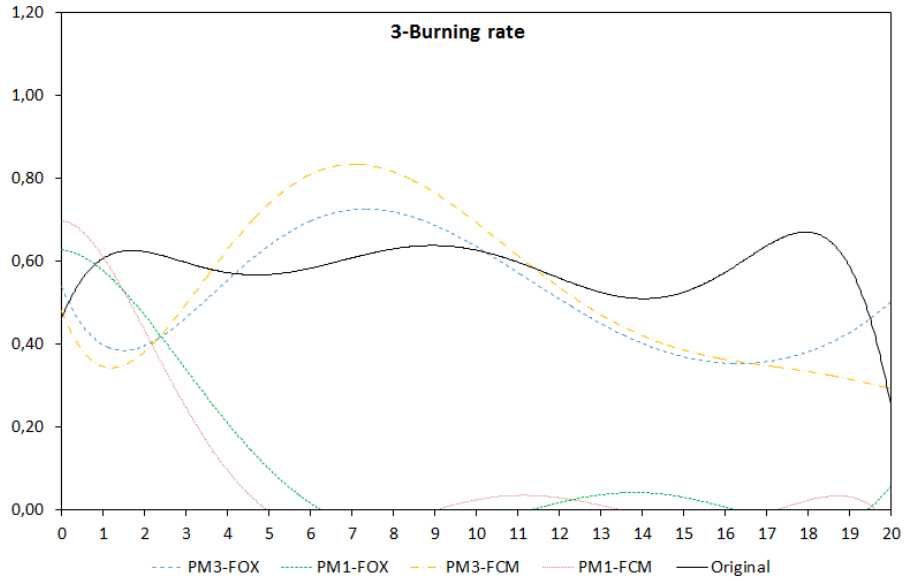
3-Burning rate
1,20
1,00
0,80
0,60
0,40
0,20
0,00
0 1 2 3 4 5 6 7 8 9 10 11 12 13 14 15 16 17 18 19 20
PM3-FOX
PM1-FOX
PM3-FCM
PM1-FCM
Original

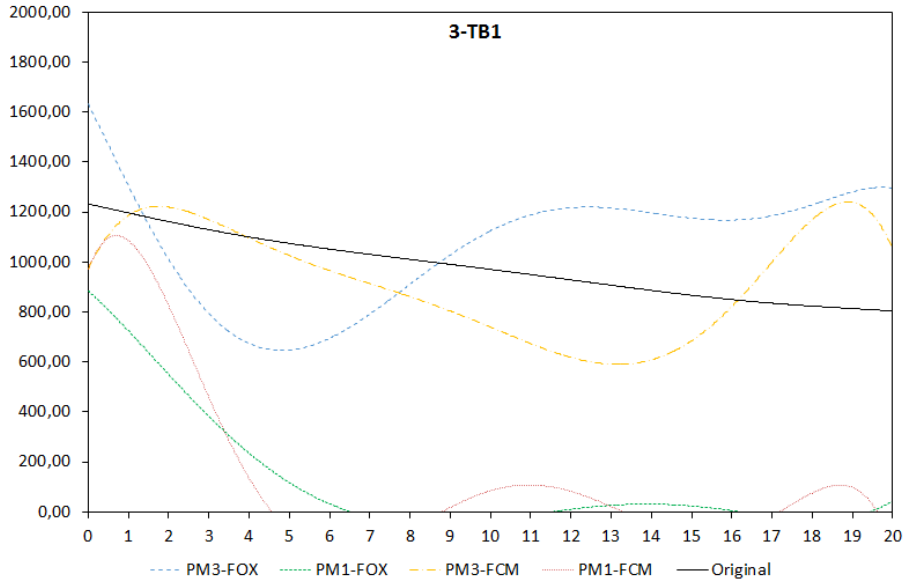
3-TB1
2000,00
1800,00
1600,00
1400,00
1200,00
1000,00
800,00
600,00
400,00
200,00
0,00
0 1 2 3 4 5 6 7 8 9 10 11 12 13 14 15 16 17 18 19 20
PM3-FOX
PM1-FOX
PM3-FCM
PM1-FCM
Original

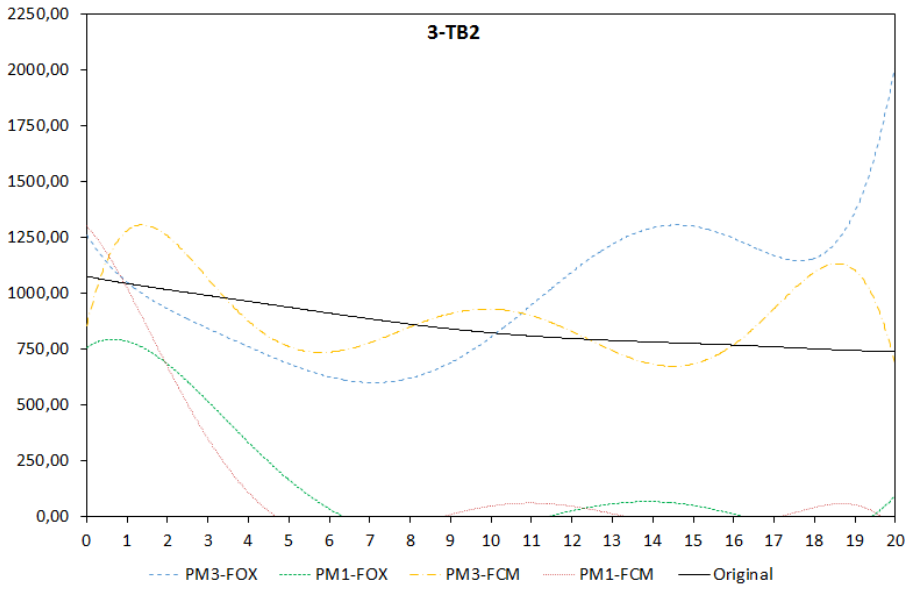
3-TB2
2250,00
2000,00
1750,00
1500,00
1250,00
1000,00
750,00
500,00
250,00
0,00
0 1 2 3 4 5 6 7 8 9 10 11 12 13 14 15 16 17 18 19 20
PM3-FOX
PM1-FOX
PM3-FCM
PM1-FCM
Original

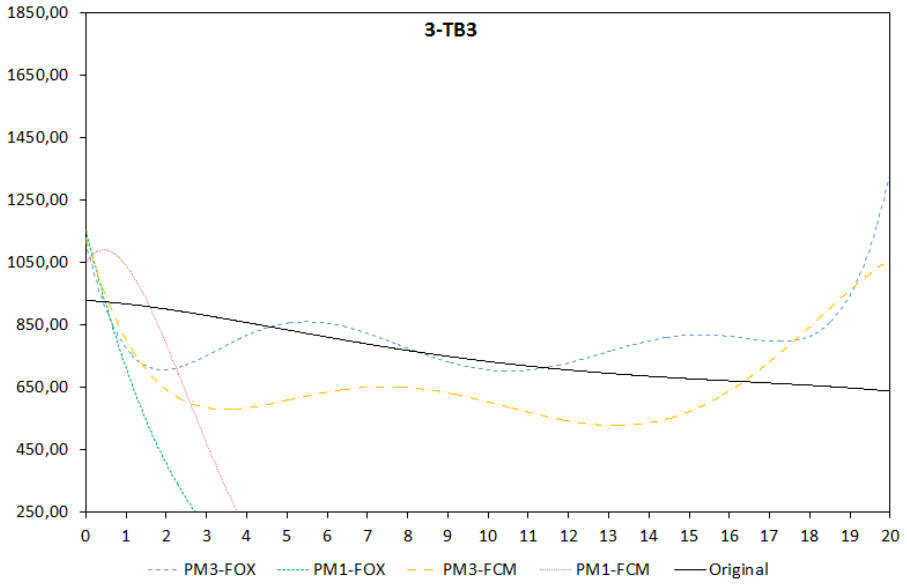
3-TB3
1850,00
1650,00
1450,00
1250,00
1050,00
850,00
650,00
450,00
250,00
0 1 2 3 4 5 6 7 8 9 10 11 12 13 14 15 16 17 18 19 20
PM3-FOX
PM1-FOX
PM3-FCM
PM1-FCM
Original

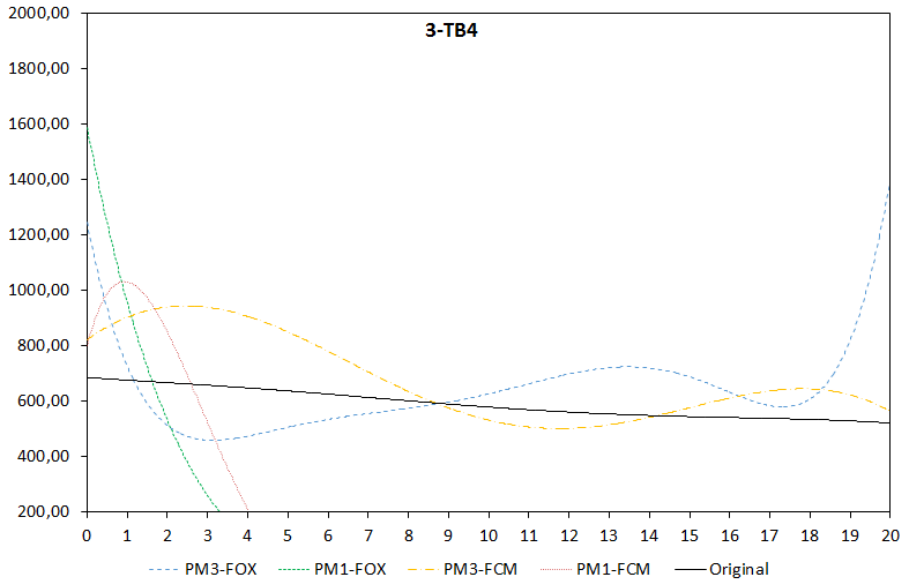
3-TB4
2000,00
1800,00
1600,00
1400,00
1200,00
1000,00
800,00
600,00
400,00
200,00
0 1 2 3 4 5 6 7 8 9 10 11 12 13 14 15 16 17 18 19 20
PM3-FOX
PM1-FOX
PM3-FCM
PM1-FCM
Original

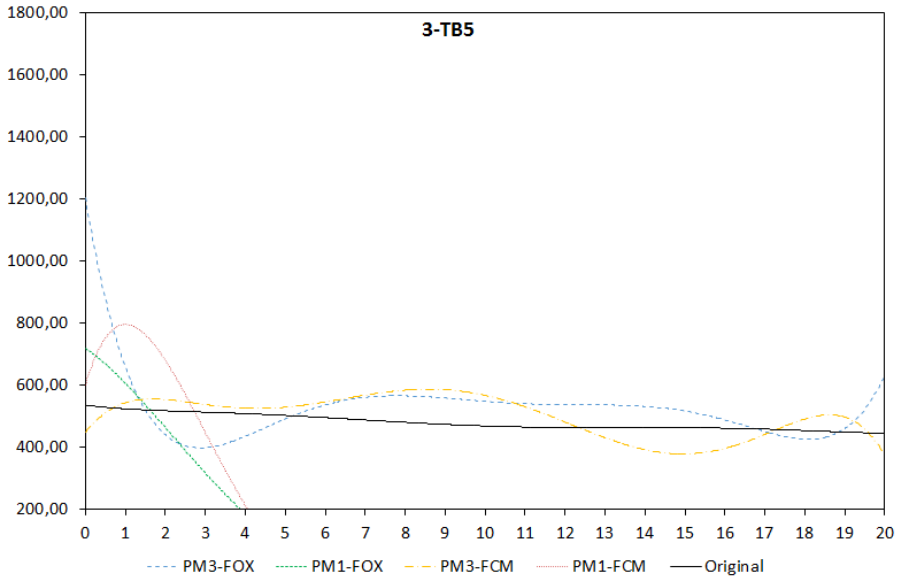
3-TB5
1800,00
1600,00
1400,00
1200,00
1000,00
800,00
600,00
400,00
200,00
0 1 2 3 4 5 6 7 8 9 10 11 12 13 14 15 16 17 18 19 20
PM3-FOX
PM1-FOX
PM3-FCM
PM1-FCM
Original

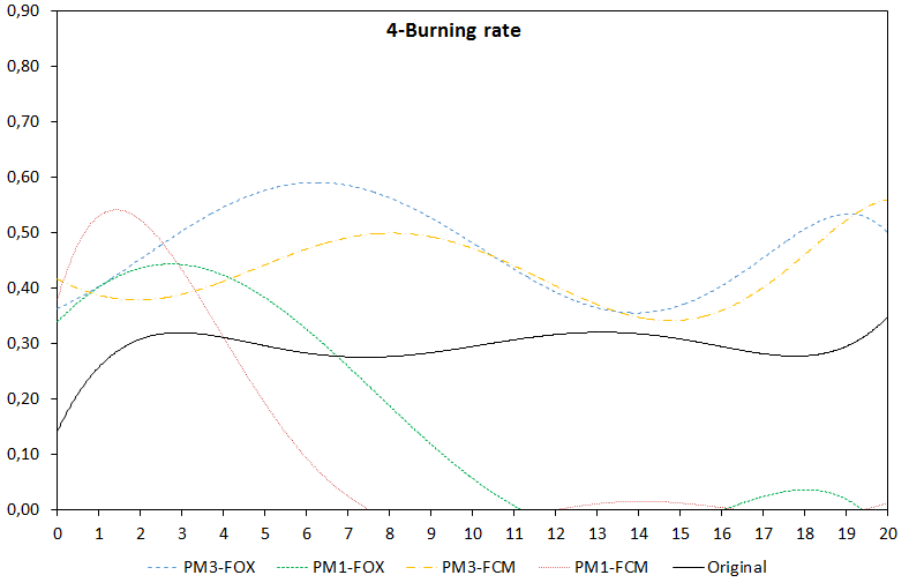
4-Burning rate
0,90
0,80
0,70
0,60
0,50
0,40
0,30
0,20
0,10
0,00
0 1 2 3 4 5 6 7 8 9 10 11 12 13 14 15 16 17 18 19 20
PM3-FOX
PM1-FOX
PM3-FCM
PM1-FCM
Original

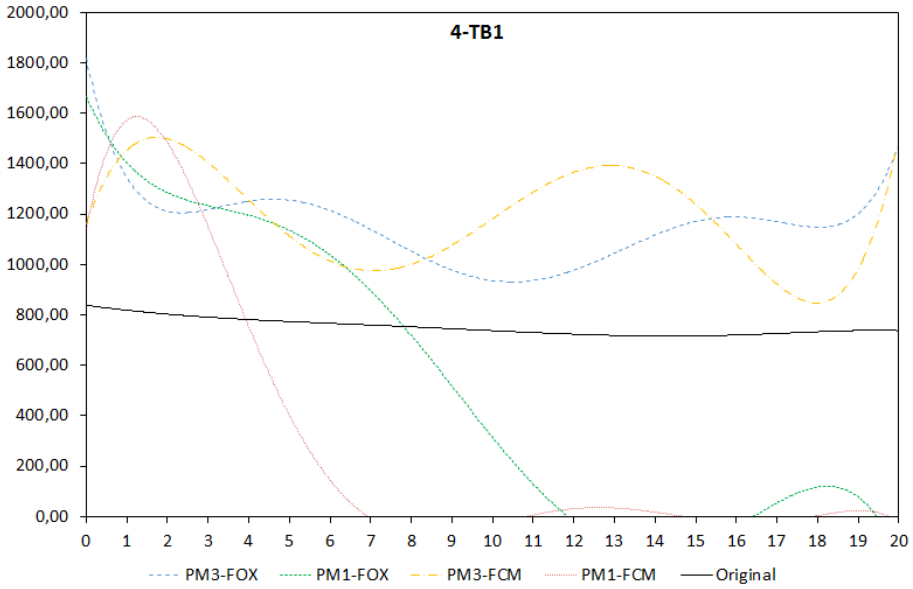
4-TB1
2000,00
1800,00
1600,00
1400,00
1200,00
1000,00
800,00
600,00
400,00
200,00
0,00
0 1 2 3 4 5 6 7 8 9 10 11 12 13 14 15 16 17 18 19 20
PM3-FOX
PM1-FOX
PM3-FCM
PM1-FCM
Original

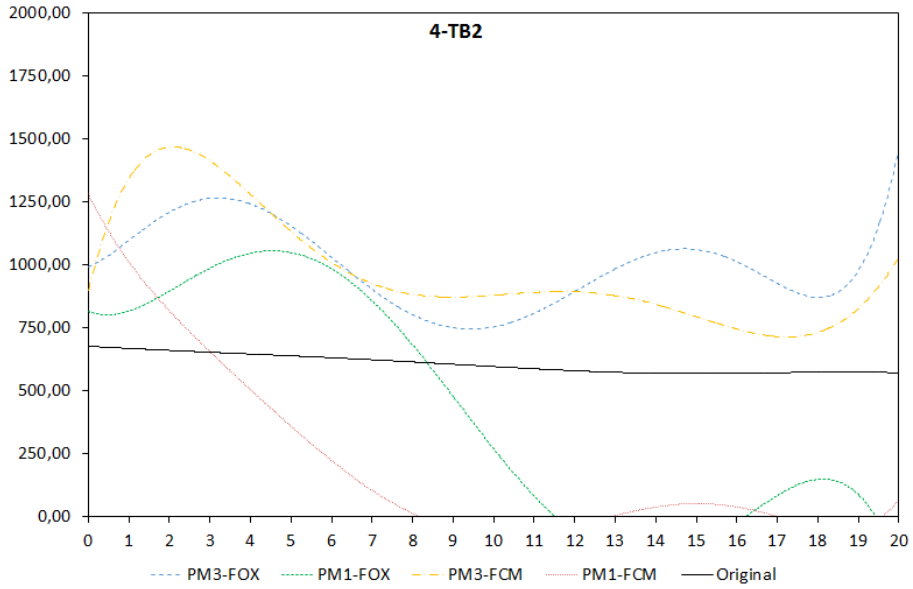
4-TB2
2000,00
1750,00
1500,00
1250,00
1000,00
750,00
500,00
250,00
0,00
0 1 2 3 4 5 6 7 8 9 10 11 12 13 14 15 16 17 18 19 20
PM3-FOX
PM1-FOX
PM3-FCM
PM1-FCM
Original

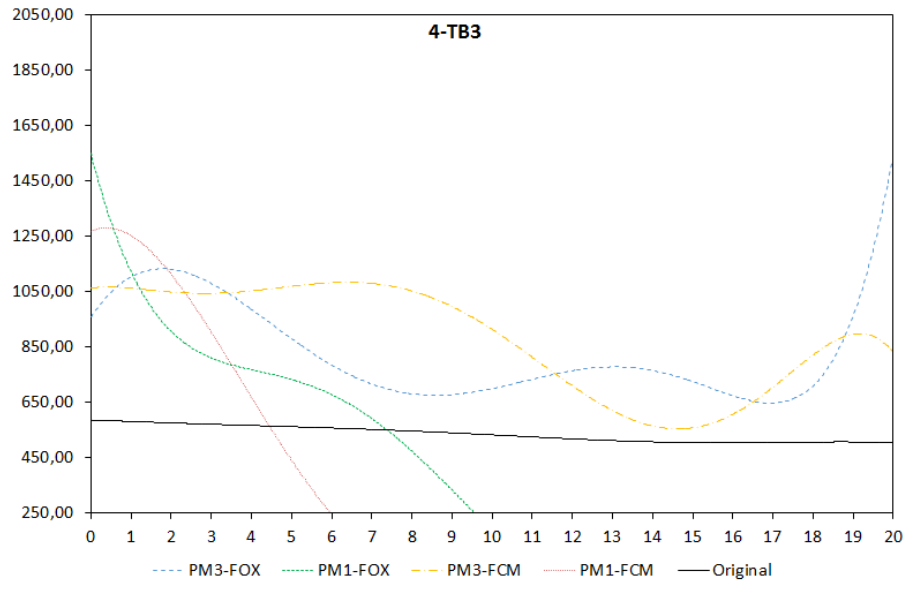
4-TB3
2050,00
1850,00
1650,00
1450,00
1250,00
1050,00
850,00
650,00
450,00
250,00
0 1 2 3 4 5 6 7 8 9 10 11 12 13 14 15 16 17 18 19 20
PM3-FOX
PM1-FOX
PM3-FCM
PM1-FCM
Original

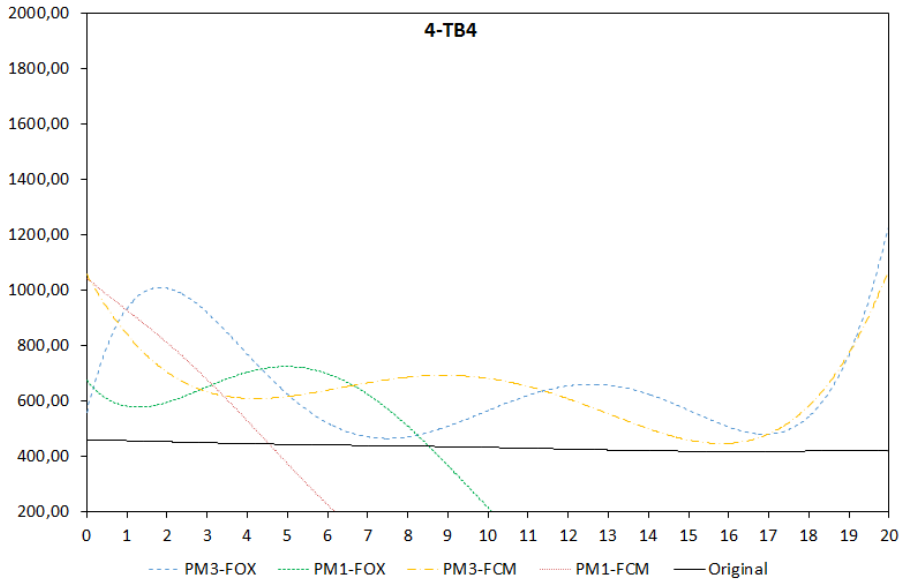
4-TB4
2000,00
1800,00
1600,00
1400,00
1200,00
1000,00
800,00
600,00
400,00
200,00
0 1 2 3 4 5 6 7 8 9 10 11 12 13 14 15 16 17 18 19 20
PM3-FOX
PM1-FOX
PM3-FCM
PM1-FCM
Original

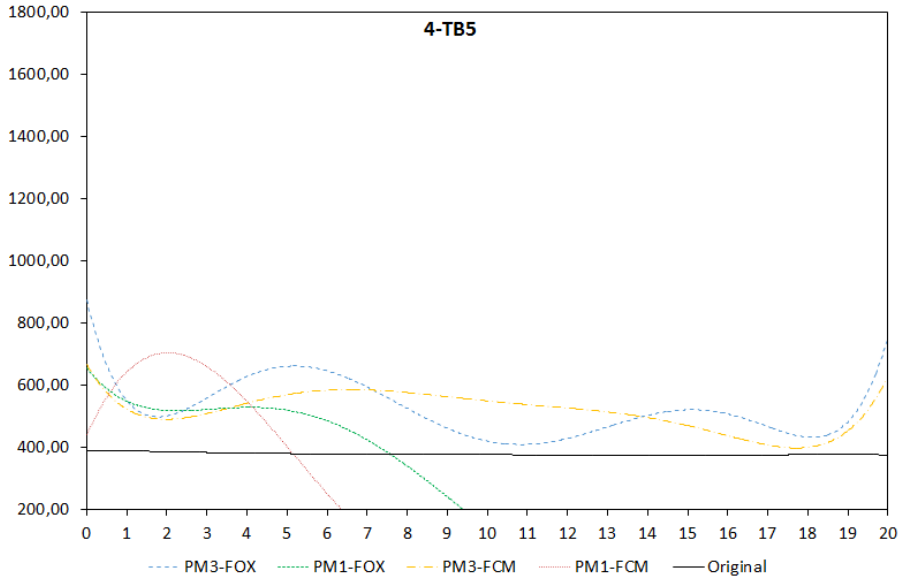
4-TB5
1800,00
1600,00
1400,00
1200,00
1000,00
800,00
600,00
400,00
200,00
0 1 2 3 4 5 6 7 8 9 10 11 12 13 14 15 16 17 18 19 20
PM3-FOX
PM1-FOX
PM3-FCM
PM1-FCM
Original

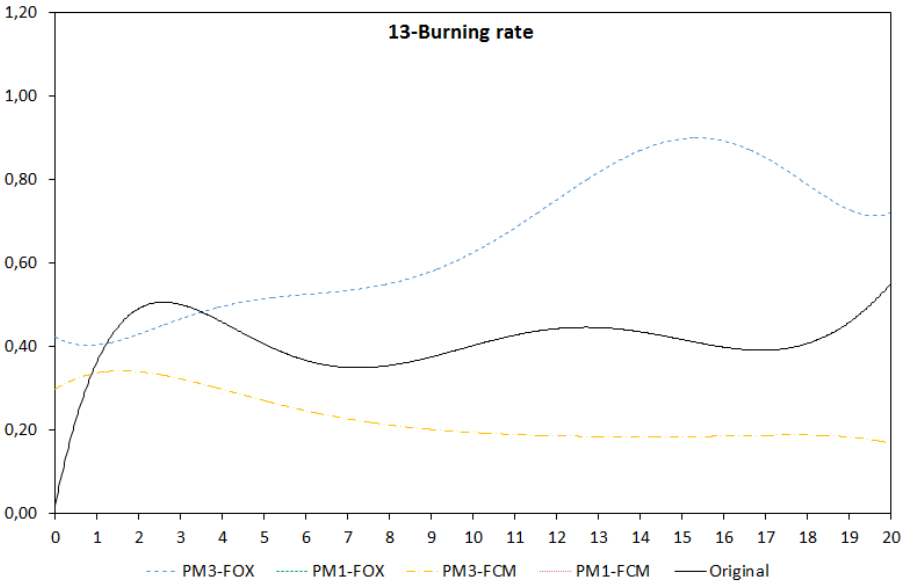
13-Burning rate
1,20
1,00
0,80
0,60
0,40
0,20
0,00
0 1 2 3 4 5 6 7 8 9 10 11 12 13 14 15 16 17 18 19 20
PM3-FOX
PM1-FOX
PM3-FCM
PM1-FCM
Original

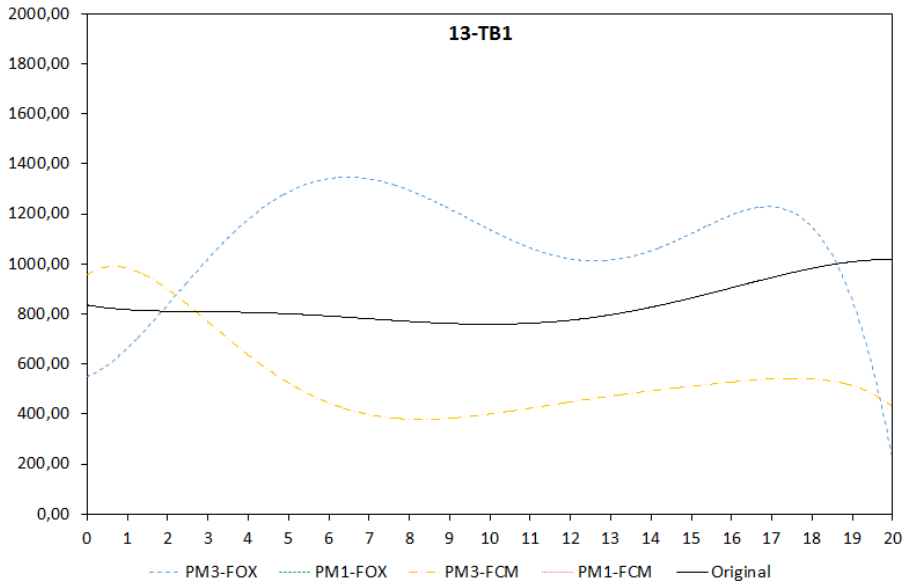
13-TB1
2000,00
1800,00
1600,00
1400,00
1200,00
1000,00
800,00
600,00
400,00
200,00
0,00
0 1 2 3 4 5 6 7 8 9 10 11 12 13 14 15 16 17 18 19 20
PM3-FOX
PM1-FOX
PM3-FCM
PM1-FCM
Original

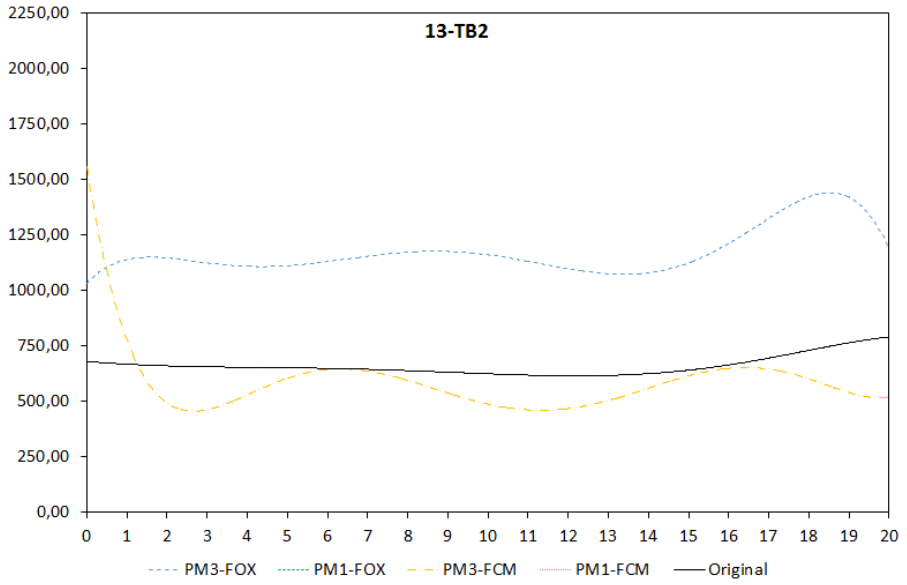
13-TB2
2250,00
2000,00
1750,00
1500,00
1250,00
1000,00
750,00
500,00
250,00
0,00
0 1 2 3 4 5 6 7 8 9 10 11 12 13 14 15 16 17 18 19 20
PM3-FOX
PM1-FOX
PM3-FCM
PM1-FCM
Original

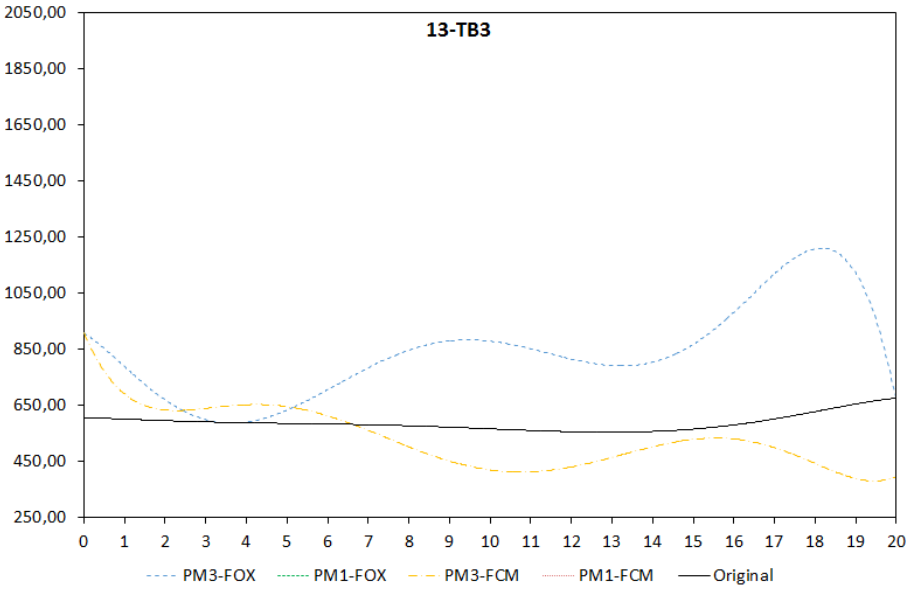
13-TB3
2050,00
1850,00
1650,00
1450,00
1250,00
1050,00
850,00
650,00
450,00
250,00
0 1 2 3 4 5 6 7 8 9 10 11 12 13 14 15 16 17 18 19 20
PM3-FOX
PM1-FOX
PM3-FCM
PM1-FCM
Original

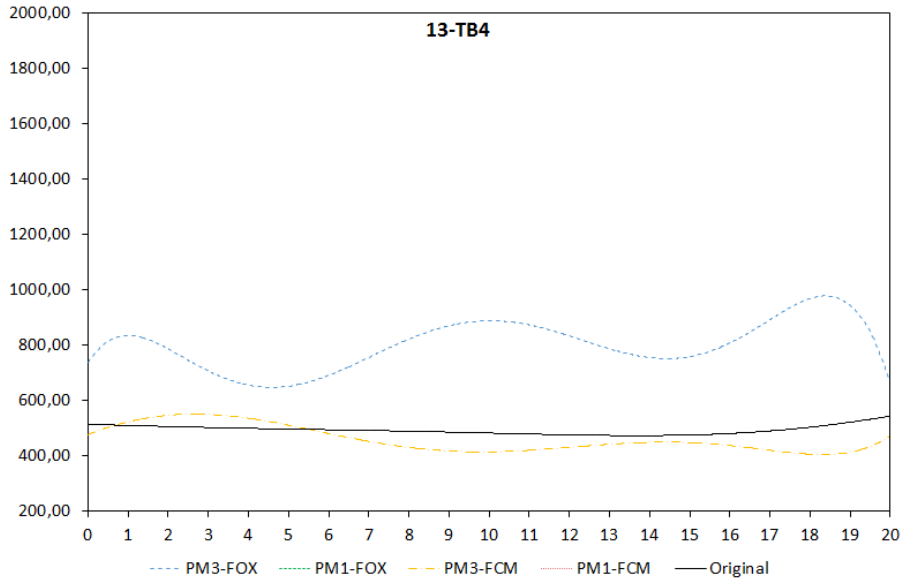
13-TB4
2000,00
1800,00
1600,00
1400,00
1200,00
1000,00
800,00
600,00
400,00
200,00
0 1 2 3 4 5 6 7 8 9 10 11 12 13 14 15 16 17 18 19 20
PM3-FOX
PM1-FOX
PM3-FCM
PM1-FCM
Original

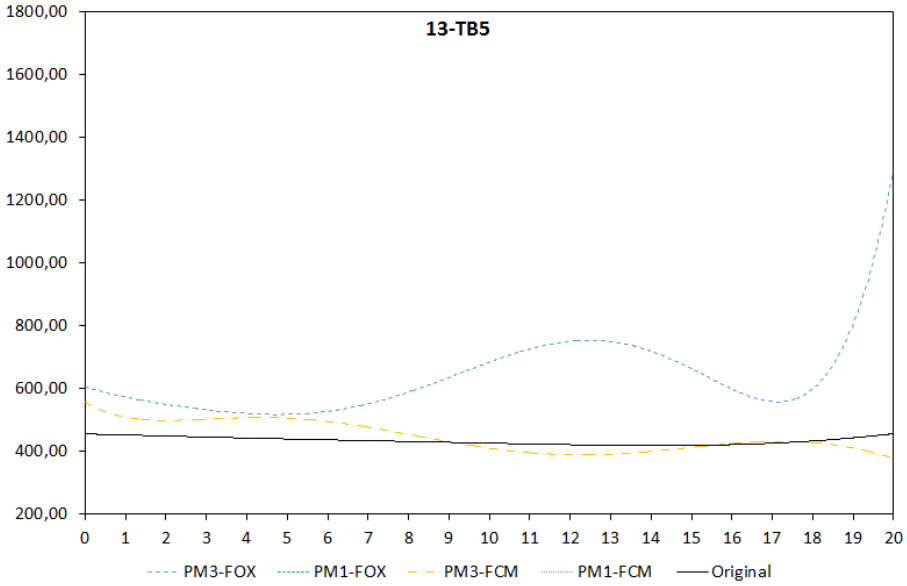
13-TB5
1800,00
1600,00
1400,00
1200,00
1000,00
800,00
600,00
400,00
200,00
0 1 2 3 4 5 6 7 8 9 10 11 12 13 14 15 16 17 18 19 20
PM3-FOX
PM1-FOX
PM3-FCM
PM1-FCM
Original

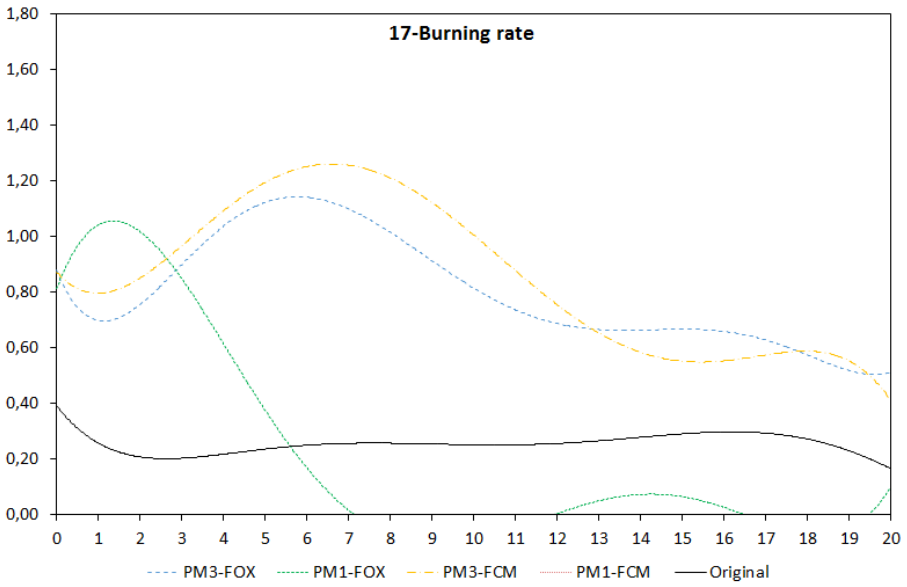
17-Burning rate
1,80
1,60
1,40
1,20
1,00
0,80
0,60
0,40
0,20
0,00
0 1 2 3 4 5 6 7 8 9 10 11 12 13 14 15 16 17 18 19 20
PM3-FOX
PM1-FOX
PM3-FCM
PM1-FCM
Original

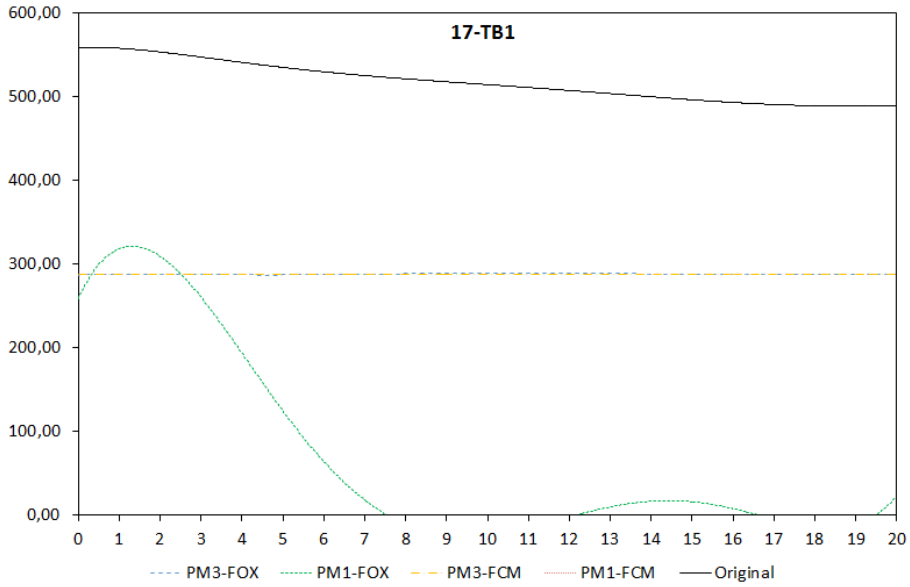
17-TB1
600,00
500,00
400,00
300,00
200,00
100,00
0,00
0 1 2 3 4 5 6 7 8 9 10 11 12 13 14 15 16 17 18 19 20
PM3-FOX
PM1-FOX
PM3-FCM
PM1-FCM
Original

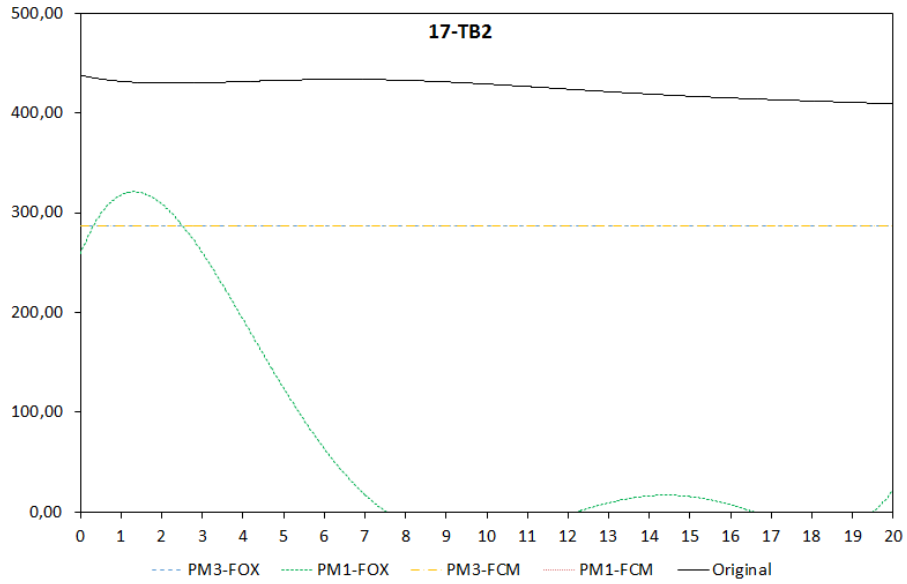
17-TB2
500,00
400,00
300,00
200,00
100,00
0,00
0 1 2 3 4 5 6 7 8 9 10 11 12 13 14 15 16 17 18 19 20
PM3-FOX
PM1-FOX
PM3-FCM
PM1-FCM
Original

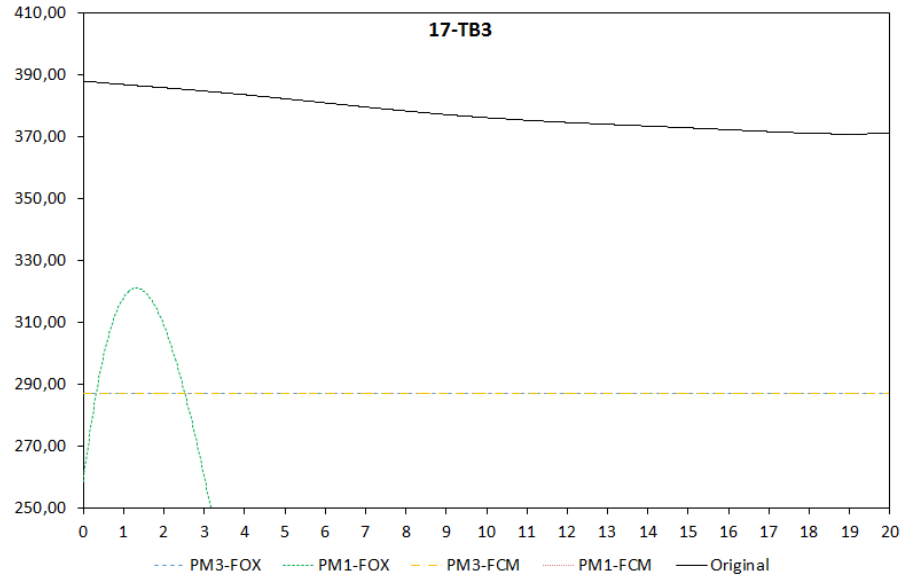
17-TB3
410,00
390,00
370,00
350,00
330,00
310,00
290,00
270,00
250,00
0 1 2 3 4 5 6 7 8 9 10 11 12 13 14 15 16 17 18 19 20
PM3-FOX
PM1-FOX
PM3-FCM
PM1-FCM
Original

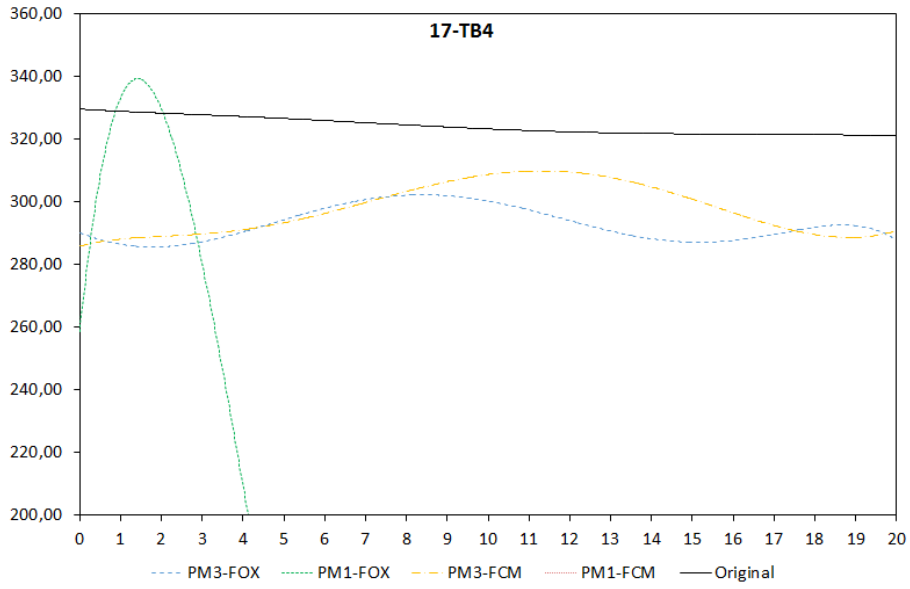
17-TB4
360,00
340,00
320,00
300,00
280,00
260,00
240,00
220,00
200,00
0 1 2 3 4 5 6 7 8 9 10 11 12 13 14 15 16 17 18 19 20
PM3-FOX
PM1-FOX
PM3-FCM
PM1-FCM
Original

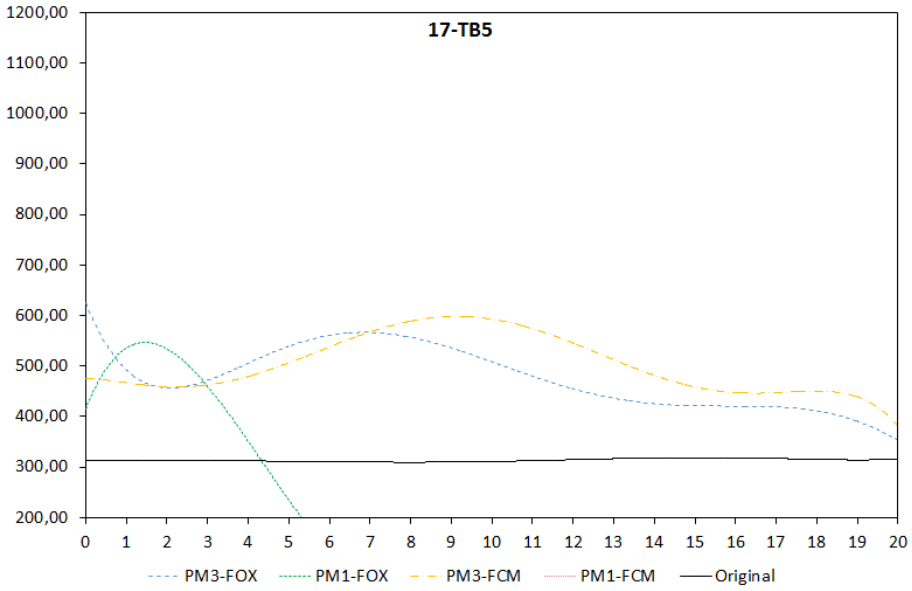
17-TB5
1200,00
1100,00
1000,00
900,00
800,00
700,00
600,00
500,00
400,00
300,00
200,00
0 1 2 3 4 5 6 7 8 9 10 11 12 13 14 15 16 17 18 19 20
PM3-FOX
PM1-FOX
PM3-FCM
PM1-FCM
Original

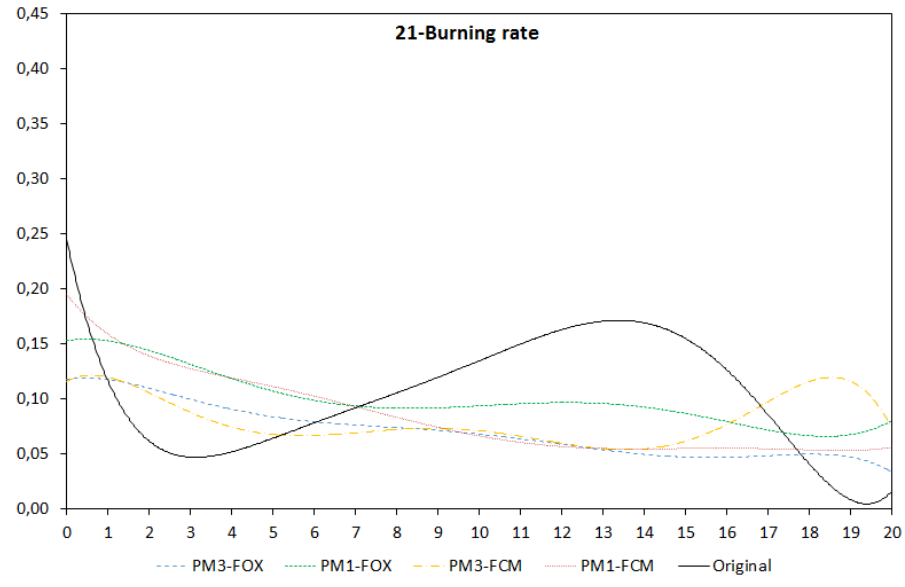
21-Burning rate
0,45
0,40
0,35
0,30
0,25
0,20
0,15
0,10
0,05
0,00
0 1 2 3 4 5 6 7 8 9 10 11 12 13 14 15 16 17 18 19 20
PM3-FOX
PM1-FOX
PM3-FCM
PM1-FCM
Original

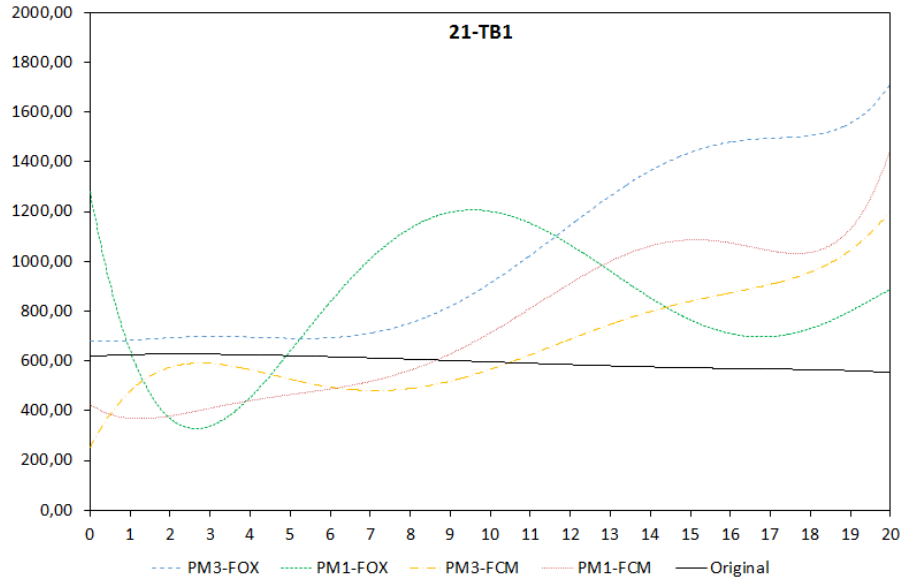
21-TB1
2000,00
1800,00
1600,00
1400,00
1200,00
1000,00
800,00
600,00
400,00
200,00
0,00
0 1 2 3 4 5 6 7 8 9 10 11 12 13 14 15 16 17 18 19 20
PM3-FOX
PM1-FOX
PM3-FCM
PM1-FCM
Original

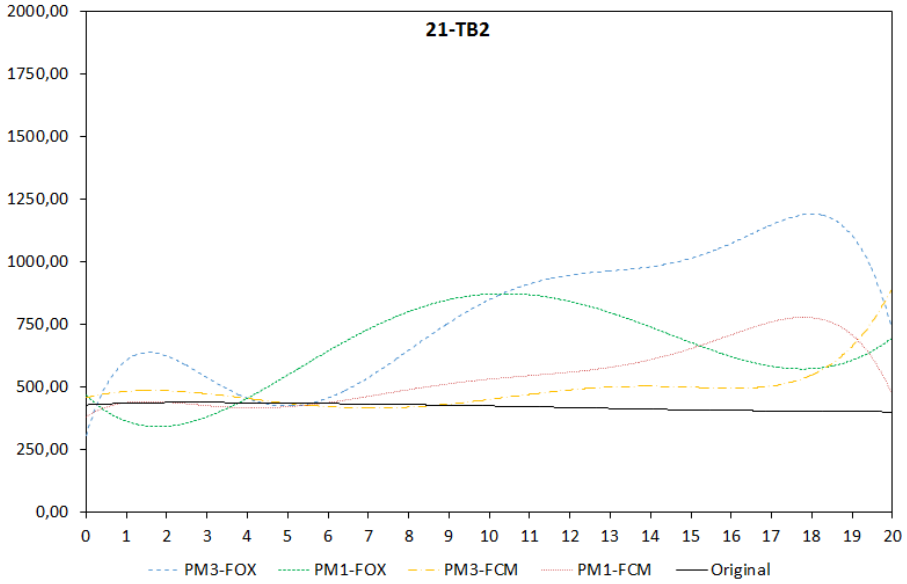
21-TB2
2000,00
1750,00
1500,00
1250,00
1000,00
750,00
500,00
250,00
0,00
0 1 2 3 4 5 6 7 8 9 10 11 12 13 14 15 16 17 18 19 20
PM3-FOX
PM1-FOX
PM3-FCM
PM1-FCM
Original

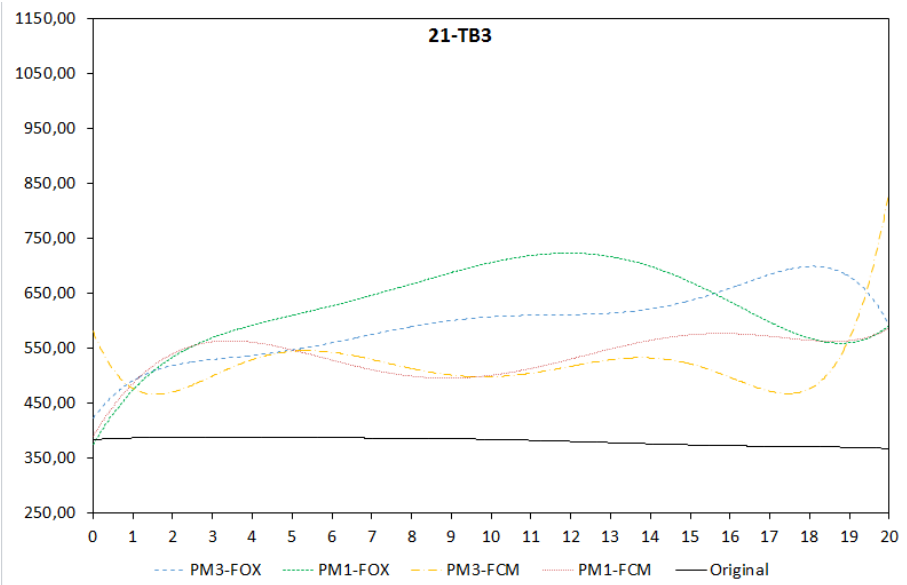
21-TB3
1150,00
1050,00
950,00
850,00
750,00
650,00
550,00
450,00
350,00
250,00
0 1 2 3 4 5 6 7 8 9 10 11 12 13 14 15 16 17 18 19 20
PM3-FOX
PM1-FOX
PM3-FCM
PM1-FCM
Original

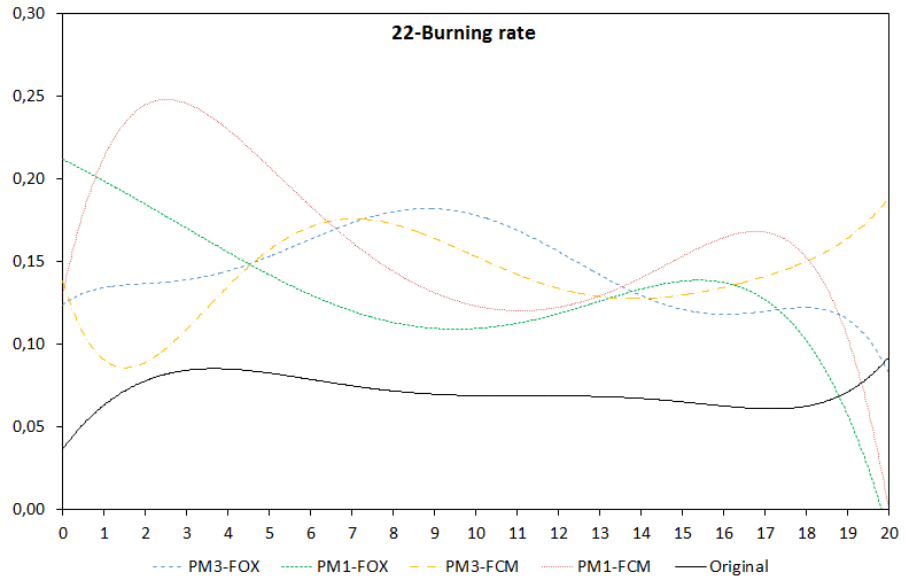
22-Burning rate
0,30
0,25
0,20
0,15
0,10
0,05
0,00
0 1 2 3 4 5 6 7 8 9 10 11 12 13 14 15 16 17 18 19 20
PM3-FOX
PM1-FOX
PM3-FCM
PM1-FCM
Original

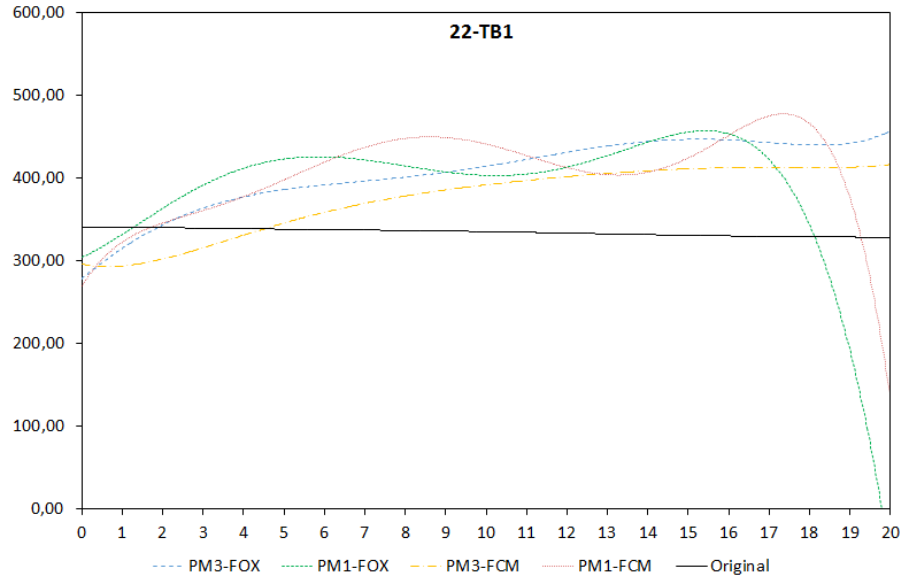
22-TB1
600,00
500,00
400,00
300,00
200,00
100,00
0,00
0 1 2 3 4 5 6 7 8 9 10 11 12 13 14 15 16 17 18 19 20
PM3-FOX
PM1-FOX
PM3-FCM
PM1-FCM
Original

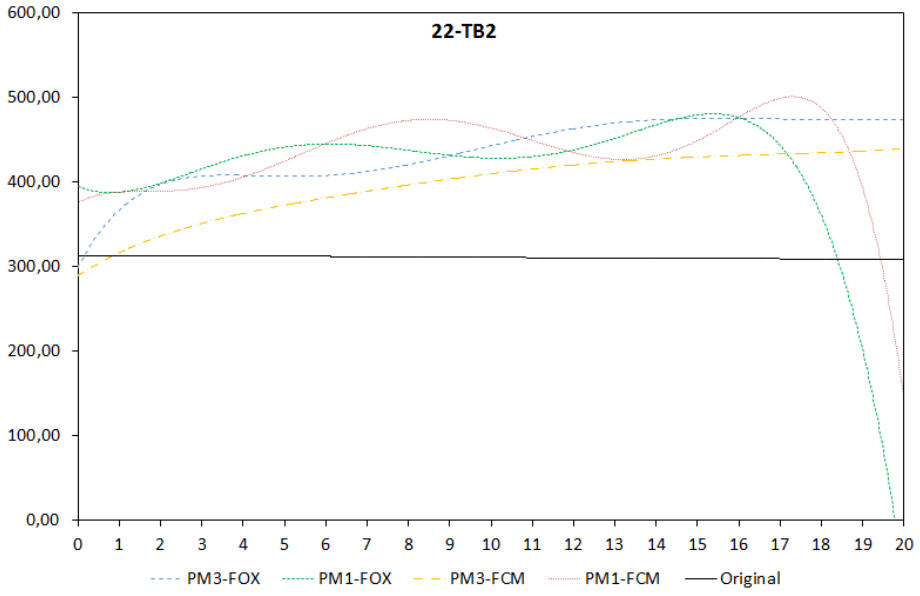
22-TB2
600,00
500,00
400,00
300,00
200,00
100,00
0,00
0 1 2 3 4 5 6 7 8 9 10 11 12 13 14 15 16 17 18 19 20
PM3-FOX
PM1-FOX
PM3-FCM
PM1-FCM
Original

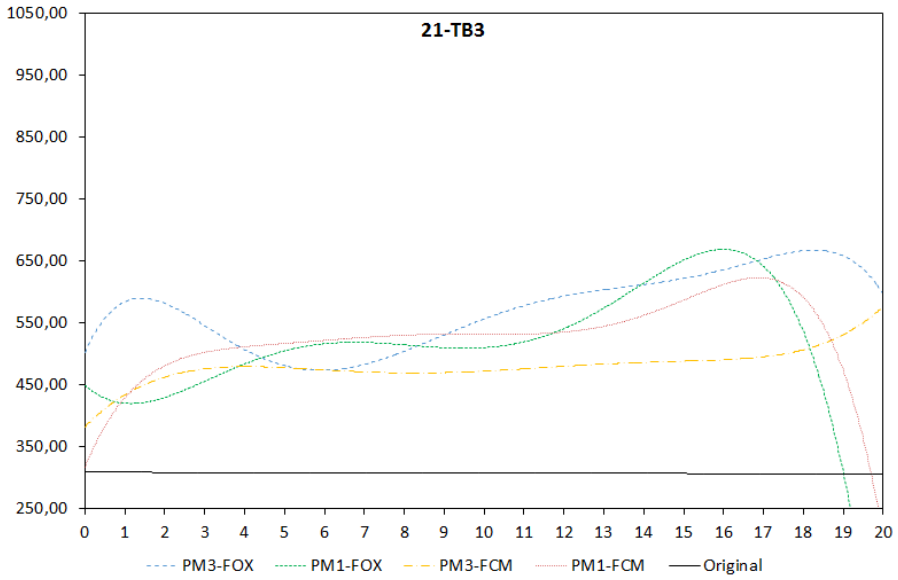

Appendix B – Quantification model uncertainty

Model uncertainty was calculated according to K. McGrattan et al. [23]. The following table is a recollection of estimations for the uncertainty that is inherent to the measurement of different variables.

Table 12: Uncertainty estimations for the measurements.

Output Quantity	Measurement uncertainty	Propagated input uncertainty	Combined uncertainty, σ_E
Gas and solid temperatures	0.05	0.05	0.07
Gas concentration	0.02	0.08	0.08
Pressure, closed compartment	0.01	0.21	0.21
Pressure, open compartment	0.01	0.15	0.15
Velocity	0.07	0.03	0.08
Heat Flux	0.05	0.10	0.11

Model uncertainty is calculated using the next equation:

$$\widetilde{\sigma_M^2} + \widetilde{\sigma_E^2} = \frac{1}{n-1}\sum_{i=1}^{n}\left[\ln\left(\frac{M_i}{E_i}\right) - \overline{\ln\left(\frac{M}{E}\right)}\right]^2 \qquad [59]$$

Where M stands for the model data, E for the experimental data, and n is the total number of values. Results for the uncertainty are posted in the table below, in percentage form:

Table 13: Model uncertainty calculations

Simulation	TB1	TB2	TB3	TB4	TB5	Rad92
01_FOX	23,7%	6,8%	113,1%	11,6%	15,7%	235,0%

01_FCM	23,7%	6,8%	11,6%	15,8%	20,4%	233,5%
03_FOX	70,9%	76,6%	69,3%	61,8%	43,5%	110,6%
03_FCM	72,4%	72,2%	67,5%	61,0%	34,3%	116,6%
04_FOX	80,7%	68,0%	89,2%	74,1%	64,0%	175,0%
04_FCM	82,7%	71,0%	85,7%	82,3%	61,1%	164,0%
13_FOX	70,3%	79,0%	81,1%	71,9%	59,7%	196,6%
13_FCM	72,3%	46,8%	48,0%	59,3%	45,0%	78,9%
14_FOX	54,3%	55,4%	33,4%	23,7%	39,2%	89,7%
14_FCM	52,6%	34,0%	38,0%	12,8%	28,3%	85,8%
17_FOX	120,7%	6,3%	67,0%	71,3%	37,2%	143,1%
17_FCM	121,3%	6,3%	68,0%	70,5%	35,5%	67,5%
21_FOX	97,5%	55,5%	101,7%			135,8%
21_FCM	62,6%	39,4%	50,6%			142,9%
22_FOX	30,8%	16,6%	86,4%			188,8%
22_FCM	28,4%	18,5%	64,7%			205,7%